

The Pennsylvania State University

The Graduate School

Department of Mathematics

CONTROL PROBLEMS  
IN INFECTIOUS DISEASE MANAGEMENT

A Dissertation in

Mathematics

by

Dongmei Zhang

©2014 Dongmei Zhang

Submitted in Partial Fulfillment  
of the Requirements  
for the Degree of

Doctor of Philosophy

December 2014

The dissertation of Dongmei Zhang was reviewed and approved\* by the following:

Alberto Bressan  
Eberly Family Professor of Mathematics  
Dissertation Co-Advisor, Co-Chair of Committee

Timothy Reluga  
Associate Professor of Mathematics  
Dissertation Co-Advisor, Co-Chair of Committee

Jinchao Xu  
Francis R. and Helen M. Pentz Professor of Science

Lyle N. Long  
Distinguished Professor of Aerospace Engineering and Mathematics

Yuxi Zheng  
Professor of Mathematics, Head of the Department of Mathematics

\*Signatures are on file in the Graduate School.

## Abstract

This dissertation presents applications of mathematical control theory to better understand and prevent infectious disease transmission in epidemiology. Control of structured epidemic models with age heterogeneity and spatial heterogeneity are formulated and analyzed separately. Age structured model is crucial for disease transmission such as HIV. We introduce continuous age structure in both course of infection of individuals and the transmission rate in the population. Not only we analyzed the disease transmission under such detailed age-structured model, we further applied game theory to identify the rational behavior accordingly. Notice that disease often spread into population from a disease reservoir nearby, we also researched a simplified spatial model in one dimension regarding how to control disease from spreading into nearby community. In both age and spatially structured model, we provide mathematical analysis of the existence and derived necessary conditions of the possible optimal strategy. Numerical simulations are also included to show ways to calculate the optimal strategy. In order to fundamentally prevent the disease spread from disease reservoir to the community nearby, we further investigate the controllability problems of the disease reservoir in two dimension, including the confinement and steering problems. The asymptotic shape of the reachable set are also analyzed.

# Contents

<b>List of Figures</b>	<b>vi</b>
<b>List of Tables</b>	<b>vi</b>
<b>Acknowledgements</b>	<b>viii</b>
<b>1 Introduction</b>	<b>1</b>
<b>2 Rational behavior in a continuously-age-structured epidemic game</b>	<b>4</b>
2.1 Background . . . . .	4
2.2 The mathematical model . . . . .	5
2.3 Model Analysis . . . . .	9
2.3.1 Necessary conditions for best responses and game equilibrium . . . .	9
2.3.2 Numerical computation to identify game equilibria . . . . .	11
2.4 Application for three transmission scenarios . . . . .	14
2.4.1 Parametrization . . . . .	14
2.4.2 Scalar infection pressure in constant transmission case . . . . .	15
2.4.3 Age-structured infection pressure in the fully separable transmission case . . . . .	17
2.4.4 Age-structured infection pressure in the non-separable transmission case . . . . .	19
2.5 Results and analysis . . . . .	19
2.6 Discussion . . . . .	23
<b>3 Social planner problem of disease reservoir in an epidemic</b>	<b>24</b>
3.1 Introduction . . . . .	24
3.2 Integral kernel model and model adjustment . . . . .	25
3.3 Analysis for the planner's problem . . . . .	27
3.3.1 Existence of steady state solution of disease dynamic . . . . .	27
3.3.2 Existence of the optimal control with penalty term . . . . .	28
3.4 Optimality condition for the optimal control . . . . .	30
3.5 Numerical algorithm and results . . . . .	31
3.6 Chattering effect analysis as $\epsilon \rightarrow 0$ . . . . .	33
3.7 Comparison with wall blocking strategy for uniform population . . . . .	38

3.8	Discussion . . . . .	39
<b>4</b>	<b>Control problems for a class of set valued evolutions</b>	<b>40</b>
4.1	Introduction . . . . .	40
4.2	Averaging and approximation results . . . . .	44
4.3	Confinement strategies . . . . .	47
4.3.1	A necessary condition . . . . .	47
4.3.2	A steering problem . . . . .	49
4.4	Asymptotic shape of a rotating solution . . . . .	53
	<b>Bibliography</b>	<b>60</b>
	<b>Appendix</b>	<b>68</b>
	<b>Details of Chapter 2</b>	<b>68</b>

# List of Figures

2.1	Example game solution when the infection pressure is independent of age. .	15
2.2	Expected values for the example game solution when the infection pressure is independent of age. . . . .	16
2.3	Population density of susceptible people and infected people. . . . .	17
2.4	Parameterization of fully separable transmission rate and an example solution of steady state infection pressure at game equilibrium. . . . .	20
2.5	Example game solution when the transmission rate is fully separable and the infection pressure is independent of age. . . . .	20
2.6	Parameterization of non-separable transmission rate. . . . .	21
2.7	Example steady state infection pressure at game equilibrium. . . . .	21
2.8	Example solution of the population game with non-separable transmission rate and age-dependent infection pressure. . . . .	22
2.9	Expected values for the example solution of the population game with non-separable transmission rate and age-dependent infection pressure. . . . .	22
3.1	Example solutions regarding various background infection rate of disease reservoir without control function. . . . .	32
3.2	Influence of basic reproduction number and diffusion rate on solutions without control function. . . . .	32
3.3	Sample solution for the model problem based on various diffusion coefficients when $R_0 > 1$ . . . . .	33
3.4	Sample solution for the model problem based on various diffusion coefficients when $R_0 < 1$ . . . . .	34
3.5	Comparison of the value of the cost functional based on different diffusion coefficient. . . . .	34
3.6	Sample solution of the Planner's Problem for $R_0 > 1$ . . . . .	34
3.7	Sample solution of the Planner's Problem for $R_0 > 1$ . . . . .	35
3.8	Sample optimal control $\theta$ for background infection rate $\eta$ . . . . .	38
3.9	Sample solution of wall blocking strategy. . . . .	39
4.1	Illustration of the vector fields $\mathbf{v}^+$ , $\mathbf{v}^-$ construction and the periodic orbit. .	56
4.2	No point of $\Gamma(t)$ can lie in the shaded area, because the interior ball condition would otherwise be violated. . . . .	58

# List of Tables

2.1	List of all symbols used in System (2.2.6). We assume all ages ( $a$ and $z$ ) are measured in the same units as time ( $t$ ). . . . .	9
3.1	List of all symbols used in System (3.3.5). . . . .	27

## Acknowledgements

Above all, I would love to express my deepest gratitude to my two advisors, Professor Alberto Bressan and Professor Timothy Reluga. It has been a great honor to be advised by Professor Bressan, whom I have admired for years as a world-leading mathematician on differential equations and control theory. Throughout the years, he guided me with his insights and motivated me with his passion. I deeply appreciate all his effort in guiding me and helping me during the tough phase of my research and in life, while at the same time giving me all the freedom in searching and pursuing my own career. Such precious memory, along with all my gratitude, will always be kept deeply in the bottom of my heart.

I am forever indebted to Professor Timothy Reluga, who introduced me to interdisciplinary research in infectious disease management. His academic achievements as a gifted young researcher have inspired me to be more courageous in my research interests. He taught me how to ask the key questions, model the problem and work efficiently in an interdisciplinary setting. I am very grateful for all the time and effort he devoted in training me to effectively communicate and apply mathematics in other fields. I can hardly imagine how could I make it through without his great support during my career search and dissertation completion.

I would love to express my great appreciation to Professor Jinchao Xu and Professor Ludmil Zikatanov for their years of guidance on my study in computational science and the support they provided in general. I was very lucky to get to know their research group and attend their group meetings for very long time. It was a great experience working with them on high order method and eigenvalue problems.

I am grateful to Professor Lyle Long for serving on my dissertation committee and supporting me during the completion of my dissertation. I also want to thank Professor Chui Liu and Professor Yuxi Zheng for welcoming me into the big math family at Penn State University and helping me adapt to a new life as a foreign student.

In addition to my professors, my greatest thanks also go to my fellows Giancarlo Facchi, Ke Han, Deling Wei and Guoliang Fang for their support in life during our graduate school years and beyond. And never would I forget Mykhailo Potomkin for all the time and effort he put in helping me tackle the many differential equations.

Finally, I especially want to thank my whole family, all my friends and my high school math teacher Dan Gu for having faith in me and supporting me all these years me in pursuing my dreams, without whom I would never have made it.



# Chapter 1

## Introduction

Infectious disease are dangerous. We need to understand how to protect ourselves from them. Epidemiology is about the studies of the origin, patterns, and effects of health and disease condition in a target population. It has long been studied as an important public health topic for modern society. John Snow is famous for his 19th century cholera epidemics outbreak investigations and is known as the father of (modern) epidemiology, see [91, 38]. His identification of the Broad Street pump as the cause of the Soho epidemic by marking data of the infected people on a map and further noticing the significantly higher death rates in two areas supplied by Southward Company. Snow later used chlorine in order to clean the water and remove the handle of the pump. These ended the outbreak. Such historical event in the history of public health shows a vivid picture of the modern science of epidemiology. This type of population-based health management has been further studied since, from investigating the transmission within the identified population and locating the origin of outbreak to further implement and evaluate interventions that are designed to improve the health of that population, see [62, 61, 44].

People have been studying disease transmission dynamic at population scale (considered as continuum, see [62]) by mathematical modeling using differential equations. Theoretical paper by Kermack and McKendrick about infectious disease models, has developed early theory in mathematical epidemiology models, see [19, 58]. Since then mathematical models have been increasingly used to elucidate the transmission of diseases, usually based on compartment models, see [14], are crucial in gaining important knowledge of the underlying aspects of the infectious diseases the spread and to evaluate the potential impact of control programs in reducing the risk of infection. More structured models can deal explicitly with time and heterogeneity like age and space. Models can further include infectious disease management component, which can be specified by certain parameters. Such models can be used to predict the impacts of various interventions like vaccination and education [81, 39, 12].

Due to resource limitation and the constraints of daily life, infectious disease management requires making trade-offs between expensive control measures and the costs of infection. It's often come into a form of optimization problem balancing the again of staying health by investment in disease control measures and the cost of infection. Intervention strategies can be modeled with the goal of understanding how they will influence

the diseases battle. Education, vaccination campaigns, preventive drugs administration and surveillance programs are all examples of prevention methods for disease prevention. As financial resources are limited, it is nature to seek insight into optimal control under constraints imposed by limited resources. Finding the optimal strategy depends on the balance of economic and epidemiological parameters that reflect the nature of the disease transmission system and the efficiency of the control method.

Simple optimization methods have been used to study many epidemiology questions, see [43, 30]. But some questions require more sophisticated approaches. In particular, questions that include some format of explicit time, age, or space dependence in the management strategy may require some form of dynamic programming and optimal control.

Optimal control is a process of verify controllability, determining control and the corresponding state trajectory for a dynamical system over a period of time in order to minimize a performance index [60]. Historically, it is an extension of the calculus of variations. The generalization of the calculus of variation to optimal control was strongly motivated by military applications such as missile control since 1950s. There are in general two diverse approach to optimal control problem. The Pontryagin Maximum Principle and the Hamilton-Jacobi-Bellman with dynamical programming. The former principle has provided research with suitable conditions for optimization problem with constraints presented as solution of differential equations, which will be the prospect we will take on here. Along with the rapid development of computer science and computational science, applications of the optimal control theory to various complex problem can be tackled. Selected examples are, in physical systems as optimal guidance of rockets, in aerospace as satellite launchers, in economics and management as energy distribution policies, as well as in biology and medicine as oncology, radiotherapy, etc. Applications in management of infectious disease have yet not been spotted much, see [7]. However, structured epidemic models with control measure with continuous dependence on age and space seem to be a nature fit for applying optimal control.

The useful containment of diseases depends on both the capacity to recognize its transmission characteristics and the efficiency to apply optimal medical and logistic policies. Here we want to investigate structured epidemic model with age and spatial heterogeneity, which can better disclose the detailed structure of disease transmission. Although there has been research papers with such heterogeneous structure, but problem as how to impose efficient control accordingly has rarely been studied.

The main goal of this dissertation is to demonstrate with some sample situations that how optimal control theory can be applied to resolve problems from epidemiology for disease management. The second chapter of the dissertation is to formulate structured epidemiological models, giving a special importance to HIV disease as a special example of the age heterogeneity. We formulate the disease management question for each individual as an optimal control problem requiring the maximization/minimization of some objective function that depends on the infected individuals and control costs, given some initial conditions. Due to the feedback of the control and the disease prevalence in the population, we eventually applied game theory to answer such management question.

Further, notice that lots of disease came from disease reservoir, see [95, 94], we ask whether it would be possible to prevent disease from spreading out of the disease reservoir

at the first place. This lead to propose a spatial structured disease transmission model in simply one dimensional space to incorporate the disease reservoir effect. After basic analysis of such disease spreading dynamic, we propose possible control measures to assess and forecast the disease burden. We proved the existence of optimal control and provided numerical simulations.

At last, motivated by the control of disease transmission in moving troops [90], we will build a more realistic model of disease reservoir in two dimension and study the controllability. This lead to necessary studies of nature question such as confinement or steering problem in two dimension, and possible asymptotic shape of the configuration.

## Chapter 2

# Rational behavior in a continuously-age-structured epidemic game

In this chapter, we investigate rational age-dependent behaviors that reduce exposure rates in epidemiological games with steady-state infectious disease transmission. A generalized Kermack–McKendrick model is formulated with continuous age structures for both age since date-of-birth and age since date-of-infection. Necessary conditions are derived for the best response of individuals to the risk of infection, and a numerical scheme is proposed to calculate the game equilibrium provided population-scale dynamics reach a steady-state. The existence, uniqueness, and stability analysis of the population-scale dynamics are also investigated. We apply our model to the issue of HIV transmission in MSM or IDU communities and find that when life is valued equally each day, equilibrium investments in social distancing are strongly correlated to the ages of greatest risk. However, if life is valued by reproductive success, it is by all means always important to invest in early age after become active in the disease contact network by reducing partner switches often. Our results provide insight into epidemic games that each individual is forced to engage in, especially the rational behavior which could be advised to the public. On the other hand, our work also lends a sample method which can be adapted to better understand ways to potentially spread a product or idea throughout the population.

### 2.1 Background

Epidemics of infectious diseases like flu, smallpox, cholera, HIV, malaria, and measles, have been major health issues around the world [4]. Since the 1960's, we have managed many infectious diseases with sanitation, hygiene, vaccination, and antibiotics. But some infectious diseases like HIV and malaria continue to reduce global health, in part because of poor treatment options and the absence of effective vaccines [89]. This leaves behavior-based interventions as primary tool for managing risk.

Although it seems natural for an individual to formulate such best behavior choice

as an optimization problem balancing benefits and costs to cope with epidemic [78]. An individual's risk of infection depends on the prevalence of disease in a community, which depends on the behavior choices of all people in that community. Thus, there is a feedback loop between behavior of the population and disease prevalence. People have proposed the use of games in epidemiology to model such feedbacks under a variety of epidemiological assumptions [25, 28, 78, 82, 84].

However, none of the previous epidemic game models is suitable for disease like HIV to capture the long term effect of age-dependency. For one, HIV has long term infection and the health condition of people changes naturally with aging process. Also, the behavior of people involved changes with their age. While, the ability of each infected individual to transmit the disease also varies according to their stage of infection. Hence, among various heterogeneous structures, the transmission of HIV has unnegligible great dependents on age-structure.

Previous research has intensively studied on age-structured models for disease transmission dynamics. Some divide the population into discrete age groups [14]. Others like [52, 53] incorporated age as a continuous variable. But few studies have been conducted for age-structured epidemic games. [40] studied discrete compartments for young and old people without aging. Reluga in [84] and [82] described models with aging between discrete and continuous age groups.

Here, we propose our game as a population game with continuous age structure. Our susceptible-infected (SI) disease-transmission model has the population-scale dynamics governed by generalizing the Kermack–McKendrick equations [56]. In addition to age-since-birth, we also consider age-since-infection to represent the infectivity change over the course of longterm infection. Lastly, we incorporate a general form of transmission rate among people to reflect various contact pattern in communities and individuals' age-dependent activity level. Within this population game, we attempt to identify the rational behavior that correspond to Nash equilibria, where every individual is playing their best strategy, conditional on the average behavior of other individuals. Although, this modified model could allow us to study strategy set with continuously-age-dependency, this is not a differential-game, as all the analysis is undertaken at certain steady-state of the disease-transmission system. This type of epidemic game with multiple continuously-age-dependency is not only relevant for HIV, but also of importance for other disease whose transmission is sensitive respect stage of infection.

The paper is organized as follows. In section 2, we propose our model game of investment choice to achieve behavioral changes and epidemiological dynamics, definitions of best response and game equilibrium condition. The corresponding necessary conditions for best response as well as game equilibrium are also derived. A numerical scheme for calculating Nash equilibria is designed for this type of epidemic game in section 3. Section 4 presents and analyzes various type of results from implementation for different cases of transmission.

## 2.2 The mathematical model

We begin by building an age-structured model of infectious disease transmission where infected individuals remain infected for the duration of their lives. The population-scale,

dynamics are governed by a pair of coupled McKendrick–Von Foerster equations, see [58]. Let  $S(a, t)$  be the age-density of age- $a$  susceptible people at time  $t$ . We make the simple assumption that births introduce susceptible individuals into the population at a constant rate  $r$ . Individuals then age at a constant rate. We also assume mortality rates in the population are age-dependent but density-independent, being specified by  $\mu(a)$ . To avoid complications associated with infinite-horizons, we assume there exists a maximum age  $a_{\max}$  such that  $\mu(a) = \infty$  for all  $a > a_{\max}$ .

Susceptible individuals may be infected when exposed to other infected individuals. The rates of infection can depend on the contact pattern and the ages of the infected individuals involved, as well as their stage of the infection at the time of exposure. Let  $I(a, t, z)$  be the age-density of age- $a$  infected people who has been infected for time  $z$  at time  $t$ . Where necessary, we will refer to  $a$  as the “age-since-birth” and  $z$  as the “age-since-infection”. The mortality rate among infected people is independent of density, but depends on both the age-since-birth and the age-since-infection, as  $\gamma(a, z)$ . We constrain the background mortality rate  $\mu(a)$  and mortality rate of infected people  $\gamma(a, z)$  such that both are positive and strictly increasing for sufficiently large  $a$ , where  $\mu(a) \leq \gamma(a, 0) \leq \gamma(a, z)$  for all  $a \geq 0$  and  $z \geq 0$ . The disease transmission rate  $\beta(a, a_I, z)$  represents the transmission rate from infected people at age  $a_I$  with age-since-infection  $z$  to susceptible people at age  $a$ . The infection pressure  $\lambda(a, t)$  is, by definition, the probability per unit of time that an susceptible at age  $a$  gets infected, which we will assume to be a linear function of the age-density of infections  $I(a, t, z)$ . We then have the disease dynamic as

$$\frac{\partial S}{\partial t} + \frac{\partial S}{\partial a} = -\mu(a)S - \lambda(a, t)S, \quad S(0, t) = r, \quad (2.2.1a)$$

$$\frac{\partial I}{\partial t} + \frac{\partial I}{\partial a} + \frac{\partial I}{\partial z} = -\gamma(a, z)I, \quad I(a, t, 0) = \lambda(a, t)S(a, t), \quad (2.2.1b)$$

$$\lambda(a, t) = \int_0^{a_{\max}} \int_0^{a_I} \beta(a, a_I, z) I(a_I, t, z) dz da_I. \quad (2.2.1c)$$

This model is a generalization the theory originally formalized by Kermack and McKendrick [56, 57]. It is very similar to the model of Inaba in [53], except that our model uses bilinear incidence instead of standard incidence. This is also a generalization with more detailed age-structure of the disease dynamic model studied in [82]. System 2.2.1 can be used to study the dynamics of several infectious diseases including HIV and syphilis. Although no sex structure has been built in this model, it is still suitable for the MSM or IV drug use communities. In many public health cases where 2.2.1 maybe applied, behavior choice is an important aspect of disease control. Changes in behavior can affect disease transmission dynamics in different ways, such as altering individuals’ resistance to infection [12, 80, 88], the progression of disease [45], and the contact network governing the spread of disease [39, 45, 96]. Such behavioral changes, if adopted by a large population, might further feed back on the infection and recover rates of the disease in a community [43], which also impacts disease prevalence. On the other hand, changes in behavior often come at a price. The behaviors that put people at risk (sex and drug use) have a high personal value to the participating individuals [11]. In such cases, people’s choices trade off the value of the risky activity against future costs of the activity [32, 39]. Hence, people’s choices of

behavior can be interpreted as balancing the risk of illness against the costs of prevention.

Suppose  $c_S(a)$  represents an individual's investment strategy in order to gain the desired behavior changes at age  $a$  (utility per unit time). Correspondingly, the aggregated investment strategy of the population at age  $a$  is described by  $\bar{c}_S(a)$ . To measure the effectiveness of behavior against risk of infection at age  $a$ , we introduce the relative exposure rates  $\sigma(a, c_S(a))$ , which lies in  $[0, 1]$  and decreases when  $c_S(a)$  increases. Based on the economic hypothesis of diminishing marginal returns, we also assume  $\sigma$  is convex in  $c_S$ . This measurement also applies to the aggregated strategy of the population  $\bar{c}_S(a)$ . With symbols listed in Table 3.2, the population-scale disease-transmission dynamic of our model with behavioral intervention is governed by

$$\frac{\partial S}{\partial t} + \frac{\partial S}{\partial a} = -\mu(a)S - \sigma(a, \bar{c}_S(a))\lambda(a, t)S, \quad (2.2.2a)$$

$$S(0, t) = r, \quad (2.2.2b)$$

$$\frac{\partial I}{\partial t} + \frac{\partial I}{\partial a} + \frac{\partial I}{\partial z} = -\gamma(a, z)I, \quad (2.2.2c)$$

$$I(a, t, 0) = \sigma(a, \bar{c}_S(a))\lambda(a, t)S(a, t), \quad (2.2.2d)$$

$$\lambda(a, t) = \int_0^{a_{\max}} \int_0^{a_I} \beta(a, a_I, z)I(a_I, t, z)dzda_I. \quad (2.2.2e)$$

Authors in [19] show that this class of epidemic models, with both demography and non-permanent immunity, can also be formulated mathematically as a scalar renewal equation for the infection pressure instead. Breda and Visetti [20] have also recently studied the existence and stability of the steady-state solutions for similar systems. We provide a similar analysis with detailed computations in the appendix to this chapter.

Now, suppose the infection pressure  $\lambda(a, t)$  is given by a time-independent (while possibly age dependent) stationary infection pressure  $\tilde{\lambda}(a)$ . In the face of this endemic risk, the probability that an individual at age  $a$  is susceptible or infected ( $p_S(a, t)$  and  $p_I(a, t, z)$  respectively) is described by

$$\frac{\partial p_S}{\partial t} = -\frac{\partial p_S}{\partial a} - \mu(a)p_S - \sigma(a, c_S(a))\tilde{\lambda}(a)p_S, \quad (2.2.3a)$$

$$p_S(a, t_0) = \delta(a), \quad (2.2.3b)$$

$$\frac{\partial p_I}{\partial t} = -\frac{\partial p_I}{\partial a} - \frac{\partial p_I}{\partial z} - \gamma(a, z)p_I, \quad (2.2.3c)$$

$$p_I(a, t, 0) = \sigma(a, c_S(a))\tilde{\lambda}(a)p_S(t, a). \quad (2.2.3d)$$

where  $\delta(\cdot)$  refers to the Delta-function while  $t_0$  serves as the date-of-birth. Since the infection pressure is stationary, all rates are independent of  $t_0$  and  $t$ . Hence, without loss of generality, we assume  $t_0 = 0$ . Integrating the hyperbolic System (2.2.3) along characteristics, where

$t - a$  is constant, gives us

$$\frac{\partial p_S}{\partial a} = -\mu(a)p_S - \sigma(a, c_S(a))\tilde{\lambda}(a)p_S, \quad (2.2.4a)$$

$$p_S(0) = 1, \quad (2.2.4b)$$

$$\frac{\partial p_I}{\partial a} + \frac{\partial p_I}{\partial z} = -\gamma(a, z)p_I, \quad (2.2.4c)$$

$$p_I(a, 0) = \sigma(a, c_S(a))\tilde{\lambda}(a)p_S(a). \quad (2.2.4d)$$

For an individual in this population, the goal might be to find a strategy  $c_S(a)$  that will maximize their lifetime expected utility, given that each individual is born susceptible. Suppose the positive functions  $u_S(a)$  and  $u_I(a, z)$  are the expected utility gains per unit time at age  $a$  of being healthy or having been infected for time  $z$  respectively. We need to assume a discounting rate  $h$  for estimating the accumulated utility gains in long term. At any given age  $a$ , the net utility gain of being health is described as  $u_S(a) - c_S(a)$ . While on the other hand, the expected utility gain of being infected at age  $a$  will be the utility gain  $u_I(a, z)$  accumulated over all ages of infection  $z$  with the corresponding probabilities  $p_I(a, z)$ . Hence, given the stationary infection pressure  $\tilde{\lambda}$ , the expected lifetime accumulated payoff as a functional of a chosen investment strategy  $c_S(\cdot)$ ,

$$\mathcal{U}(c_S; \tilde{\lambda}) \doteq \int_0^{a_{\max}} e^{-ha} \left\{ [u_S(a) - c_S(a)]p_S(a) + \int_0^a u_I(a, z)p_I(a, z)dz \right\} da. \quad (2.2.5)$$

We naturally restrict the rate of utility gain for susceptible  $u_S(a)$  is never less than that of an infected individual of the same age ( $u_I(a, z) \leq u_S(a)$  for all ages  $a$  and  $z$ ).

But an individual's strategy must be consistent with the actions of all other players, due to the feed back loop between behavior and disease prevalence. As one individual is seeking to find investment strategy  $c_S(a)$ , others are looking for the aggregated investment strategy  $\bar{c}_S(a)$  of the population as a whole, which eventually drives the stationary infection pressure to be  $\tilde{\lambda}(a)$ .

$$\mathcal{U}(c_S; \bar{c}_S, \tilde{\lambda}) = \int_0^{a_{\max}} e^{-ha} \left\{ [u_S(a) - c_S(a)]p_S(a) + \int_0^a u_I(a, z)p_I(a, z)dz \right\} da \quad (2.2.6a)$$

$$\frac{\partial p_S}{\partial a} = -\mu(a)p_S - \sigma(a, c_S(a))\tilde{\lambda}(a)p_S, \quad p_S(0) = 1, \quad (2.2.6b)$$

$$\frac{\partial p_I}{\partial a} + \frac{\partial p_I}{\partial z} = -\gamma(a, z)p_I, \quad p_I(a, 0) = \sigma(a, c_S(a))\tilde{\lambda}(a)p_S(a), \quad (2.2.6c)$$

$$c_S(a) \geq 0, \quad (2.2.6d)$$

$$\frac{\partial S}{\partial a} = -\mu(a)S - \sigma(a, \bar{c}_S(a))\tilde{\lambda}(a)S, \quad S(0) = r, \quad (2.2.6e)$$

$$\frac{\partial I}{\partial a} + \frac{\partial I}{\partial z} = -\gamma(a, z)I, \quad I(a, 0) = \sigma(a, \bar{c}_S(a))\tilde{\lambda}(a)S(a) \quad (2.2.6f)$$

$$\tilde{\lambda}(a) = \int_0^{a_{\max}} \int_0^a \beta(a, a_I, z)I(a_I, z)dzda_I. \quad (2.2.6g)$$



Symbol	Interpretation
$S(a)$	density (number per unit area) of susceptible people at age $a$
$I(a, z)$	density (number per unit area) of infected people at age $a$ with age-since-infection $z$
$p_S(a)$	the probability that an individual at age $a$ is susceptible
$p_I(a, z)$	the probability that an individual at age $a$ is infected with age-since-infection $z$
$r$	birth rate (number per unit time) of the population
$\mu(a)$	background mortality rate (per unit time) of the population at age $a$
$\gamma(a, z)$	mortality rate (per unit time) of infected people at age $a$ with age-since-infection $z$
$\beta(a, a_I, z)$	transmission rate per infected individual at age $a_I$ infected for time $z$ to age- $a$ susceptibles (per person per unit time)
$h$	discounting rate (per unit time)
$u_S(a)$	the expected utility gains per unit time at age $a$ of being healthy
$u_I(a, z)$	the expected utility gain at age $a$ of being infected with age-since-infection $z$
$\bar{c}_S(a)$	the aggregated investment strategy of the population at age $a$ (utility per unit time)
$c_S(a)$	the investment strategy of the individual at age $a$ (utility per unit time)
$\sigma(a, c_S(a))$	the relative exposure rate (dimensionless) depending on age $a$ and investment $c_S(a)$
$\lambda(a)$	the infection pressure (per unit time) in the population at age $a$

Table 2.1: List of all symbols used in System (2.2.6). We assume all ages ( $a$  and  $z$ ) are measured in the same units as time ( $t$ ).

## 2.3 Model Analysis

Given the utility  $\mathcal{U}(c_S; \bar{c}_S, \tilde{\lambda})$ , we want to find what types of equilibria the population game possesses, how to calculate these equilibria, and how those equilibria depend on model parameters.

### 2.3.1 Necessary conditions for best responses and game equilibrium

If there is a stationary infection pressure  $\tilde{\lambda}(a)$  of system (2.2.2) which is driven by the aggregated investment strategy of the population  $\bar{c}_S(a)$ , then the best-response correspondence can be defined as

$$c_S^B(\bar{c}_S, \tilde{\lambda}) \doteq \operatorname{argmax}_{c_S} \mathcal{U}(c_S; \bar{c}_S, \tilde{\lambda}). \quad (2.3.1)$$

Nash equilibria are strategies which are best responses to themselves. A strategy  $c_S^*$  is a Nash equilibrium if it is a solution of the set inclusion relation

$$c_S^* \in c_S^B(c_S^*, \tilde{\lambda}). \quad (2.3.2)$$

In this population game, each individual needs to maximize the utility by trading off the lifetime cost of illness and cost of prevention. So, the problem of finding a Nash equilibrium can be formulated iteratively as constrained optimization to identify best response in each iteration. There are two different approach to solve this type of optimization problem where constraints consisting of ordinary and partial differential equations. One way of computing the optimal control is first discretizing the constraints and utility function and then solve the finite-dimensional optimization problem which is known as *discretize-then-optimize* approach [59]. Alternatively, we can derive the continuous optimality system using adjoint calculus based on the Lagrangian form, then discretize this system and find the optimal control. This is the *optimal-then-discretize* approach.

Here we take the second approach. To derive the optimality condition, notice that our Lagrangian has an integral form because of the continuous state-space individuals occupied. Denote our utility function  $\mathcal{U}(p_S, p_I, c_S)$  as functional of  $p_S(\cdot)$ ,  $p_I(\cdot, \cdot)$  and  $c_S(\cdot)$ . Given  $c_S(\cdot)$ , for the two differential equation type of constraints on  $p_S(\cdot)$  and  $p_I(\cdot, \cdot)$  respectively, we denote the curve defined by the solutions of the differential equations for  $p_S$  and  $p_I$  with matching terminal conditions as  $C(p_S(\cdot), p_I(\cdot, \cdot), c_S(\cdot)) = 0$ . The Lagrangian of our utility function has general form

$$\mathcal{L} = \mathcal{U}(p_S, p_I, c_S) - \langle V, C(p_S, p_I, c_S) \rangle, \quad (2.3.3)$$

where  $V = (V_S, V_I, V_{c_S})$  is the adjoint functions of  $(p_S(\cdot), p_I(\cdot, \cdot), c_S(\cdot))$  and  $\langle \cdot, \cdot \rangle$  is inner product. Applying the standard adjoint calculus, details shown in Appendix A, we derived the necessary conditions on the continuous level for a given  $\tilde{\lambda}(a)$  as following

$$-\frac{dV_S}{da} = u_S - c_S^B + \sigma(a, c_S^B) \tilde{\lambda}[V_I(0) - V_S] - [h + \mu] V_S, \quad (2.3.4a)$$

$$V_S(a_{\max}) = 0, \quad (2.3.4b)$$

$$-\frac{dV_I}{da} - \frac{dV_I}{dz} = u_I - [h + \gamma] V_I, \quad (2.3.4c)$$

$$V_I(a_{\max}, z) = 0, \quad (2.3.4d)$$

$$0 = \left\{ \frac{\partial \sigma}{\partial c_S} \Big|_{c_S^B} - \frac{1}{\tilde{\lambda}[V_I(0) - V_S]} \right\} c_S^B, \quad c_S^B \geq 0. \quad (2.3.4e)$$

The adjoint variables  $V_S(a)$  and  $V_I(a, z)$  represent the shadow prices which give the marginal utility gains of relaxing the corresponding probabilities  $p_S$  and  $p_I$  when the system reaches the optimal solution. On the other hand, we want to point out that the integrated form of System (2.3.4) can also be interpreted as the expected value (utility gains) of a certain age state.

Integrating along the characteristic lines of Eq. (2.3.4), we see for infected people with a certain age  $a$  and age-since-infection  $z$ ,

$$V_I(a, z) = \int_0^{a_{\max}-a} \underbrace{e^{-\int_0^w \gamma(a+v, z+v) dv}}_{PA} \times \underbrace{\int_0^w u_I(a+v, z+v) e^{-hv} dv}_{EV} \underbrace{\gamma(a+w, z+w) dw}_{PD}. \quad (2.3.5)$$

$PA$  is the probability of living  $w$  more years,  $PD$  is the probability a sick individual at exactly  $w$  years later in life, and  $EV$  represents the expected value during the next  $w$  years of being infected but alive. Then integrating over all the possible  $w$  up to the maximum year yet to live  $a_{\max} - a$ , this gives the expected value of infected individual at age  $a$  and age-since-infection  $z$ . Similarly, the solution  $V_S$ , which depends on the stationary infection pressure  $\tilde{\lambda}(a)$  as well as the individual's behavior  $c_S$ , is described by

$$V_S(a; c_S, \tilde{\lambda}) = \int_a^{a_{\max}} \underbrace{e^{-\int_a^\alpha \tilde{\lambda}(\tau) \sigma(\tau, c_S(\tau)) + \mu(\tau) d\tau}}_{PH} \underbrace{\left[ \tilde{\lambda}(\alpha) \sigma(\alpha, c_S(\alpha)) + \mu(\alpha) \right]}_{PR} \times \left\{ \underbrace{\frac{\tilde{\lambda}(\alpha) \sigma(\alpha, c_S(\alpha))}{\tilde{\lambda}(\alpha) \sigma(\alpha, c_S(\alpha)) + \mu(\alpha)}}_{PI} \underbrace{V_I(\alpha, 0) e^{-h(\alpha-a)}}_{EVI} + \underbrace{\frac{\mu(\alpha)}{\tilde{\lambda}(\alpha) \sigma(\alpha, c_S(\alpha)) + \mu(\alpha)}}_{PD} + \underbrace{\int_a^\alpha [u_S(v) - c_s(v)] e^{-h(v-a)} dv}_{EVH} \right\} d\alpha. \quad (2.3.6)$$

$PH$  represent the probability of staying healthy from age  $a$  up to a future age  $\alpha$ .  $PRd\alpha$  is the probability to be removed from susceptible state due to either infection or death at exact future age  $\alpha$ .  $PI$  is the conditional probability of getting infected but still alive,  $PD$  instead represent the conditional probability of getting infected and die. Hence,  $EVI$  is the expected value of getting infected at age  $\alpha$  and  $EVH$  is the expected value (net utility gains) of staying healthy from age  $a$  up to the future age  $\alpha$ . The discounting rate is considered and included respectively. Integrating over all possible future ages  $\alpha$  up to the maximum gives us the expected value of susceptible individual at age  $a$ .

### 2.3.2 Numerical computation to identify game equilibria

After defining the best response condition Eq. (2.3.1) and game equilibrium condition Eq. (2.3.2), and taking the optimality conditions (2.3.4) into account, we can reformulate

the task of finding game equilibrium candidates as finding  $c_S^B(a)$  such that

$$\bar{c}_S = c_S^B \quad (2.3.7a)$$

$$-\frac{dV_S}{da} = u_S - c_S^B + \sigma(a, c_S^B) \tilde{\lambda}(a) [V_I(0) - V_S] - [h + \mu] V_S, \quad (2.3.7b)$$

$$V_S(a_{\max}) = 0, \quad (2.3.7c)$$

$$-\frac{dV_I}{da} - \frac{dV_I}{dz} = u_I - [h + \gamma] V_I, \quad (2.3.7d)$$

$$V_I(a_{\max}, z) = 0, \quad (2.3.7e)$$

$$0 = \left\{ \frac{\partial \sigma}{\partial c_S} \Big|_{c_S^B} - \frac{1}{\tilde{\lambda} [V_I(0) - V_S]} \right\} c_S^B, \quad c_S^B \geq 0, \quad (2.3.7f)$$

$$\frac{\partial S}{\partial a} = -\mu S - \sigma(a, \bar{c}_S) \tilde{\lambda} S, \quad S(0) = r, \quad (2.3.7g)$$

$$\frac{\partial I}{\partial a} + \frac{\partial I}{\partial z} = -\gamma I, \quad I(a, 0) = \sigma(a, \bar{c}_S) \tilde{\lambda} S, \quad (2.3.7h)$$

$$\tilde{\lambda}(a) = \int_0^{a_{\max}} \int_0^a \beta(a, a_I, z) I(a_I, z) dz da_I. \quad (2.3.7i)$$

We can now compute the game equilibria since the best response  $c_S^B$  for given infection pressure  $\tilde{\lambda}$  can be calculated from Eq. (2.3.3). Therefore, we do not need to compute neither of the original variables  $p_S$  and  $p_I$  in order to evaluate the payoff function  $\mathcal{U}$ , nor its gradient for searching direction of the optimizer  $c_S^B$ . But we do need to keep the state equations of the disease dynamics, because the aggregated behavior strategy may induce a different infection pressure.

Our approach is to focus on numerically solving the System (2.3.7) iteratively. All individuals in the population game are solving a constrained optimization problem, when the population dynamic reaches a stationary solution with a known infection pressure  $\tilde{\lambda}$ . We can try to identify game equilibria by first taking care of way to compute the disease infection pressure  $\tilde{\lambda}$ , where Eqs. (2.2.2) is satisfied for a given aggregated strategy. Usually we can start by assuming no one is making any special behavior changes in the community, meaning  $\bar{c}_S = 0$ . Notice that the differential equations in Eqs. (2.2.2) have characteristic lines that never intersect each other. We derive the following steady-state condition on infection pressure, which can be applied to any given aggregated investment strategy of the population  $\bar{c}_S$  later on in each iteration. Integrate along characteristics of the population dynamics Eqs. (2.2.2),

$$S(a) = r e^{-\int_0^a \mu(\tau) + \sigma(\bar{c}_S(\tau), \tau) \tilde{\lambda}(\tau) d\tau}, \quad (2.3.8a)$$

$$I(a, z) = \sigma(a - z, \bar{c}_S(a - z)) \tilde{\lambda}(a - z) S(a - z) e^{-\int_0^z \gamma(a - z + \tau, \tau) d\tau}, \quad (2.3.8b)$$

$$\tilde{\lambda}(a) = \int_0^{a_{\max}} \int_0^a \beta(a, a_I, z) I(a_I, z) da_I dz. \quad (2.3.8c)$$

If we define integral function  $F$  of  $\tilde{\lambda}(a)$  for given  $\bar{c}_S(a)$  as

$$F \doteq \int_0^{a_{\max}} \int_0^{a_I} \beta(a, a_I, z) \tilde{\lambda}(a_I - z) \sigma(a_I - z, \bar{c}_S(a_I - z)) \times \\ r e^{-\int_0^{a_I - z} \tilde{\lambda}(\tau) \sigma(\tau, \bar{c}_S(\tau)) + \mu(\tau) d\tau} e^{-\int_0^z \gamma(a_I - z + \tau, \tau) d\tau} dz da_I, \quad (2.3.9)$$

then the steady-state condition for infection pressure  $\tilde{\lambda}(a)$  is

$$\tilde{\lambda}(a) = F[\tilde{\lambda}(a); \bar{c}_S(a)]. \quad (2.3.10)$$

To compute  $\tilde{\lambda}(a)$  using Eq. (2.3.10), we can use fixed-point iteration choosing proper numerical integration scheme, such as Guass quadrature on triangular domain [21]. Alternatively,  $\tilde{\lambda}(a)$  can be achieved by solving the differential-integral equations in Eq. (2.2.2) numerically using iterative method.

Next, to calculate the best response  $c_S^B(\bar{c}_S, \tilde{\lambda})$ , we plug  $\tilde{\lambda}(a)$  into Eqs. (2.3.4) and apply proper numerical method to solve the differential equations. Notice that since the value function  $V_I(a, z)$  is independent of strategy choice and disease prevalence, we can precompute it and store the value  $V_I(a, 0)$  as the lifetime expected value of getting sick at age  $a$  at the beginning. Hence, we only need to compute  $V_S(a)$  and  $c_S^B(a) = c_S(a)$  in each iteration.

The game equilibrium condition Eq. (2.3.2) indicates that when one individual finds the best investment strategy  $c_S^B(a)$ , others must adopt the same as the aggregated investment strategy of the population  $\bar{c}_S(a) = c_S^B(a)$ . Therefore, in order to identify the game equilibrium  $c_S^*$ , we need to update  $\bar{c}_S$  to be  $c_S^B(\bar{c}_S, \tilde{\lambda})$ . Up to now, we stated all the steps in one iteration, then we go back to compute the new  $\tilde{\lambda}(a)$  as in the next iteration until convergence. The stopping criteria can be setup as the convergence of  $c_S^B(a)$ .

As long as the disease dynamic has a unique endemic steady state  $\tilde{\lambda} > 0$ , identifying a game equilibrium is equivalent as locating stationary infection pressure  $\tilde{\lambda}$  in equations

$$F[\tilde{\lambda}; c_S^*] = \tilde{\lambda}, \text{ where } c_S^* \in c_S^B(c_S^*, \tilde{\lambda}), \text{ for all } a \geq 0. \quad (2.3.11)$$

Therefore, the stopping criteria can set as the convergence of  $\tilde{\lambda}$  as alternative to  $c_S^B$ . For the implementation, we suggest mesh size comparable with the data. The numerical integration scheme should be suitable for triangular domain.

Notice that Eq. (2.3.10) always has  $\tilde{\lambda} = 0$  as a stationary solution. Hence,  $c_S^*(a; \tilde{\lambda} = 0) = 0$  is always a Nash equilibria. This case matches our intuition that when there is no disease, we can all agree that the best strategy is to do nothing. But we are more interested in finding non-trivial game equilibria which corresponds to positive infection pressure  $\tilde{\lambda}(\cdot) > 0$ . Currently, the existence of general non-trivial game equilibria has not been established, but it depends in part on the details of the transmission pattern and also costs of disease. We can always attempt to run this iterative numerical scheme to compute the game equilibria if it converges to a unique one, then check it for the optimality condition. But, there is no guarantee.

For our model problem, the existence and uniqueness of non-trivial Nash equilibria is closely related to the properties of the transmission rate  $\beta(a, a_I, z)$ . Here, we list some analysis and results for transmission rate in some special but commonly seen forms in the following section.

## 2.4 Application for three transmission scenarios

We begin investigating the HIV risk management with our model by first study the simplest transmission rate as a uniform scaler. Later we will parametrize more detailed transmission pattern to acquire age-dependent transmission rate. Within each transmission scenario, we will study the population dynamic steady-state and its properties first before moving on to identify our game analysis. So, the all following content will be organized in such order respectively.

### 2.4.1 Parametrization

Before getting into details, there are several assumptions we have to specify. For our problems, we consider the relative exposure rate

$$\sigma(a, c_S(a)) = \frac{1}{1 + m(a)c_S(a)}, \quad (2.4.1)$$

where  $m(a)$  measure the efficiency of the investment  $c_S(a)$  on social distancing strategy at different age  $a$ . Here, we simply take  $m(a) = 100$ . Within each iteration of searching for a game equilibrium, the necessary condition (2.3.4) for local optimality yields that the best response  $c_S^B(a; \tilde{\lambda})$ , for any particular age  $a$ , must be either equal to 0 or satisfies

$$\frac{-m(a)}{[1 + m(a)c_S^B]^2} = \frac{1}{\tilde{\lambda}(a)[V_I(a, 0) - V_S(a)]}, \quad c_S^B(a; \tilde{\lambda}) \geq 0, \quad (2.4.2)$$

which yields

$$c_S^B(a; \tilde{\lambda}) = \max \left\{ 0, \frac{-1 + \sqrt{m(a)\tilde{\lambda}(a)[V_S(a) - V_I(a, 0)]}}{m(a)} \right\}. \quad (2.4.3)$$

To further parametrize our model, we give details regarding demography, transmission, removal rates and costs. Based on the CDCs mortality schedule for the US in 2003 (Arias, 2006), the mortality rate for generic individuals in the US can be approximated by  $\mu(a) = \exp(k_0 + k_1 a)$ , where  $k_0 = -9.46$ ,  $k_1 = 0.085$  with assumption that the average life expectancy at birth is  $a_{\max} = 80$ , see [87]. We also take the birth rate as  $r = 1$  in order to normalize our population structure. Disease transmission will be presented separately in each of the following cases. The mortality rate of infected people  $\gamma(a, z) = \mu(a)$  for all  $z$ . Here, we assume there is no mortality rate increase due to infection, Instead, we incorporate such changes in health as a drop in utility gains for infected people. We define utility gains of being susceptible as

$$u_S(a) = \min\{1, 1 - (a - 30)/(a_{\max} - 30)\},$$

where the change at age  $a = 30$  is to model the slow loss of function due to the aging process. On the other hand, due to the disease progression pattern of HIV, there is an approximately 10 years period for infected individual with HIV to live without any symptoms before

progressing to the final AIDS stage. Assume the utility gains as being infected  $u_I(a, z)$  only drop to 10 percent of the corresponding  $u_S(a)$  once individual progresses into AIDS period, and keep decreasing thereafter,

$$u_I(a, z) = \begin{cases} u_S(a) & \text{if } z < 10, \\ u_S(a)/(1 + 10(z - 10)^2) & \text{if } z \geq 10. \end{cases}$$

The background annual discount rate is set around three percent  $h = 0.03$  as published on the WHO report.

#### 2.4.2 Scalar infection pressure in constant transmission case

We start discussion regarding our numerical computation of Nash equilibria with a simple case, where the transmission rate is assumed to be a scalar constant. We know that this is a fair assumption for diseases transmission that are not sensitively depend on both the age-since-birth and the age-since-infection of people involeed. That being the case, we have the infection pressure in our model being independent of age at steady state of the disease transmission dynamic. An example solution of this type is shown in Figure 2.1.

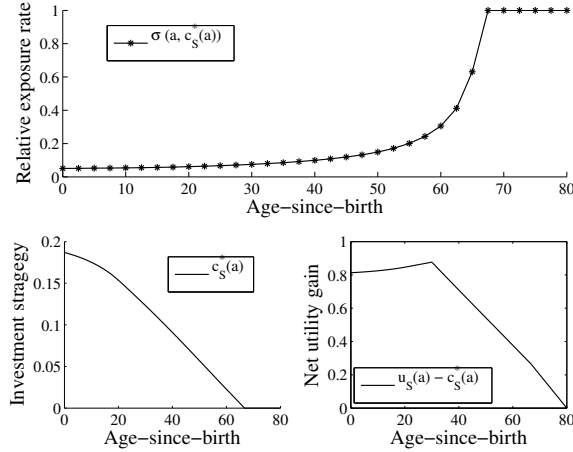


Figure 2.1: Example game solution when the infection pressure is independent of age. The plot on top shows the Nash equilibrium strategy  $\sigma(c_S^*)$  at steady state infection pressure  $\tilde{\lambda} = 0.4254$ , given the transmission rate is scalar constant  $\beta = 0.01$  defined in (2.4.6). The corresponding investment strategy and net utility gain are listed on the bottom.

To compute the positive stationary infection pressure, recall Eq. (2.3.10), we cancel  $\tilde{\lambda}$  on both side of the equation to achieve a form that admit only non-zero stationary infection pressure  $\tilde{\lambda}$  as its solution.

$$F(\tilde{\lambda}) \doteq \int_0^{a_{\max}} \int_0^a \beta \sigma(\bar{c}_S(a-z)) r e^{-\int_0^{a-z} \sigma(\bar{c}_S(\tau)) \tilde{\lambda} + \mu(\tau) d\tau} e^{-\int_0^z \gamma(a-z+\tau) d\tau} dz da = 1. \quad (2.4.4)$$

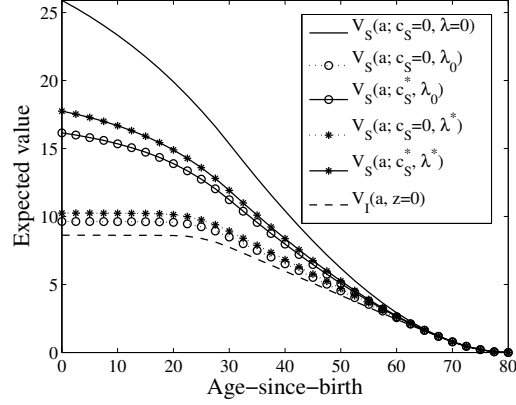


Figure 2.2: Expected values for the example game solution when the infection pressure is independent of age. This plot illustrates expected values for age  $a$  infected people  $V_I(a, 0)$  and susceptible people  $V_S(a)$  adapting different strategies when facing steady state infection pressure  $\tilde{\lambda}$ . Parameters are the same as in Figure 2.1. The first shows the case of being disease free. The following two comparisons show a drastic increase of expected value for susceptible people from engaging in the rational behavior when facing the endemic.

Notice that  $F(\tilde{\lambda}) \rightarrow 0$  as  $\tilde{\lambda} \rightarrow \infty$ , we expect to find at least one positive root of  $F(\tilde{\lambda}) = 1$ , provided that  $F(0) > 1$ . With this intuition and detailed analysis in Appendix B, we state the following conclusions about the steady state solution regarding the population-scale disease dynamic.

Define basic reproduction number  $R_0 = G(0)$  from Eq. (2.4.4),

$$R_0 \doteq \int_0^{a_{\max}} \int_0^a \beta \sigma(\bar{c}_S(a-z)) r e^{-\int_0^{a-z} \mu(\tau) d\tau} e^{-\int_0^z \gamma(a-z+\tau) d\tau} dz da. \quad (2.4.5)$$

If  $R_0 < 1$ , there exist a unique disease-free equilibrium. If  $R_0 > 1$ , there exist a unique endemic equilibrium. Not only  $R_0$  is an indicator of the existence and uniqueness of the steady-state solution, but also grant the stability of the disease-free equilibrium as: If  $R_0 < 1$ , the disease-free equilibrium is stable. If  $R_0 > 1$ , the disease-free equilibrium is unstable.

For the game equilibrium, we observe from numerical simulation and Eq. (2.4.3) that the best response  $c_S^B$  is uniquely defined by  $\tilde{\lambda}$  at any given age  $a$ . Moreover it is a non-decreasing function of  $\tilde{\lambda}$ . Notice that the disease-free infection pressure is unstable, although we have no conclusion about the stability of the endemic infection pressure, but the uniqueness of the endemic equilibria is sufficient to guarantee the converged best response is the only endemic game equilibria. Therefore, we have conclusions about existence and uniqueness of game equilibrium as following: If  $R_0 < 1$ , there exist a unique game equilibrium  $c_S^* = 0$  with disease-free infection pressure  $\lambda^* = 0$ . If  $R_0 > 1$ , there exist a unique non-trivial game equilibrium  $c_S^* > 0$  with endemic infection pressure  $\lambda^* > 0$ .

This type of model with a scalar transmission rate can be efficiently simulated numerically and provide a simple prediction for an epidemiology game. However, the density of



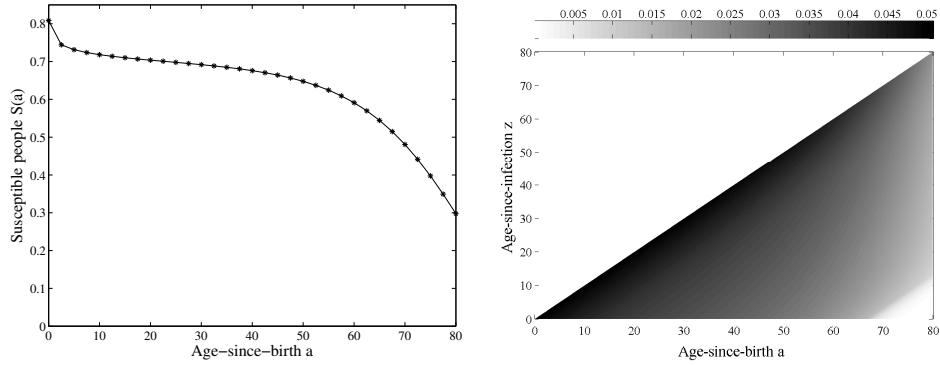


Figure 2.3: Population density of susceptible people  $S(a)$  and infected people  $I(a, z)$  at endemic game equilibria as steady state infection pressure  $\lambda^* = 0.4254$ , given the transmission rate is constant  $\beta = 0.01$ . The drop in density of susceptible people  $S$  at early age is due to disease infection, while the latter drop is due to nature aging process. The density of infected people provide forecast for potential targeted age group to conduct education and disease prevention.

infected people indicated in Figure 2.3 is not realistic for diseases as HIV. Notice that most infected people being children in the community does not match the real data we see around the world. Children should bear low risk until the age of maturity. This brought our attention to address the issue that risk should be age dependent. Moreover, transmission rate should not be assumed as constant but varies with people's state of infection as well as people's chronological age, where the latter one may have influence on the choice of contact network. Hence, heterogeneous structure should be incorporated in transmission rate.

We model the transmission rate with age heterogeneity in a form of

$$\beta(a, a_I, z) \doteq \Theta(a, a_I)\phi(z), \quad (2.4.6)$$

where  $\Theta(a, a_I)$  represents the contact patten (per unit time) between age-since-birth  $a$  susceptibles and age-since-birth  $a_I$  infected people, and  $\phi(z)$  is the relative infectivity (probability of transmission, per contact with a susceptible) at age-since-infection  $z$ . The underline assumption here is that there is no correlation between age-since-infection and contact pattern.

### 2.4.3 Age-structured infection pressure in the fully separable transmission case

Here, we consider a transmission rate which is separable respect to age-since-birth for people involved under the assumption of fully random mixing contact pattern. Such transmission pattern is suitable in male homosexual population under the bathhouse assumption [41, 79], meaning all the contacts were fairly indiscriminate, casual and promiscuous. We performed numerical experiment for HIV restricted for this subgroup of population. This is a study

of importance since 97% the new grow of AIDS cases in the United State are in this group according to database provided by the CDC in 2010. Hence, given the population being uniformly distributed with respect to age since birth, for our simulation we suppose

$$\Theta(a, a_I) = \xi(a)\xi(a_I), \quad (2.4.7)$$

where  $\xi(\cdot)$  represent the contact rate counting as partner acquisition rate in the population with respect to age-since-birth. Here, we also take into account that infected people may progress with HIV at different speeds, which satisfy a normal distribution  $\mathcal{N}(7.5, 1)$  to get the relative infectivity  $\phi(z)$  from the viral load data of HIV [79]. An example solution of this type is listed in Figure 2.4 and Figure 2.5.

For this separable transmission rate case, the steady state infection pressure Eq. (2.3.10) can be reduced to

$$\tilde{\lambda}(a) = \xi(a) \int_0^{a_{\max}} \int_0^{a_I} \xi(a_I) \phi(z) I(a_I, z; \tilde{\lambda}(a_I - z)) dz da_I. \quad (2.4.8)$$

Hence, we can conquer the task similar as previous by reforming the infection pressure as  $\tilde{\lambda}(a) = A \cdot \xi(a)$ . The interfere of disease free equilibria can be automatically eliminate by noticing that constant A satisfies

$$\begin{aligned} & \int_0^{a_{\max}} \int_0^{a_I} \xi(a_I) \phi(z) \xi(a_I - z) \sigma(\bar{c}_S(a_I - z)) \\ & \times r e^{-\int_0^{a_I-z} A \xi(\tau) \sigma(\bar{c}_S(\tau)) + \mu(\tau) d\tau} e^{-\int_0^z \gamma(a_I - z + \tau) d\tau} dz da_I = 1. \end{aligned} \quad (2.4.9)$$

Define the right hand side of Eq. (2.4.9) as function of  $A$ , denote as  $G(A)$ . Similar to the previous part, we state the following conclusions regarding disease transmission leaving the details in the Appendix B.

Define basic reproduction number  $R_0 = G(0)$  as

$$\begin{aligned} R_0 & \doteq \int_0^{a_{\max}} \int_0^{a_I} \xi(a_I) \phi(z) \xi(a_I - z) \sigma(a_I - z, \bar{c}_S(a_I - z)) \\ & \times r e^{-\int_0^{a_I-z} \mu(\tau) d\tau} e^{-\int_0^z \gamma(a_I - z + \tau) d\tau} dz da_I. \end{aligned} \quad (2.4.10)$$

If  $R_0 < 1$ , there exist an unique disease-free equilibrium for the dynamic which is also stable. If  $R_0 > 1$ , there exist an unique endemic equilibrium, together with the unstable disease-free equilibrium. Numerical results by iterative method indicate the endemic equilibrium is stable, but no rigorous proof is achieved yet.

Although, the best response equation Eq. (2.4.3) yields a uniquely defined  $c_S^B(a; \tilde{\lambda}(a))$  as solution, we still have hard time proving the uniqueness of the endemic Nash equilibria. However, the fact that the disease-free infection pressure being unstable and the uniqueness of the endemic infection pressure  $\tilde{\lambda}(a)$  guarantee that our numerical solution is the unique game equilibria as long as the numerical solution converge.

#### 2.4.4 Age-structured infection pressure in the non-separable transmission case

As mentioned earlier, the random mixing pattern can be applied in certain community, however, once the population is stratified by sex, age and maybe further activity class it is necessary to consider assortative mixing within and between the different strata of the population. Here we investigate a general transmission case, where the contact pattern is non-separable to address the assortative mixing. But we still restrict our model without differentiate sex and activity classes. Suppose the transmission rate takes the form of

$$\Theta(a, a_I) = \frac{\max\{0, 1 - k(a - a_I)^2\}}{\int_0^{a_{\max}} \max\{0, 1 - k(a - a_I)^2\} da_I} \xi(a) \xi(a_I) \bar{\beta}, \quad (2.4.11)$$

where  $\xi(\cdot)$  represent the contact rate counting as partner acquisition rate in the population with respect to age-since-birth, parameter  $k$  represents the assortativity of mixing with respect to age-since-birth and  $\bar{\beta}$  is a constant to rescale transmission rate between per contact and per partner. Here, we still assume people mixed randomly within the preferred age range for both susceptibles and infected people. An example solution of this type is listed in Figure 2.7 and Figure 2.8.

When the transmission rate is still separable between contact pattern and age-since-infection, the steady state condition given by Eq. (2.3.10) yields

$$\begin{aligned} \tilde{\lambda}(a) = \int_0^{a_{\max}} \Theta(a, a_0) \tilde{\lambda}(a_0) \sigma(c_S(a_0)) r e^{-\int_0^{a_0} \tilde{\lambda}(\tau) \sigma(\tau, c_S(\tau)) + \mu(\tau) d\tau} \\ \times \left\{ \int_0^{a_{\max} - a_0} \phi(z) e^{-\int_0^z \gamma(a_0 + \tau) d\tau} dz \right\} da_0. \end{aligned} \quad (2.4.12)$$

Due to the complexity of the transmission rate, there is no theoretical analysis regarding the existence and uniqueness of the endemic state for the disease transmission dynamic, let alone the endemic game equilibrium. Unlike the fully separable case which can be reduced to the scalar case shown in Eq. (2.4.8), the general transmission kernel lacks the needed symmetry. However, our numerical simulation shows the possible existence of the unique endemic game equilibrium by approaching it with fix point iteration as the the general nonlinear solver. Like most iterative algorithm, our algorithm is sensitive with respect to the initial guess as well. For random initial guess, the algorithm easily converge to the disease free steady state. Notice that the general kernel given by Eq. (2.4.11) is related to the separable kernel Eq. (2.4.7), we suggest the homotopy approach by taking the solution of the corresponding fully separable case as the convenient initial guess. For arbitrary kernel, homotopy approaches (ref.) may be suggested.

## 2.5 Results and analysis

The following figures illustrate example solutions of epidemic game with separable and non-separable transmission case. At the game equilibrium, Individuals are better off adapting

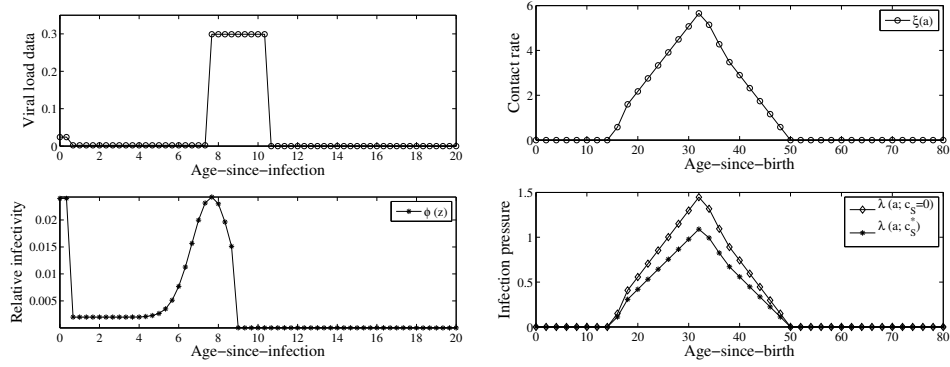


Figure 2.4: Parameterization of fully separable transmission rate and an example solution of steady state infection pressure at game equilibrium. On the left is the plot for Viral loads and relative infectivity. Variation in viral loads over the course of a typical untreated individual's HIV infection [3]. On the right list the contact rate [41] and the steady state infection pressure at game equilibrium. The age period of being sexually active matches the age range associates with positive risk of infection pressure. The correlation of the magnitude of the two shows that the infection pressure has the approximate shape of the contact rate which may only up to rescaling.

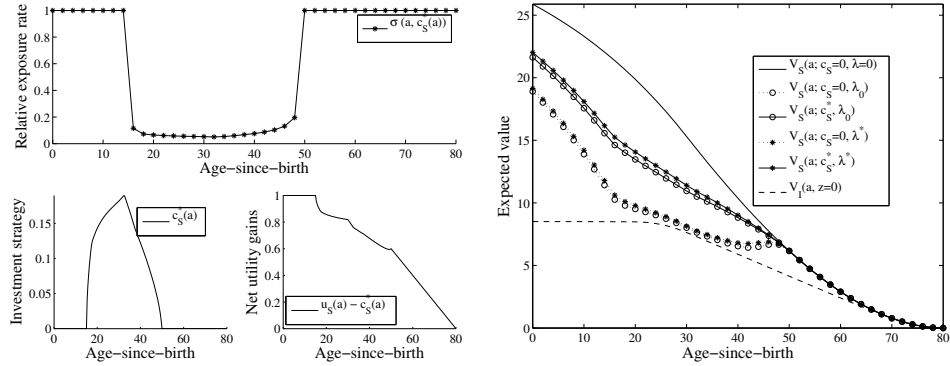


Figure 2.5: Example game solution when the transmission rate is fully separable and the infection pressure is independent of age. Upper left plot shows the rational behavior  $\sigma(c_S^*)$  with steady state infection pressure  $\lambda^*(a)$  shown in figure 2.4 at game equilibrium where transmission rate  $\beta$  is defined in Eq. (2.4.6). The corresponding investment strategy and net utility gain are listed on the bottom. Plot on the right illustrated expected values for infected people  $V_I(a, 0)$  and susceptible people  $V_S(a)$  adapting different strategies when facing different steady state infection pressures, where  $\lambda_0$  stands for steady state infection pressure when no one makes investment and  $\lambda^*$  represent the game equilibrium infection pressure. The comparison shows drastic increase of expected value for susceptible people by engaging in the rational behavior when facing the endemic.

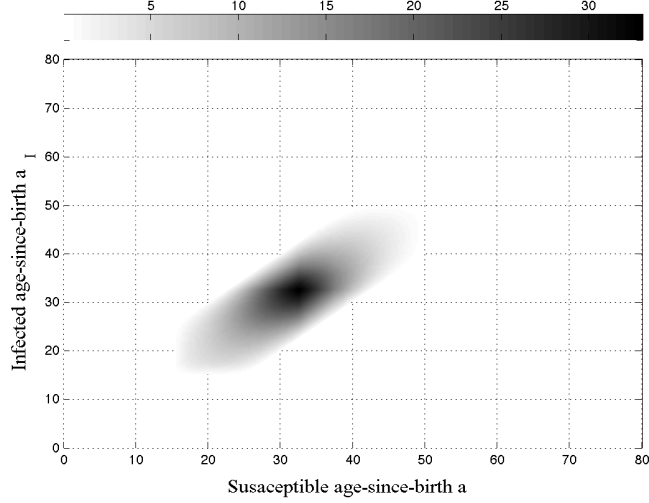


Figure 2.6: Parameterization of non-separable transmission rate defined in Eq. (2.4.11). This plot shows the contact pattern of assortative mixing, where  $k = 0.01$  and  $\beta = 40$ . Relative infectivity  $\phi(z)$  is the same as in Figure 2.4.

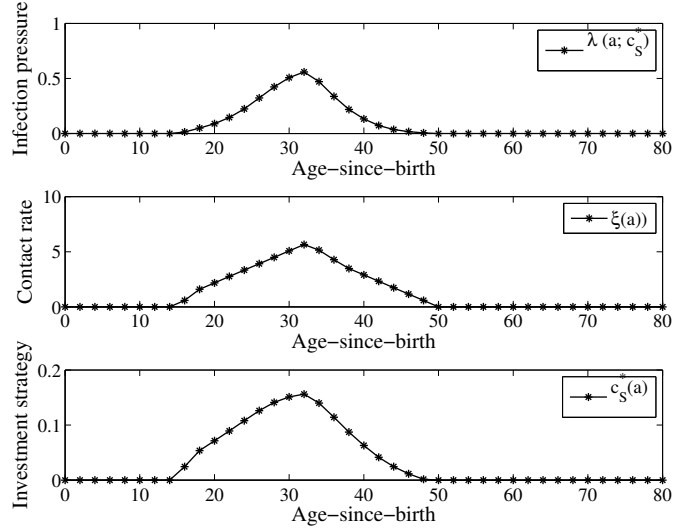


Figure 2.7: Example steady state infection pressure at game equilibrium. These plots illustrate the steady state infection pressure at game equilibrium (top) as well as the contact rate (middle) [41] and equilibrium investment strategy (bottom). The age period with positive risk of infection pressure shows correlation with age being sexually active, while the changes in magnitude of the two are not exactly synchronized. But changes seem more at the same pace as shown in the investment strategy and the infection pressure.

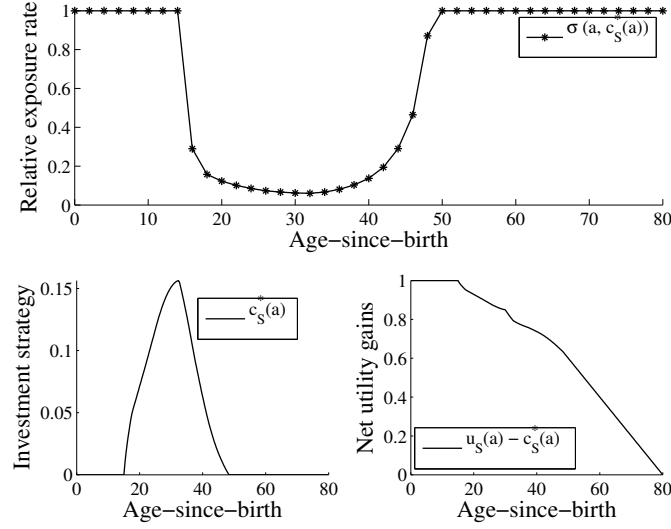


Figure 2.8: Example solution of the population game with non-separable transmission rate and age-dependent infection pressure. The upper plot shows the rational behavior  $\sigma(c_S^*(a))$  with steady state infection pressure  $\lambda^*(a)$  at game equilibrium for transmission rate defined in (2.4.11). The corresponding investment strategy and net utility gain are listed on the bottom.

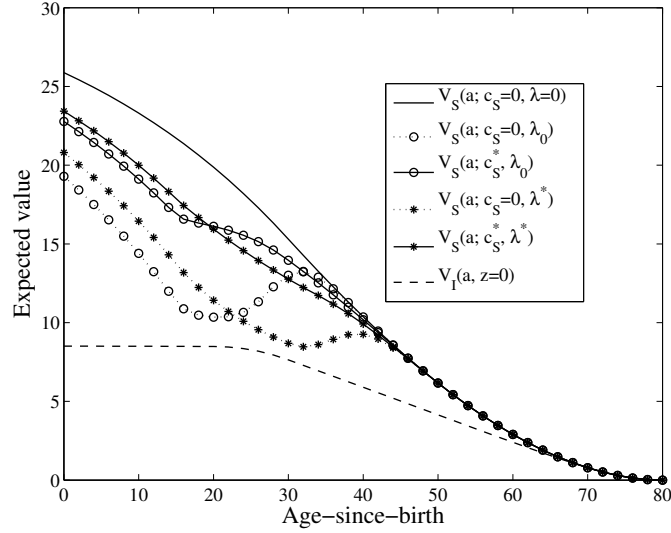


Figure 2.9: Expected values for the example solution of the population game with non-separable transmission rate and age-dependent infection pressure. This plot illustrates expected values for infected people  $V_I(a, 0)$  and susceptible people  $V_S(a)$  adapting different strategies when facing different steady state infection pressures, where  $\lambda_0$  stands for steady state infection pressure when no one makes investment and  $\lambda^*$  represent the game equilibrium infection pressure. The comparison shows drastic increase of expected value for susceptible people by engaging in the rational behavior when facing the endemic.

the game equilibrium strategy compare to laissez-faire strategy where one does not make investment.

In comparison of the two predictive infection disease model, we observe that: At the game equilibrium, people spend more in the fully separable transmission model Eq. (2.4.7) than in the assortative mixing model represented by our general non-separable transmission case Eq. (2.4.11), where the assortativity is more concentrated around the age of high risk. Besides, people are more strongly mixed in the separable model, where the risk and the investment are more even across the ages. Young people in the assortative mixing model engaged in more activities among people with similar age, so they face lower risk compare to the separable case where the partners are evenly distributed across age. Because of the higher average number of partners in separable fully random mixing model, young people would have higher risk of infection. If one decide to take no action, the expected value will be a lot less which could be even close to the case of being infected. However, one should keep in mind that the result is generalized from the fully separable transmission model with the bathhouse assumption, which count per new partner as per activity at risk. Previous research shows couples have less risk of HIV transmission even one party is infected, see [51]. Therefore, one can manage risk by reducing number of switch in partners.

## 2.6 Discussion

It has been the purpose of this paper to model epidemic games with behavior changes as the premier choice of disease prevention and to address the computational aspects of such matters in the proposed generalized  $SI$  model with continuous age structure which also tracking the time since infection continuously. The efficient and precise algorithms for computing game equilibrium strategy has real-world meanings. In our paper we elaborated how to formulated and solve a model of social behavior in a HIV-like epidemic. Designing a rational response to an epidemic at its steady state can depend on determining infection pressure as we have discussed. Our results place an emphasis on the search for efficient and quick methods that give good approximations when applied to real-world problems such as HIV. Result of simulation support one's intuition. But theoretical analysis of such game equilibrium still remains as open questions, along with the question regarding endemic steady state analysis of the disease dynamics for general transmission kernel. It would be great to draw the attention of both mathematicians and epidemiologists to such questions in order to move forward. Further work will be applying our model for analyze potential impact of different interventions and the model could be generalized to incorporate more heterogeneous structures, such as various activity level groups combine with more complicated mixing pattern.

## Chapter 3

# Social planner problem of disease reservoir in an epidemic

Public policies intended to induce behavioral change, specifically incentives to reduce inter-personal contacts or to build up medical facilities, play a prominent role in public disease response strategies when facing major epidemics. Elementary theories consider strong mixing hypotheses, but spatial segregation can strongly influence transmission patterns and potentially policy design [1]. In this work, we explore the impact of spatial heterogeneity on infectious disease management policy. Different from social planner results usually published, we not only compare desired policy and outcomes under central and decentralized social planner conditions, but also provide rigorous mathematical analysis regarding the controllability and corresponding model adjustment. Optimality conditions are derived for the controlled social planner case with an efficient numerical algorithm proposed. Our results provide insight into epidemic control that each individual and the government are forced to engage in, especially the rational behavior which could be advised to the public. On the other hand, our work also apply to the case of controlling the infectious disease of plant as well as how to better manage potentially spread a product or idea throughout the population with spatial heterogeneity.

### 3.1 Introduction

Disease reservoirs from animals and other environmental sources present a risk to human populations. A systematic literature survey [95] suggests that many new species of human pathogens have a global distribution and are mostly associated with human interactions with spatially segregated animal or environmental reservoirs.

Disease reservoirs are important and often spatially separated from large human communities to which they pose the highest risk. Take dengue fever as an example. It is transmitted to people by the bite of a dengue virus infected *Aedes* mosquito but cannot be spread directly from person to person [2]. Monkeys may serve as a reservoir in some parts of Asia and Africa[48]. Similar examples are current Ebola epidemic and Cholera epidemic [77, 93]. In the geographic analysis of disease transmission, infection risks decrease as the



distance from reservoirs increase and infected individuals decreases [17]. If we want to design efficient disease controls that reduce risk to communities, we should take into account this spatial structure.

There exist various spatial epidemiology models. Popular approaches to spatial epidemiology include models that involve actual geographical entities and those do not. The explicit spatial approach include mapping the spatial distribution of infectious diseases based on distributions of vectors, reservoirs and disease incidence [17]. A variety models have been used, such as lattice models [68, 92, 35], individual-based model [49], continuous space models represented by diffusion equations [27, 34, 55, 71], integro-differential equations [69, 83] and integro-difference equations [54, 62, 85]. Spatial structure can also be incorporated implicitly as in network models [13, 36, 73] and metapopulation models [65, 46, 86]. More detailed reviews on spatial epidemiology can be found in [17, 46, 47, 49, 67, 75].

People have studied the optimal control of spatially structured epidemics, but not the management of the on-going risk from disease reservoirs. Regarding the application of disease control, optimal control theory has been use to model epidemic scenarios in previous work [7, 63]. The types of control functions imposed in the objective functional, vary between linear ('bang-bang') control [15, 62] and the usual quadratic [18, 54, 74] form to guarantee the existence of the optimal solution. But here we look into the case where a switching cost term is present as penalty in the objective functional.

Our goal is to characterize the most cost-effective spatially-explicit strategy for local reductions in disease transmission rate at steady state epidemic. In this paper, we take the distributed-contact approach to study the continuous spatiotemporal spread of disease among a population of susceptible ( $S$ ) and infected ( $I$ ) individuals in presence of a disease reservoir. Our result shows that chattering effect of the control may happen when there are no switching penalty in the objective cost functional. With the switching costs, we can construct suitable optimal strategy for various epidemic scenarios.

In Section 2, we present the model in a general framework and form the associated optimal control problem. Principles in optimal control theory are applied in Section 3 and 4 to characterize the optimal strategy. For illustration, Sections 5 to 7 provide numerical approximations of optimal spatial strategies with various epidemic parameters. Discussion and conclusion are provided at the end.

## 3.2 Integral kernel model and model adjustment

To investigate the control problem of the disease transmission when a disease reservoir is near the susceptible community, we simplify the problem to model the space as a finite interval. This is suitable when the region where the disease put risk on is large. And the disease reservoir is indeed bounded in a region near the population. For the disease transmission model, notice that numerous infectious disease confer no long-term immunity, we take the SIS model with constant total population.

In the model problem, we consider an uniformly distributed homogeneous population on one-dimensional finite spatial space represented by  $\Omega = [-1, 1]$ . Let  $S(x, t)$  be the density of susceptible and  $I(x, t)$  represent infected people respectively in location  $x$  at time  $t$ . To introduce the spatial structure, see [19, 75], we assume the background transmission

rate at location  $x$  to be  $\eta(x)$ , where  $\eta(x) \in [0, \bar{\eta}]$  is a decreasing function representing the disease reservoir, and the recovery rate of the infected people to be  $\gamma$ . The population-scale disease-transmission dynamics is governed by

$$\frac{\partial I}{\partial t} = [\eta(x) + \lambda(x, t)]S(x, t) - \gamma I(x, t), \quad (3.2.1a)$$

$$\frac{\partial S}{\partial t} = -\frac{\partial I}{\partial t}, \quad (3.2.1b)$$

$$I(x, 0) = I_0, I_x(-1, t) = I_x(1, t) = 0, \quad (3.2.1c)$$

$$S(x, 0) = 1, \quad (3.2.1d)$$

$$S(x, t) + I(x, t) = 1. \quad (3.2.1e)$$

Under the distributed-contacts hypothesis [83], approximate infection pressure  $\lambda(x, t)$  for any give time  $t$  as  $\lambda(x, t) = \int_{\Omega} \kappa(x, y)I(y, t)dy$ , where  $\kappa$  is the distributed contact kernel.

Consider the steady state density of the infected  $I(x)$ , as detailed in [72], with isotropic kernels [i.e.,  $\kappa(\Delta) = \kappa(-\Delta)$ ], one have the following

$$[\eta(x) + \alpha I_{xx} + \beta I](1 - I) - \gamma I = 0, \quad (3.2.2)$$

where  $\alpha = \langle \Delta^2 \rangle / 2 = \int_{\Omega} \Delta^2 \kappa(\Delta) d\Delta$  is the positive diffusion coefficient. This type of model was first proposed in [75].

Consider the distributed control function denote as

$$\sigma(a, u(x)) = \exp\{-a u(x)\}, \quad (3.2.3)$$

where the investment  $u(\cdot)$  is nonnegative and uniformly bounded from above by  $M$ , and parameter  $a$  represent the effectiveness of the strategy  $u(\cdot)$  in reducing the transmission. The steady state population-scale disease-transmission dynamics is now governed by

$$e^{-a u(x)}[\eta(x) + \alpha I_{xx} + \beta I](1 - I) - \gamma I = 0, \quad (3.2.4a)$$

$$I_x(-1) = I_x(1) = 0. \quad (3.2.4b)$$

Given the approximated stationary modified infection pressure  $\tilde{\lambda}(x) \approx e^{-a u(x)}(\alpha I_{xx}(x) + \beta I(x))$ , define the expected accumulated payoff as a functional of a chosen investment strategy  $u(\cdot)$  as  $\mathcal{J}(u; I)$ , we reformulate our best planner's problem as a minimization problem,

$$\min_{u(x) \in [0, M]} \mathcal{J}(u(x); I(x)) \quad (3.2.5a)$$

$$e^{-a u(x)}[\eta(x) + \beta I + \alpha I''] (1 - I) - \gamma I = 0, \quad (3.2.5b)$$

$$I'(-1) = I'(1) = 0. \quad (3.2.5c)$$

In this paper, we will focus on the analysis of System (3.2.5) with a proper choice of  $\mathcal{J}(u; I)$ .

Symbol	Interpretation
$S(x, t)$	density of susceptible people at location $x$ and time $t$
$I(x, t)$	density of infected people at location $x$ and time $t$ with age-since-infection $z$
$\eta(x)$	background transmission rate (per person per unit time) of the population at location $x$
$\lambda(x, t)$	the infection pressure of the population at location $x$ and time $t$
$\gamma$	recovery rate (per unit time) of infected people
$\alpha$	the spatial diffusion parameter (utility per unit time)
$\beta$	transmission rate per infected individual to susceptibles (per person per unit time)
$u(x)$	the investment strategy at location $x$ (utility per unit time)
$a$	the scaling factor for effectiveness of the strategy in reducing the transmission rate (dimensionless)
$c$	the expected utility costs per unit time of being infected
$\epsilon$	the weight of the penalty term for switching in the objective functional

Table 3.1: List of all symbols used in System (3.3.5).

### 3.3 Analysis for the planner's problem

Equation in (3.2.4) is the steady state condition for solutions of the nonlinear heat equation (3.2.1). Although it is hard to give general solutions of this nonlinear equation, we still could conduct sufficient analysis for solutions in the region of our interest  $I(x) \in [0, 1]$  due to the biological meaning of our model variables.

**Lemma 1.** For every solution  $I(x) \in H^1([-1, 1])$  of the steady-state equation in (3.2.5):  $I(x) \neq 1$ , for all  $x \in [-1, 1]$ , provided the parameter  $\gamma \neq 0$ .

*Proof.* Suppose there exist a point  $x_0 \in [-1, 1]$  with  $I(x_0) = 1$ . Notice that  $I(x) \in H^1([-1, 1])$  and plug  $I(x_0) = 1$  into the Eq. (3.2.5), then  $-\gamma = 0$ , which contradict to our assumption that  $\gamma \neq 0$ .  $\square$

This result suggests that we can try to prove that there is a positive solution  $I(x) \in (0, 1)$ , since the solution will never cross  $I(\cdot) = 1$ . We believe that with an adequate initial guess  $I_0(x) \in (0, 1)$ , the steady state solution won't intersect or be larger than  $I(\cdot) = 1$ .

#### 3.3.1 Existence of steady state solution of disease dynamic

The steady state conditions for the disease dynamic equation specify a two point boundary value problem for a system of differential equations. Generally, the existence of solutions to such problems must be handled on a case-by-case basis. Therefore, we rewrite Eq. (3.2.4)

as

$$\alpha I''(x) \doteq F(x, I(x)) = e^{a u(x)} \gamma \frac{I(x)}{1 - I(x)} - \beta I(x) - \eta(x), \quad (3.3.1a)$$

$$I'(-1) = I'(1) = 0. \quad (3.3.1b)$$

Without lost of generality, we assume  $\alpha = 1$ .

Here, we give the condition for the parameters value to guarantee the existence of steady state solution of the disease dynamic equation (3.3.1). For the detailed proof and computation, we refer to Appendix A.

**Theorem 2.** Suppose all the parameters in Eq. (3.3.1) are non-negative,  $\eta(x)$  continuous and there exist  $\bar{\eta} > 0$  such that  $0 \leq \eta(x) \leq \bar{\eta}$ . Then, there exist solution  $I(x) \subset [0, 1]$  of Eq. (3.3.1), provided the non-negative control function  $u(x) \in \mathcal{C}([-1, 1])$  or if  $u(x)$  is bounded on  $\Omega$ .

*Proof.* We take the upper and lower solution approach, see [33] for detailed definition. To simplify the problem, one can check that

$$\mu_{upper} \doteq -\frac{\bar{\eta} - \beta + \gamma}{2\beta} + \sqrt{\left(\frac{\bar{\eta} - \beta + \gamma}{2\beta}\right)^2 + \frac{\bar{\eta}}{\beta}}, \quad \text{and} \quad \mu_{lower} \doteq 0, \quad (3.3.2)$$

are constant upper and lower solutions respectively of Eq. (3.3.1). To verify that  $\mu_{upper} < 1$ , we can take square of both said of the rearranged  $\sqrt{\left(\frac{\bar{\eta} - \beta + \gamma}{2\beta}\right)^2 + \frac{\bar{\eta}}{\beta}} < 1 + \frac{\bar{\eta} - \beta + \gamma}{2\beta}$ . After canceling the same terms, the only requirement for the inequality to hold is  $\gamma > 0$ , which is naturally satisfied by the model set up. Therefore, there exist an solution  $I(x) \in [\mu_{lower}, \mu_{upper}] \subset [0, 1]$ . To see these, we only need to show that  $\mu_{upper}$  indeed is an upper solution. Suppose we have a possible constant upper solution  $\mu$ ,

$$\mu'' = 0 \leq F(x, \mu) = e^{a u(x)} \gamma \frac{\mu}{1 - \mu} - \beta \mu - \eta(x).$$

Then,  $\mu$  only need to satisfy

$$0 \leq F(x, \mu; u = 0, \eta = \bar{\eta}) = \gamma \frac{\mu}{1 - \mu} - \beta \mu - \bar{\eta}. \quad (3.3.3)$$

Notice that the first term in the right hand side is a hyperbola, with coefficient  $\gamma > 0$ , we can always find  $\mu \in (0, 1)$  big enough to over come the linear negative terms in condition (3.3.3), which in particular being  $\mu = \mu_{upper}$ .  $\square$

### 3.3.2 Existence of the optimal control with penalty term

To construct the expected accumulated payoff  $\mathcal{J}$  as a functional of a chosen investment strategy  $u(x)$ . One can always rescale the cost for the control  $u(\cdot)$  as unit price. Then the cost of being sick can be assume to be a positive constant  $c$ , which is independent of the location  $x$ , To account the potential costs of control strategy switching, we introduce the

term  $u_x^2(\cdot)$  as a penalty term for building various facilities with a positive relaxed weight coefficient  $\epsilon > 0$ . Finally, we can formulate the expected accumulated payoff  $\mathcal{J}$  as

$$\mathcal{J}^\epsilon(u; I) \doteq \int_{-1}^1 c I(x) + u(x) + \frac{\epsilon}{2} (u'(x))^2 dx, \quad (3.3.4)$$

where we naturally assume the cost of being sick  $c > 0$  is a constant independent of the location. Finally, we reformulate our best planner's problem as a minimization problem,

$$\min_{u(x) \in [0, M]} \mathcal{J}^\epsilon(u; I) = \int_{-1}^1 c I(x) + u(x) + \frac{\epsilon}{2} (u'(x))^2 dx, \quad (3.3.5a)$$

$$e^{-a u(x)} [\eta(x) + \beta I + \alpha I''] (1 - I) - \gamma I = 0, \quad (3.3.5b)$$

$$I'(-1) = I'(1) = 0. \quad (3.3.5c)$$

In order to prove the existence of an optimal pair  $x \mapsto (u^*(x), I^*(x))$  of our control problem. We prove first the convergence of the minimizing sequence in Lemma 3. Then we show there is some corresponding solution sequence  $I_n$ , which converge to  $I^*$ . At the end, we show there exist an optimal pair  $(u, I)$  in Theorem 4.

**Lemma 3.** Suppose  $\{u_n\}$  is the minimizing sequence of the admissible control for the steady state optimization problem (3.3.5), then there exist admissible control  $u$  such that  $u_n \rightarrow u$  uniformly on  $L^2([1, 1])$ .

*Proof.* Notice that the penalty term of  $u'$  guarantee that there is a constant  $C$  such that

$$\int_{-1}^1 (u')^2 dx \leq C. \quad (3.3.6)$$

Constant  $C$  can be constructed from any minimizing sequence  $\{u_n\}$  since  $u$  is supposed to be the minimizer. By the Poincar inequality [37],  $u_n \in H^1([-1, 1])$  and  $u'_n \in L^2([-1, 1])$ .  $u_n$  is Hölder continuous with Holder constant  $1/2$  [37]. Hence,  $u_n \rightarrow u$  uniformly on  $L^2([-1, 1])$ .  $\square$

For any given control  $u_n$ , pick one  $I_n$  that solves:

$$\alpha I'' = e^{a u_n(x)} \gamma \frac{I_n}{1 - I_n} - \beta I_n - \eta(x), \quad (3.3.7)$$

$$I'(-1) = I'(1) = 0, \quad (3.3.8)$$

which has the minimal  $\mathcal{H}^\epsilon(u_n, I_n)$ .

Without the penalty term, notice that if control  $u_n(x) \in [0, \bar{u}]$  is uniformly bounded, we consider directly  $\sigma_n = \sigma(u_n) = \exp a u_n$ . So,  $\sigma_n \in [\delta, 1]$  where  $\delta > 0$ . Then  $\int_{\Omega} -\frac{1}{a} \ln \sigma(u_n) dx$  is bounded. Hence  $\sigma_n, 1/\sigma_n \in L^\infty([-1, 1])$ ,  $\sigma_n \rightharpoonup \sigma, 1/\sigma_n \rightharpoonup 1/\sigma$  weakly. On the other hand, there exist constant  $C_0 > 0$ , such that  $\|I''(x)\| < C_0$ . Then  $I' \in \mathcal{C}([-1, 1])$  and  $I_n \rightarrow I$  uniformly.

**Theorem 4.** There exist an optimal pair  $(u, I)$  in  $L^2([-1, 1])$  for optimization problem (3.3.5).

*Proof.* Given the convergence of the minimizing sequence  $\{u_n\}$  and the corresponding  $\{I_n\}$ , we need to show that for the pair  $(u, I)$ ,  $I$  satisfies same equation Eq. (3.3.7) with  $u$ . Consider Eq. (3.3.7) in a different form

$$\alpha I'_n(x_2) - \alpha I'_n(x_1) = \int_{x_1}^{x_2} e^{a u_n(\nu)} \gamma \frac{I_n(\nu)}{1 - I_n(\nu)} - \beta I_n(\nu) - \eta(\nu) d\nu, \quad (3.3.9)$$

Since  $1/\sigma_n \rightharpoonup 1/\sigma$  weakly, which means  $e^{a u_n} \rightharpoonup e^{a u}$  weakly, and  $I_n \rightarrow I$  uniformly, we can pass the limit into the integral. Hence, then pair  $(e^{a u}, I)$  satisfy Eq. (3.3.7). Notice that our objective function  $\mathcal{H}_\epsilon$  is lower semicontinuous due to the convexity, we have  $(u, I)$  is an optimal pair for the problem (3.3.5).  $\square$

### 3.4 Optimality condition for the optimal control

Recall our optimal control problem (3.3.5). We denote the state equation (3.3.1) as  $C(I, u) = 0$ , which is the appropriate formulation of the steady state solution of our PDE with initial data in the domain  $\mathcal{B}$  that guarantee existence of solution defined in Theorem 2. We can now state our PDE-constrained optimization problem of the form

$$\min_{I \in \mathcal{B}, u \in U} \mathcal{J}^\epsilon(I, u) \quad \text{subject to} \quad C(I, u) = 0. \quad (3.4.1)$$

Here  $u \in U$  is the control living in a Banach space  $U$ .

The Lagrangian function for (3.4.1) is given by

$$\mathcal{L}(I, u, f) = \mathcal{J}^\epsilon(I, u) + \langle f, C(I, u) \rangle. \quad (3.4.2)$$

By standard optimality theory we obtain the following result, see details in Appendix.

**Proposition 3.4.1.** Assume that  $\mathcal{J}^\epsilon : \mathcal{B} \times U \rightarrow \mathbb{R}$ ,  $C : \mathcal{B} \times U \rightarrow \mathcal{B}$  are continuously differentiable. If  $(I, u)$  is a local solution of (3.4.1), then there exists a Lagrange multiplier (adjoint state)  $f \in \mathcal{B}^*$  with

$$\mathcal{L}_I(I, u, f) = \mathcal{J}_I^\epsilon(I, u) + (C_I)^*(I, u)f = 0 \quad (\text{Adjoint equation}), \quad (3.4.3a)$$

$$\mathcal{L}_u(I, u, f) = \mathcal{J}_u^\epsilon(I, u) + (C_u)^*(I, u)f = 0 \quad (\text{Stationarity equation}), \quad (3.4.3b)$$

$$C(I, u) = 0 \quad (\text{State equation}). \quad (3.4.3c)$$

To be precise, we have adjoint equation

$$-\alpha f'' + (-\beta + e^{au} \gamma \frac{1}{(1-I)^2})f + c = 0, \quad f'(-1) = f'(1) = 0, \quad (3.4.4)$$

Stationarity equation

$$-ae^{au} \gamma \frac{I}{1-I} f + 1 - \epsilon u'' = 0, \quad u'(-1) = u'(1) = 0, \quad (3.4.5)$$

and State equation at the steady state of the disease dynamic

$$e^{-au} [\eta + \beta I + \alpha I_{xx}] (1 - I) - \gamma I = 0, \quad (3.4.6a)$$

$$I(0, x) = I_0 \in \mathcal{B}, \quad I_x(t, -1) = I_x(t, 1) = 0. \quad (3.4.6b)$$

**Remark.** Similarly, we can consider the distributed control function where  $\sigma(a, u(x)) = \exp\{-a u(x)\}$ . affecting only the infection pressure  $\lambda(t, x)$ , which modify the infection pressure as  $\sigma(x)\lambda(t, x)$ . Then the optimization problem will be modified as

$$\min_{u(x) \geq 0} \mathcal{J}^\epsilon(u; I) = \int_{-1}^{+1} c I(x) + u(x) + \frac{\epsilon}{2} u_x^2(x) dx, \quad (3.4.7a)$$

$$[\eta(x) + e^{-a u(x)}(\beta I(x) + \alpha I_{xx}(x))](1 - I(x)) - \gamma I(x) = 0, \quad (3.4.7b)$$

$$I_x(-1) = I_x(1) = 0. \quad (3.4.7c)$$

Then, we can follow similar argument to proof the existence of optimal pair for this modified problem and derive the corresponding optimality conditions.

### 3.5 Numerical algorithm and results

The general principle for computing the desired optimal control is iteratively adopting Newtown's method. Here we present a brief description of the computation step. For detailed algorithm, see Appendix B.

**Algorithm 1. (Numerical algorithm).**

Input: parameters for the disease dynamic and initial guess of the control.

Output: the optimal control and the associated infected population.

Given: Tolerance level for accuracy,

1. Compute  $I(u)$ ,  $\mathcal{H}(u)$  for the current guess  $u$ .
2. Compute an adjoint state  $f$ .
3. Check if  $u$  and  $I(u)$  is KKT point.
4. Compute the tangential step  $\delta u$  from Eq. 3.4.5.
5. Update  $u$  if needed.

#### Analysis of parameters in the disease dynamic

First, we investigate the influence of background infection rate when no control function is at present, see Figure. 3.1. With minor disease invasion force  $R_0 < 1$ , we still see the spread of disease from the reservoir. The higher the background infection rate  $\eta_{max}$ , the wider and higher infection outside the boarder of reservoir.

Besides the dominating effect of the disease invasion force which was represented by the basic reproduction number, we also notice from Figure. 3.2 that the diffusion parameter determines how wide the disease will spread outside the disease reservoir, even when the disease transmission is minor factor  $R_0 < 1$ .

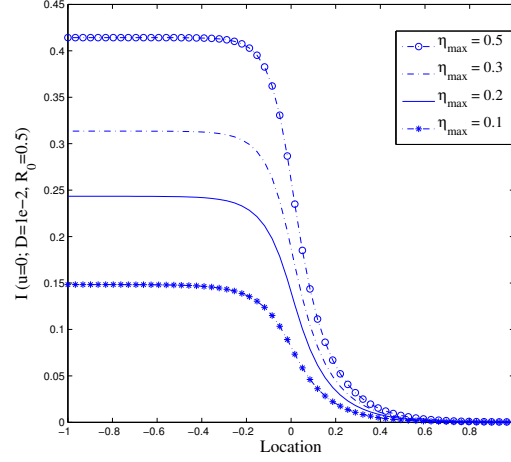


Figure 3.1: Example solutions regarding various background infection rate of disease reservoir without control function.

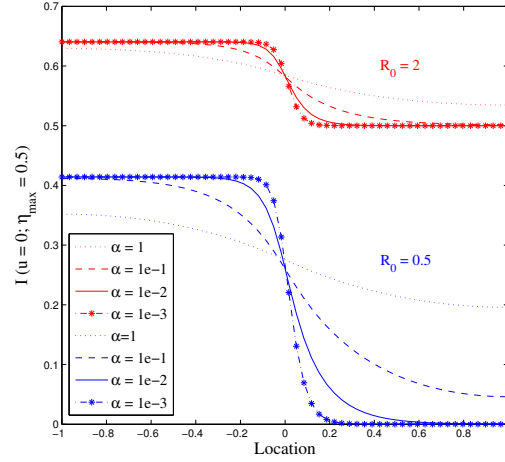


Figure 3.2: Example solutions regarding various basic reproduction number  $R_0$  and diffusion rate  $\alpha$  of disease reservoir without control function. Additional parameters used  $a = 10$ ,  $c = 1$ , and  $\gamma = 1.0$ .

### Optimal control and the cost under various diffusion coefficients

Knowing the basic row of the background parameters in the disease dynamic, we consider the efficiency of our optimal control. By observing Figure. 3.3 and Figure. 3.4, our algorithm is robust for a wide range of parameters. The computed optimal control sufficiently reduced the infected population. With continuously applied optimal control, the disease can be almost confined within the disease reservoir, provided the diffusion remain small.



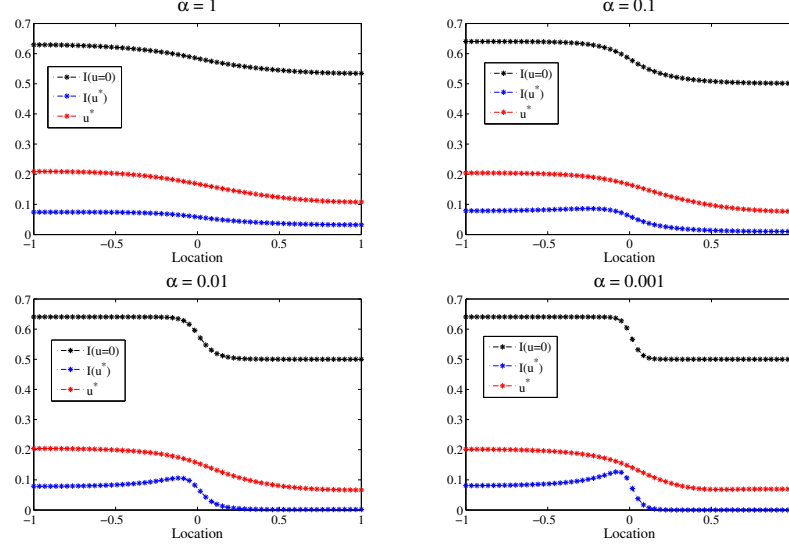


Figure 3.3: Sample solution for the model problem based on various diffusion coefficients  $\alpha$  at  $R_0 = 2, a = 10$  and  $\eta_{max} = 0.5$ .

In Figure. 3.5, one can observe the sufficient improvement of the total cost by adapting the optimal control.

### Influence of the basic reproduction number on the optimal control

The basic reproduction number  $R_0$  dominant the disease spread in the whole area without control, see fig:RInf. However, by compare Figure. 3.3 and Figure. 3.4 accordingly, we can still find the optimal control to reduce the disease spread out of the reservoir if the diffusion is relatively small, as also shown in Figure. 3.6.

## 3.6 Chattering effect analysis as $\epsilon \rightarrow 0$

Here, in Figure. 3.7, we demonstrate numerically the important role of the introduced penalty term in the cost functional defined in Eq. (3.3.5).

As the weight of the penalty term decrease to zero, one has the linear expected accumulated payoff  $\mathcal{J}(u(x); I(x))$  would be

$$\mathcal{J}(u; I) \doteq \int_{-1}^1 c I(x) + u(x) dx. \quad (3.6.1)$$

For the original nonlinear control problem (3.3.1), the set of velocities may not be convex. If  $u(x) \in [0, M]$ , it may sometime be convenient to chatter between  $u = 0$  and  $u = M$ . In the following, we show such chattering effect may happen with this linear payoff. This leads to replace Eq. (3.3.1) with the chattering system, which is linear with respect to the

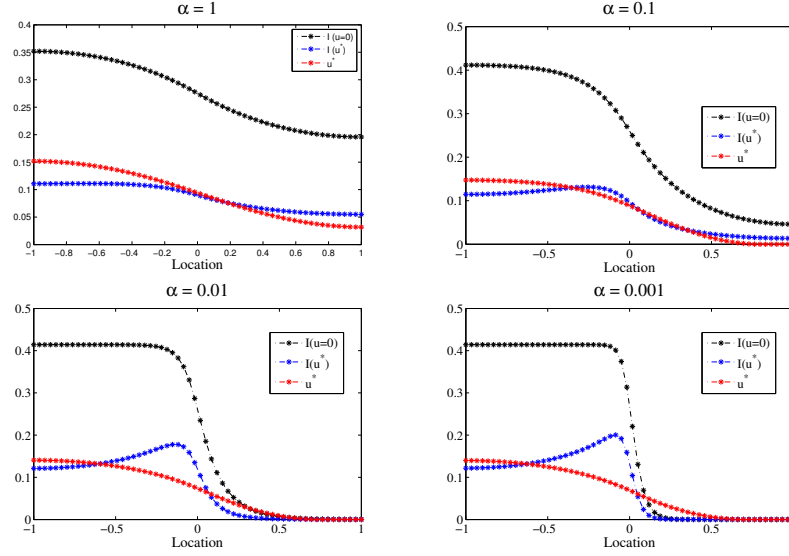


Figure 3.4: Sample solution for the model problem based on various diffusion coefficients  $\alpha$  at  $R_0 = 0.5$ ,  $a = 10$  and  $\eta_{max} = 0.5$ .

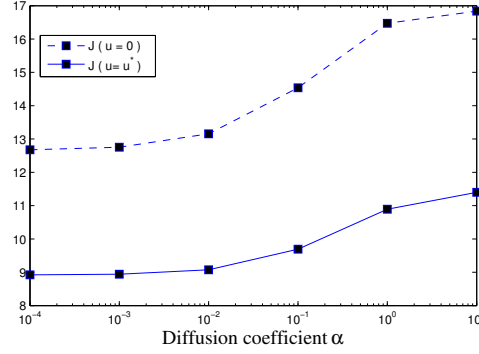


Figure 3.5: Comparison of the value of the cost functional based on different diffusion coefficient  $\alpha$ .

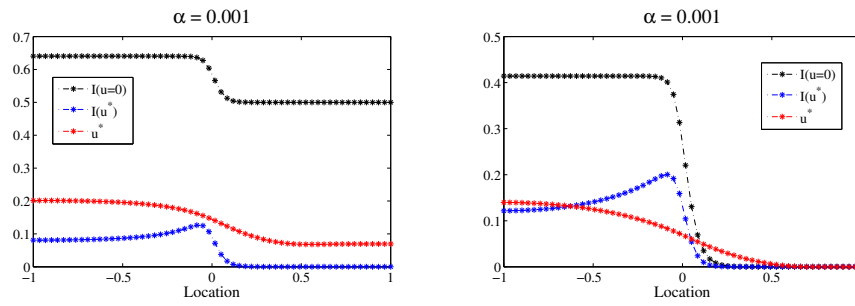


Figure 3.6: Sample solution of the Planner's Problem for  $R_0 = 2$  V.S.  $R_0 = 0.5$ , where  $\alpha = 0.001$ ,  $a = 10$  and  $\eta_{max} = 0.5$ .

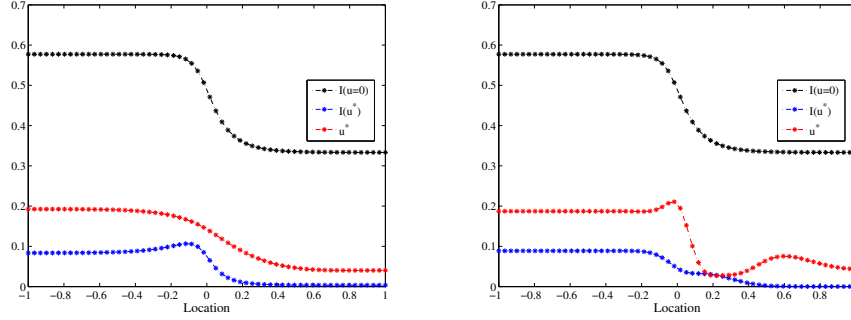


Figure 3.7: Sample solution for the comparison on weight of penalty term,  $\epsilon = 1$ (left) V.S.  $\epsilon = 0.01$ (right), where  $\eta_{max} = 0.5$ ,  $R_0 = 1.5$ ,  $\alpha = 0.01$  and  $a = 10$ .

control variable  $\theta(x)$ ,

$$\alpha I''(x) = \frac{\gamma I(x)}{1 - I(x)} + \theta(x)(e^{aM} - 1) \frac{\gamma I(x)}{1 - I(x)} - \beta I(x) - \eta(x), \quad (3.6.2a)$$

$$I'(-1) = I'(1) = 0. \quad (3.6.2b)$$

As we analyze the optimal control problem at the steady state of the disease dynamic, we rewrite Eq. (3.2.4) as a first order system with column vector  $x \mapsto (\xi_1(x), \xi_2(x))^T = (I(x), I'(x))^T$ ,

$$\min_{\theta \in [0,1]} \int_{-1}^1 c \xi_1(x) + \theta(x) M dx, \quad (3.6.3a)$$

$$\dot{\xi}_1 = \xi_2, \quad (3.6.3b)$$

$$\dot{\xi}_2 = \frac{1}{\alpha} \left[ \frac{\gamma \xi_1}{1 - \xi_1} + \theta(e^{aM} - 1) \frac{\gamma \xi_1}{1 - \xi_1} - \beta \xi_1 - \eta \right], \quad (3.6.3c)$$

$$\xi_2(-1) = \xi_2(1) = 0. \quad (3.6.3d)$$

For this new problem, since the control  $\theta$  enters linearly both in the cost functional and the dynamic system, the existence of an optimal control  $\theta$  is a classical result given in many textbooks on optimal control, see [23].

Let  $x \mapsto \theta^*(x)$  be an optimal control and  $t \mapsto I^*(x) = I(x, u^*) = \xi_1^*(x)$  be an optimal trajectory correspondingly for the minimization problem. By the Pontryagin's maximum principle, we have the necessary conditions for this chattering control, where  $\theta = 0$  or  $\theta = 1$  correspond to a genuine control  $u = 0$  or  $u = M$ .

A common approach is to define the Hamiltonian, as follows

$$\mathcal{H} = c \xi_1 + \theta M + \lambda_1 \xi_2 + \lambda_2 \left[ \frac{1}{\alpha} \left[ \frac{\gamma \xi_1}{1 - \xi_1} + \theta(e^{aM} - 1) \frac{\gamma \xi_1}{1 - \xi_1} - \beta \xi_1 - \eta \right] \right], \quad (3.6.4)$$

where  $\lambda_i, i = 1, 2$  are often referred to as the adjoint variables.

Applying the PMP one can show that there exist non-zero row vector  $x \mapsto (\lambda_1(x), \lambda_2(x))$  such that the adjoint equations are in the following form

$$-\dot{\lambda}_1 = \lambda_2 \frac{1}{\alpha} \left[ \frac{\gamma}{(1 - \xi_1)^2} + \theta(e^{aM} - 1) \frac{\gamma}{(1 - \xi_1)^2} - \beta \right] + c, \quad (3.6.5a)$$

$$-\dot{\lambda}_2 = \lambda_1, \quad (3.6.5b)$$

$$\lambda_1(-1) = \lambda_1(1) = 0. \quad (3.6.5c)$$

$$\theta^* = \arg \min_{\theta \in [0,1]} \mathcal{H}(\xi_1, \xi_2, \lambda_1, \lambda_2, \theta). \quad (3.6.6)$$

Since the Hamiltonian  $\mathcal{H}$  is linear in control  $\theta$ , we define

$$\Phi(x) = \lambda_2 \frac{e^{aM} - 1}{\alpha} \frac{\gamma \xi_1}{1 - \xi_1} + M. \quad (3.6.7)$$

$$\mathcal{H} = \Phi(x)\theta(x) + c\xi_1 + \lambda_1 \xi_2 + \lambda_2 \frac{1}{\alpha} \left[ \frac{\gamma \xi_1}{1 - \xi_1} - \beta \xi_1 - \eta \right], \quad (3.6.8)$$

Hence, the necessary condition leads to the following form of the  $\theta^*$  by PMP

$$\theta^*(x) = \begin{cases} 1 & \text{if } \Phi(x) < 0, \\ 0 & \text{if } \Phi(x) > 0. \end{cases} \quad (3.6.9)$$

$\Phi(\cdot)$  can be seen as the switching function and its zeros can be interpreted as the switching times. If the switching function contains only isolated zeros, the problem is regular and we can achieve an optimal control by finite switch of the two extreme states of the control. However, if  $\Phi(\cdot)$  is zero along an open interval, then such interval is the singular arc, along which  $\dot{\Phi}(x) = \psi(\xi_1, \xi_2, \lambda_1) = 0$ .

Hence, for a monotone decreasing background infection rate  $\eta(x) \geq 0$ ,

- $\theta = 0 \mapsto I(x; \theta = 0)$ :

$$\dot{\xi}_1 = \xi_2, \quad (3.6.10a)$$

$$\dot{\xi}_2 = \frac{1}{\alpha} \left[ \frac{\gamma \xi_1}{1 - \xi_1} - \beta \xi_1 - \eta \right], \quad (3.6.10b)$$

$$\xi_2(-1) = \xi_2(1) = 0. \quad (3.6.10c)$$

- $\theta = 1 \mapsto I(x; \theta = 1)$ :

$$\dot{\xi}_1 = \xi_2, \quad (3.6.11a)$$

$$\dot{\xi}_2 = \frac{1}{\alpha} \left[ e^{aM} \frac{\gamma \xi_1}{1 - \xi_1} - \beta \xi_1 - \eta \right], \quad (3.6.11b)$$

$$\xi_2(-1) = \xi_2(1) = 0. \quad (3.6.11c)$$

- $\theta \in (0, 1) \mapsto I(x; \theta)$ :

$$\dot{\xi}_1 = \xi_2, \quad (3.6.12a)$$

$$\dot{\xi}_2 = \frac{1}{\alpha} \left[ \frac{\gamma \xi_1}{1 - \xi_1} + \theta(e^{aM} - 1) \frac{\gamma \xi_1}{1 - \xi_1} - \beta \xi_1 - \eta \right], \quad (3.6.12b)$$

$$\dot{\lambda}_1 = -\lambda_2 \frac{1}{\alpha} \left[ \frac{\gamma}{(1 - \xi_1)^2} + \theta(e^{aM} - 1) \frac{\gamma}{(1 - \xi_1)^2} - \beta \right] - c, \quad (3.6.12c)$$

$$\dot{\lambda}_2 = -\lambda_1, \quad (3.6.12d)$$

$$\xi_2(-1) = \xi_2(1) = 0, \quad \lambda_1(-1) = \lambda_1(1) = 0, \quad (3.6.12e)$$

$$\psi(\xi_1, \xi_2, \lambda_1) = \lambda_1 \left( \frac{e^{aM} - 1}{\alpha} \right)^2 \left( \frac{\gamma \xi_1}{1 - \xi_1} \right)^2 + \frac{\gamma M}{(1 - \xi_1)^2} \xi_2 = 0. \quad (3.6.12f)$$

For special case where the background infection rate  $\eta(x) = \bar{\eta}$  being constant, we can explicitly compute the control and the corresponding cost. Notice that in such case the infected population  $I$  and the optimal control  $u$  are constants as well, we can use the standard lagrangian multiplier approach

- $\theta = 0 \mapsto I(\theta = 0)$ :

$$I_0 = \frac{-(\gamma - \beta + \bar{\eta}) + \sqrt{(\gamma - \beta + \bar{\eta})^2 + 4\beta\bar{\eta}}}{2\beta}, \quad (3.6.13a)$$

$$\mathcal{J}_0 = \frac{c}{\beta} [-(\gamma - \beta + \bar{\eta}) + \sqrt{(\gamma - \beta + \bar{\eta})^2 + 4\beta\bar{\eta}}], \quad (3.6.13b)$$

where as  $\bar{\eta} \rightarrow +0$ ,

$$I_0 \rightarrow \begin{cases} 0 & \text{if } \beta < \gamma \\ 1 - \frac{\gamma}{\beta} & \text{if } \beta > \gamma \end{cases}, \quad (3.6.14)$$

$$\mathcal{J}_0 \rightarrow \begin{cases} 0 & \text{if } \beta < \gamma \\ 2c(1 - \frac{\gamma}{\beta}) & \text{if } \beta > \gamma \end{cases}. \quad (3.6.15)$$

- $\theta = 1 \mapsto I(\theta = 1)$ :

$$I_1 = \frac{-(\gamma e^{aM} - \beta + \bar{\eta}) + \sqrt{(\gamma e^{aM} - \beta + \bar{\eta})^2 + 4\beta\bar{\eta}}}{2\beta}, \quad (3.6.16a)$$

$$\mathcal{J}_1 = \frac{c}{\beta} [-(\gamma e^{aM} - \beta + \bar{\eta}) + \sqrt{(\gamma e^{aM} - \beta + \bar{\eta})^2 + 4\beta\bar{\eta}}] + 2M. \quad (3.6.16b)$$

where as  $\bar{\eta} \rightarrow +\infty$ ,  $I_1 \rightarrow 1$ . (Taylor series of  $(1 + x)^{0.5} = 1 + \frac{1}{2}x + o(x^2)$ .)

- $\theta_s \in (0, 1) \mapsto I(\theta_s)$ :

$$\theta_s = \frac{c\gamma(e^{aM} - 1) - 2\beta M}{\gamma(e^{aM} - 1)M} \sqrt{\frac{\bar{\eta}M}{c\gamma(e^{aM} - 1) - \beta M}} - \frac{\gamma - \beta + \bar{\eta}}{\gamma(e^{aM} - 1)} \quad (3.6.17a)$$

$$I_s = \sqrt{\frac{\bar{\eta}M}{c\gamma(e^{aM} - 1) - \beta M}}, \quad (3.6.17b)$$

$$\mathcal{J}_s = 2cI_s + 2M\theta_s \quad (3.6.17c)$$

$$\lambda_s = -\frac{2M}{c\gamma(e^{aM} - 1) - 2\beta M} \sqrt{\frac{c\gamma(e^{aM} - 1) - \beta M}{\bar{\eta}M}}. \quad (3.6.17d)$$

Hence, if  $\bar{\eta}$  is small, the optimal control is  $u = 0$  ( $\theta = 0$ ). If  $\bar{\eta}$  is large, the optimal control is  $u = M$  ( $\theta = 1$ ). For other intermediate values of  $\bar{\eta}$ , one could expect the chattering control  $\theta_s \in (0, 1)$  as defined in Eq. (3.6.17).

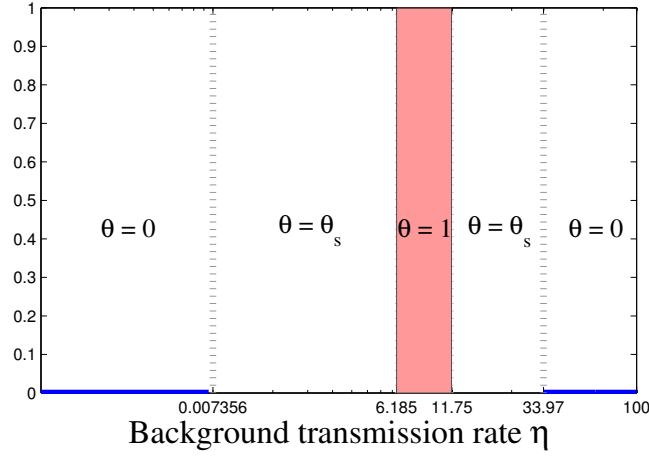


Figure 3.8: Example optimal control  $\theta$  for background infection rate  $\eta$ . This is an sample case to show the possible rise of chattering case, where parameters are taken as  $\beta = 0.5, \gamma = 1, a = 10, M = 0.22, c = 1$ .

### 3.7 Comparison with wall blocking strategy for uniform population

Consider building a wall to block the spread of disease from the reservoir. We consider a simple form control  $u(x)$  as a Gaussian shape function,

$$u(x) = C_r * e^{-\frac{(x-\mu)^2}{2\sigma^2}}. \quad (3.7.1)$$

We observe from figure 3.9 that the wall can efficiently block the transmission when  $R_0 < 1$ . When  $R_0$  is large, even with small diffusion parameter, a simple wall placed at the boarder can not stop the transmission spread out the disease reservoir.

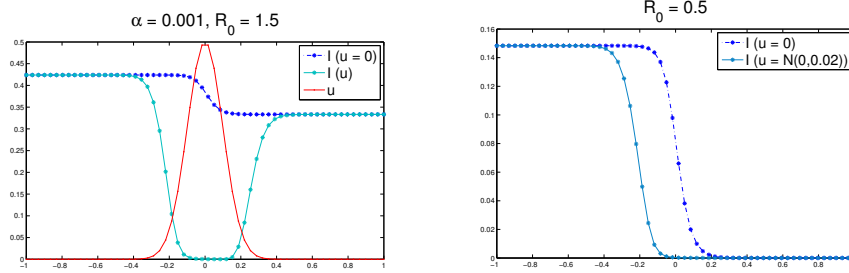


Figure 3.9: Sample solution for model problem based on various  $R_0$ , where  $\eta_{max} = 0.1$ ,  $R_0 = 1.5$  and  $a = 10$ .

However, the Allee effect question shows the possibility that this model fail to capture the possible wall blocking strategy in reality. Demographic and mathematical model studies show that the existence of an Allee effect can prevent biological invasions [42].

### 3.8 Discussion

Here we proposed a spatial model for disease control problem with disease reservoir. We analyzed the underlying dynamic when the control is imposed. Optimal pair of the disease control problem has been proved to exist with suitable choice of the cost functional. Later sections are served to show ways of calculating the optimal control pair in the various applicable scenarios. With carefully, designed the control strategy, one can hope to confine the infectious disease within a close distance around the reservoir. Although our model study one dimensional space, which may seem simple at first sight, it is applicable for large regions which can be simplified as uniform on the other direction as an approximation. Future work can be expanding the model to two dimension case, which we will try to tackle in the following chapter.

## Chapter 4

# Control problems for a class of set valued evolutions

In this chapter, we study controllability problems for the reachable set of a differential inclusion. These were originally motivated by models of control of a flock of animals. Conditions are derived, for the existence or nonexistence of a strategy which confines the reachable set within a given bounded region, at all sufficiently large times. Steering problems and the asymptotic shape of the reachable set are also investigated.

### 4.1 Introduction

The analysis and control of evolution equations on a general metric space has been the topic of several investigations [8, 9, 66]. In particular, this provides a convenient setting for the control of the evolution of a set  $S(t)$ , depending on time.

Aim of this paper is to analyze a specific class of control problems for a moving set. A version of this model, involving conservation laws, was first proposed by R. Colombo and M. Mercier [31] to describe the controlled motion of a flock of animals. Let  $\rho = \rho(t, x)$  denote the density of individuals at time  $t$  at the location  $x \in \mathbb{R}^2$ . The conservation equation takes the form

$$\rho_t + \operatorname{div}(\rho \mathbf{v}) = 0. \quad (4.1.1)$$

It is assumed that individuals choose their velocity  $\mathbf{v}$  with two goals in mind:

- (i) spread out toward less crowded areas,
- (ii) move away from a repelling source, located at a variable position  $\xi(t) \in \mathbb{R}^2$ .

To model (i), a meaningful choice is to set

$$\mathbf{v} = \mathbf{v}(\rho, \nabla \rho) = - \frac{\nabla \rho}{\sqrt{\rho^2 + \frac{1}{c^2} |\nabla \rho|^2}}, \quad (4.1.2)$$



for some constant  $c > 0$  determined by the maximum speed. This yields the conservation law

$$\rho_t - \operatorname{div} \left( \frac{\rho \nabla \rho}{\sqrt{\rho^2 + \frac{1}{c^2} |\nabla \rho|^2}} \right) = 0. \quad (4.1.3)$$

The equation (4.1.3), which coincides with the relativistic heat equation, was studied in [5]. The Cauchy problem has globally defined, unique solutions.

To model (ii), let  $\xi = \xi(t) \in \mathbb{R}^2$  be the position of the repelling source. For example, this could be the position of a dog, controlling a flock of sheep. The velocity of an individual (a sheep) located at  $x$  will be described as

$$\mathbf{v}(x, \xi) = \varphi(|x - \xi|) \frac{x - \xi}{|x - \xi|}. \quad (4.1.4)$$

A natural set of assumptions on the function  $\varphi$  is:

**(A1)** *The map  $\varphi : \mathbb{R}_+ \mapsto \mathbb{R}_+$  is a non-increasing function, with  $\varphi(s) \rightarrow 0$  as  $s \rightarrow +\infty$ .*

For example, one may take

$$\varphi(r) = ae^{-br}. \quad (4.1.5)$$

In alternative, one can also consider

$$\varphi(r) \doteq \begin{cases} \alpha & \text{if } r \leq \sigma, \\ 0 & \text{otherwise,} \end{cases} \quad (4.1.6)$$

or

$$\varphi(r) \doteq \min \{ \beta, \alpha r^{-\gamma} \}. \quad (4.1.7)$$

It will be convenient to represent the function  $\mathbf{v}$  in (4.1.4) as

$$\mathbf{v}(x, \xi) = \nabla_x \Phi(|x - \xi|), \quad \Phi(r) \doteq \int_0^r \varphi(s) ds, \quad (4.1.8)$$

where the gradient is taken w.r.t. the  $x$ -variable. Combining the two terms (4.1.2)-(4.1.4), the conservation law (4.1.1) takes the form

$$\rho_t - \operatorname{div} \left( \frac{\rho \nabla \rho}{\sqrt{\rho^2 + \frac{1}{c^2} |\nabla \rho|^2}} \right) = \operatorname{div} (\rho \nabla \Phi(x, \xi(t))). \quad (4.1.9)$$

Following [31], we regard (4.1.9) as a controlled PDE, where  $\xi(\cdot)$  is the control function.

In the present paper, instead of the density function  $\rho$  itself, we focus on the control of the *support* of  $\rho$ . This will be denoted as

$$S(t) \doteq \operatorname{Supp}(\rho(t, \cdot)) = \overline{\{x \in \mathbb{R}^2; \rho(t, x) > 0\}},$$

where the overline indicates the closure of a set.

For the equation (4.1.3) with smooth initial data  $\rho(0, x) = \rho_0(x)$ , a major result proved in [6] states that the support of the density  $\rho(t, \cdot)$  expands with speed  $c$  in all directions. Namely,

$$S(t) = \left\{ x \in \mathbb{R}^2 ; d(x, S(0)) \leq ct \right\} = S(0) + \overline{B}(0, ct). \quad (4.1.10)$$

Here and in the sequel,  $B(y, r)$  and  $\overline{B}(y, r)$  denote respectively the open and closed disc centered at  $y$  with radius  $r$ .

Motivated by (4.1.10), we introduce a model for the evolution of the region  $S(t) \subset \mathbb{R}^2$  occupied by a flock of animals at time  $t$ , formulated in terms of a differential inclusion. Intuitively for  $x, \xi \in \mathbb{R}^2$ , it is natural to consider the set of velocities

$$G(x, \xi) \doteq \overline{B} \left( \varphi(|x - \xi|) \frac{x - \xi}{|x - \xi|}, c \right)$$

However, the multifunction  $G$  defined in this way would fail to be upper semicontinuous (at points  $x, \xi$  such that either  $x = \xi$  or else  $\varphi$  is discontinuous at  $s = |x - \xi|$ ). Throughout the following, we shall thus work with the upper semicontinuous convex valued regularization of the above multifunction. This is obtained by setting

$$G(x, \xi) \doteq \left\{ y ; \left| y - \lambda \frac{x - \xi}{|x - \xi|} \right| \leq c \text{ for some } \lambda \in [\varphi(s+), \varphi(s-)] \right\} \text{ if } x \neq \xi, \quad (4.1.11)$$

$$G(x, x) = \overline{B}(0, \varphi(0) + c). \quad (4.1.12)$$

Under the assumptions (A1), one easily checks that the multifunction  $G$  in (4.1.11)-(4.1.12) is upper semicontinuous with compact, convex values. Moreover, it satisfies the uniform bound

$$G(x, \xi) \subseteq \overline{B}(0, \varphi(0) + c) \quad \text{for all } x, \xi \in \mathbb{R}^2. \quad (4.1.13)$$

Calling  $S_0$  the region occupied at time  $t = 0$ , we let  $S(t)$  be the reachable set for the differential inclusion

$$\dot{x} \in G(x, \xi(t)), \quad x(0) \in S_0. \quad (4.1.14)$$

In other words,

$$S(t) \doteq \left\{ x(t) ; x(0) \in S_0, \dot{x}(\tau) \in G(x(\tau), \xi(\tau)) \text{ for a.e. } \tau \in [0, t] \right\}. \quad (4.1.15)$$

As a first model, one may consider any continuous function  $\xi : [0, \infty[ \rightarrow \mathbb{R}^2$  as an admissible control. If  $\xi(\cdot)$  denotes the position of a dog initially located at  $\xi_0$ , that can run at a maximum speed  $\sigma$ , a more realistic model would include the assumption

**(A2)** *The control function  $t \mapsto \xi(t) \in \mathbb{R}^2$  is Lipschitz continuous, with*

$$|\dot{\xi}(t)| \leq \sigma, \quad \xi(0) = \xi_0. \quad (4.1.16)$$

As for the fire confinement problem [22, 24], this model leads to some natural questions.

**1 - Global confinement.** Assume that the initial set  $S_0$  is bounded. Is it possible to keep the set  $S(t)$  uniformly bounded for all positive times?

We thus seek conditions which provide the existence (or nonexistence) of a radius  $R > 0$  and a control  $\xi(\cdot)$  such that

$$S(t) \subseteq \overline{B}(0, R) \quad \text{for all } t \geq 0. \quad (4.1.17)$$

A related question is the following. Let two points  $P_1, P_2 \in \mathbb{R}^2$  be given, together with radii  $r_1, r_2 > 0$ . Assuming that  $S_0 \subseteq \overline{B}(P_1, r_1)$ , is it possible to find a control  $\xi(\cdot)$  that, at some later time  $\tau > 0$ , one has  $S(\tau) \subseteq \overline{B}(P_2, r_2)$ ?

**2 - Steering with constant speed.** Assume we want to steer the flock, say in the direction of the  $x_1$ -axis, with constant speed  $\lambda \geq 0$ . When is this possible?

Here we wish to understand in which cases there exists a radius  $R > 0$  and a control  $t \mapsto \xi(t)$  such that

$$S(t) \in B(t\lambda e_1, R) \quad \text{for all } t \geq 0. \quad (4.1.18)$$

By  $e_1$  we denote the unit vector parallel to the  $x_1$ -axis.

**3 - Quasi-stationary domains.** A further problem is to identify the family of compact sets  $S_0$  for which the following stabilization property holds: For every  $\varepsilon > 0$ , there exists a control  $\xi(\cdot)$  such that the corresponding sets  $S(t)$  in (4.1.15) satisfy

$$d_H(S(t), S_0) \leq \varepsilon \quad \text{for all } t \geq 0. \quad (4.1.19)$$

In the analysis of controllability properties, a key role is played by rotating controls, where the point  $\xi(t)$  rotates along a circle  $\gamma$  with constant speed. For this reason, in the last section we study this situation in more detail. In the setting we are considering, from general results about periodic orbits of dynamical systems [64, 70] it already follows that the map  $t \mapsto S(t)$  converges to a time periodic function as  $t \rightarrow +\infty$ , w.r.t. the Hausdorff distance. In the present case, a stronger result can be shown. Namely, in a set of rotating coordinates, for all times  $t$  sufficiently large the boundary of the set  $S(t)$  is a Lipschitz curve that admits a polar coordinate representation  $r = r(t, \theta)$ . Moreover, as  $t \rightarrow \infty$ , one has the uniform convergence  $r(t, \theta) \mapsto r_\infty(\theta)$ , for a smooth function  $r_\infty$ , characterized as the unique  $2\pi$ -periodic orbit of a suitable ODE. Section 2 of this paper contains a standard approximation theorem. Given a probability measure  $\mu$  on  $\mathbb{R}^2$  and a corresponding “averaged” multifunction  $x \mapsto G(x, \mu)$ , we consider the differential inclusion

$$\dot{x}(t) \in G(x(t), \mu), \quad S(0) = S_0. \quad (4.1.20)$$

One can then construct a sequence of control functions  $\xi_n(\cdot)$  such that the corresponding reachable sets  $S_n(t)$  for (4.1.14) are “almost contained” in the reachable sets for (4.1.20).

In Section 3 we give some necessary and some sufficient conditions in order that the global confinement problem or the steering problem admit a solution. Finally, Section 4 analyzes in more detail the case where stabilization is achieved by means of a uniformly rotating control function  $\xi(\cdot)$ . In this case, it is shown that the reachable set  $S(t)$  converges in a strong sense to periodic multifunction.

For the basic theory of multifunctions and differential inclusions we refer to [10, 50]. A survey of different models describing the motion of flocks of animals can be found in the recent paper [16].

## 4.2 Averaging and approximation results

Let  $G = G(x, \xi)$  be a bounded, upper semicontinuous multifunction on  $\mathbb{R}^2 \times \mathbb{R}^2$  with compact, convex values. To fix the ideas, assume

$$G(x, \xi) \subseteq \overline{B}(0, M) \quad \text{for all } x, \xi \in \mathbb{R}^2. \quad (4.2.1)$$

Call  $\mathcal{P}$  the family of all probability measures on  $\mathbb{R}^2$ . For  $\mu \in \mathcal{P}$ , consider the “averaged” multifunction

$$G(x, \mu) \doteq \int G(x, \xi) d\mu(\xi) \doteq \left\{ \int g(\xi) d\mu(\xi); g \text{ measurable, } g(\xi) \in G(x, \xi) \text{ for all } \xi \right\}. \quad (4.2.2)$$

**Lemma 1.** *The multifunction  $x \mapsto G(x, \mu)$  in (4.2.2) is bounded, upper semicontinuous, with compact convex values.*

**Proof. 1.** Introducing the constant  $M = \varphi(0) + c$ , by the uniform bound (4.1.13) it is clear that  $G(x, \mu) \subseteq \overline{B}(0, M)$  for all  $x \in \mathbb{R}^2$ . Moreover, since all sets  $G(x, \xi)$  are convex,  $G(x, \mu)$  is convex as well.

**2.** To show that each set  $G(x, \mu)$  is closed, consider a sequence of points

$$y_n = \int g_n(\xi) d\mu(\xi) \in G(x, \mu).$$

with  $y_n \rightarrow y$  as  $n \rightarrow \infty$ . Taking a subsequence, we can assume the weak convergence  $g_n \rightharpoonup g$  in  $L^1_\mu$ , for some function  $g$ . The convexity of all sets  $G(x, \xi)$  implies  $g(\xi) \in G(x, \xi)$ . Hence

$$y = \lim_{n \rightarrow \infty} \int g_n(\xi) d\mu(\xi) = \int g(\xi) d\mu(\xi) \in G(x, \mu),$$

proving that the set  $G(x, \mu)$  is closed, hence compact.

**3.** Finally, we check that the map  $x \mapsto G(x, \mu)$  is upper semicontinuous. Fix a point  $\bar{x}$  and let  $\varepsilon > 0$  be given. By the upper semicontinuity of the map  $(x, \xi) \mapsto G(x, \xi)$ , we can find a measurable function  $\xi \mapsto r(\xi) > 0$  such that

$$G(x, \xi) \subset B(G(\bar{x}, \xi), \varepsilon/3) \quad \text{for all } x \in B(\bar{x}, r(\xi)). \quad (4.2.3)$$

Choose  $\delta > 0$  such that

$$\mu(\{\xi; r(\xi) \leq \delta\}) < \frac{\varepsilon M}{3}. \quad (4.2.4)$$

We claim that this choice yields

$$G(x, \mu) \subseteq B(G(\bar{x}, \mu), \varepsilon) \quad \text{for all } x \in B(\bar{x}, \delta). \quad (4.2.5)$$

Indeed, assume that  $x \in B(\bar{x}, \delta)$  and consider an arbitrary element

$$y = \int g(\xi) d\mu(\xi) \in G(x, \mu),$$

for some function  $\xi \mapsto g(\xi) \in G(x, \xi)$ . Calling  $\pi \circ g(\xi)$  the perpendicular projection of  $g(\xi)$  on the compact convex set  $G(\bar{x}, \xi)$ , by (4.2.3)-(4.2.4) we have

$$\begin{aligned} d(y, G(\bar{x}, \mu)) &\leq \int_{r(\xi) > \delta} |g(\xi) - \pi \circ g(\xi)| d\mu + \int_{r(\xi) \leq \delta} |g(\xi) - \pi \circ g(\xi)| d\mu \\ &< \frac{\varepsilon}{3} + 2M \cdot \mu(\{\xi; r(\xi) \leq \delta\}) < \varepsilon. \end{aligned}$$

This establishes (4.2.5), and hence the upper semicontinuity of the multifunction  $x \mapsto G(x, \mu)$ .  $\square$

Given a probability measure  $\mu$  and a compact set  $S_0$  as initial data, we denote by  $S^\mu(t)$  the reachable sets for the differential inclusion (4.1.20). Moreover,  $\bar{B}(A, \varepsilon)$  will denote the closed  $\varepsilon$ -neighborhood around a set  $A$ . In our analysis of confinement and steering problems, the following approximation result will be repeatedly used.

**Theorem 1.** *In the above setting, for any  $T, \varepsilon > 0$  there exists a smooth control function  $\xi : [0, T] \mapsto \mathbb{R}^2$  such that the reachable sets  $S^\xi, S^\mu$  for the differential inclusions (4.1.14), (4.1.20) satisfy*

$$S^\xi(t) \subseteq \bar{B}(S^\mu(t), \varepsilon) \quad \text{for all } t \in [0, T]. \quad (4.2.6)$$

**Proof. 1.** Assume  $S_0 \subseteq \bar{B}(0, M_0)$  for some constant  $M_0$ . In view of (4.2.1) for  $t \in [0, T]$ , all trajectories starting in  $S_0$  will satisfy the a priori bound

$$|x(t)| \leq M_0 + MT \quad \text{for all } t \in [0, T]. \quad (4.2.7)$$

Hence, changing the values of the multifunction  $G(x, \xi)$  for  $|x| > M_0 + MT$  does not affect the solutions of the differential inclusion. For simplicity, we shall thus assume that  $G$  is constant for  $|x|$  large, namely

$$G(x, \xi) = \bar{B}(0, M) \quad \text{for all } |x| \geq M_0 + MT, \quad \xi \in \mathbb{R}^2.$$

In essence, the analysis can be restricted to the compact disc  $\bar{B}(0, M_0 + MT) \subset \mathbb{R}^2$ .

**2.** By upper semicontinuity, there exists  $\delta^\sharp > 0$  small enough such that the following holds. If  $G^\sharp$  is any multifunction such that

$$G^\sharp(x) \subseteq co \left( \bigcup_{|x' - x| \leq \delta^\sharp} B(G(x', \mu), \delta^\sharp) \right), \quad (4.2.8)$$

then the reachable sets  $S^\sharp(t)$  for the differential inclusion

$$\dot{x}(t) \in G^\sharp(x(t)), \quad S(0) = S_0, \quad (4.2.9)$$

satisfy

$$S^\sharp(t) \subseteq \bar{B}(S^\mu(t), \varepsilon/2) \quad \text{for all } t \in [0, T]. \quad (4.2.10)$$

**3.** We now approximate  $\mu$  by a purely atomic measure  $\mu^\sharp$ . More precisely, denote by  $\delta_y$  the Dirac measure concentrating a unit mass at the point  $y \in \mathbb{R}^2$ . We can then find points  $y_k \in \mathbb{R}^2$  and coefficients  $\lambda_k \in [0, 1]$  with  $\sum_{k=1}^m \lambda_k = 1$  such that the probability measure

$$\mu^\sharp \doteq \sum_{k=1}^m \lambda_k \delta_{y_k} \quad (4.2.11)$$

yields a multifunction

$$G^\sharp(x) \doteq G(x, \mu^\sharp) = \sum_{k=1}^m \lambda_k G(x, y_k) \quad (4.2.12)$$

satisfying (4.2.8). In particular, this implies (4.2.10).

**4.** Using the upper semicontinuity of the multifunctions  $G(\cdot, y_k)$  and  $G^\sharp$  in (4.2.12), we can choose  $\delta > 0$  small enough so that the following holds. If  $G_1, \dots, G_m$  are multifunctions such that

$$G_k(x) \subseteq \left( \bigcup_{|x'-x| \leq 2\delta} G(x', y_k) \right), \quad k = 1, \dots, m, \quad (4.2.13)$$

then the reachable sets  $S^*(t)$  for the differential inclusion

$$\dot{x}(t) \in G^*(x(t)) \doteq \sum_{k=1}^n \lambda_k G_k(x(t)), \quad S(0) = S_0, \quad (4.2.14)$$

satisfy

$$S^*(t) \subseteq \overline{B}(S^\sharp(t), \varepsilon/4) \quad \text{for all } t \in [0, T]. \quad (4.2.15)$$

**5.** The control function  $\xi(\cdot)$  can now be constructed as follows. Choose an integer  $n$  large enough so that  $TM/n < \delta$  and divide the time interval  $[0, T]$  into  $n$  equal subintervals, inserting the points  $t_i = iT/n$ ,  $0 \leq i \leq n$ . Each interval  $I_i = [t_{i-1}, t_i]$  is further partitioned into subintervals  $I_{i,k}$  whose lengths are proportional to the coefficients  $\lambda_k$ ,  $k = 1, \dots, m$  in (4.2.11). We then define

$$\xi_n(t) = y_k \quad \text{for } t \in \bigcup_{i=1}^n I_{i,k}. \quad (4.2.16)$$

The reachable sets for the differential inclusion

$$\dot{x} \in G(x, \xi_n(t)), \quad x(0) \in S_0 \quad (4.2.17)$$

will be denoted by  $S_n(t)$ .

**6.** Let  $x(\cdot)$  be any solution of (4.2.17). By (4.2.1), for  $t \in [t_{i-1}, t_i]$  it follows

$$|x(t) - x(t_{i-1})| \leq M \cdot \frac{T}{n}. \quad (4.2.18)$$

Consider the polygonal approximation

$$x^*(t) \doteq x(t_{i-1}) + (t - t_{i-1}) \cdot \frac{x(t_i) - x(t_{i-1})}{t_i - t_{i-1}} \quad \text{for all } t \in [t_{i-1}, t_i].$$

By definition  $x^*(t_i) = x(t_i)$  for all  $i = 0, \dots, n$ . If  $t \in [t_{i-1}, t_i]$ , then

$$|x^*(t) - x(t)| \leq 2M(t - t_{i-1}) \leq \frac{2MT}{n}. \quad (4.2.19)$$

Moreover, our previous construction yields

$$\begin{aligned} \dot{x}^*(t) &= \frac{x(t_i) - x(t_{i-1})}{t_i - t_{i-1}} \in \sum_{k=1}^m \lambda_k \cdot \left( \bigcup_{|x' - x(t_{i-1})| \leq \delta} G(x', y_k) \right) \\ &\subseteq \sum_{k=1}^m \lambda_k \cdot \left( \bigcup_{|x' - x^*(t)| \leq 2\delta} G(x', y_k) \right). \end{aligned} \quad (4.2.20)$$

Recalling (4.2.13)-(4.2.15), we thus obtain

$$x^*(t) \in \overline{B}(S^\sharp(t), \varepsilon/4). \quad (4.2.21)$$

Choosing  $n$  so large that  $\frac{2MT}{n} < \frac{\delta}{4}$ , using (4.2.19), (4.2.21), and then (4.2.10), we obtain

$$x(t) \in \overline{B}\left(S^\sharp(t), \frac{\varepsilon}{4} + \frac{\varepsilon}{4}\right) \subseteq \overline{B}(S^\mu(t), \varepsilon).$$

Since  $x(\cdot)$  was an arbitrary solution of the differential inclusion (4.2.17), we have shown that the control function  $\xi(t) = \xi_n(t)$  in (4.2.16) yields the desired estimate (4.2.6).

**7.** To achieve the proof, we need to modify the piecewise constant function  $\xi_n(\cdot)$ , making it smooth on the entire interval  $[0, T]$ . Relying again on the upper semicontinuity of the reachable sets, if the new function  $\xi(\cdot)$  coincides with the  $\xi_n(\cdot)$  on a set of times having sufficiently small Lebesgue measure, after this modification the bound (4.2.6) will be replaced by

$$S^\xi(t) \subseteq \overline{B}(S^\mu(t), 2\varepsilon) \quad \text{for all } t \in [0, T].$$

Since  $\varepsilon > 0$  was arbitrary, this completes the proof.  $\square$

## 4.3 Confinement strategies

### 4.3.1 A necessary condition

We start by deriving a necessary condition for the existence of a confining strategy. The following result shows that, if the initial set  $S_0$  is already large, then, no matter how fast the controller  $\xi$  can move, it cannot prevent the reachable sets  $S(t)$  from becoming arbitrarily large, as  $t \rightarrow +\infty$ . Consider the variables

$$A \doteq \pi r^2, \quad \Phi \doteq \int_{B_r} \operatorname{div} \mathbf{v} = 2\pi r \varphi(r).$$

We regard  $\Phi$  as a function of  $A$ , so that

$$\Phi(A) = 2\pi\sqrt{\frac{A}{\pi}}\varphi\left(\sqrt{\frac{A}{\pi}}\right) = \int_0^A \left[\frac{d}{dA}\Phi(A)\right].$$

Motivated by the previous computations, in the following theorem, we let  $s \mapsto \hat{\varphi}(s)$  be the non-decreasing rearrangement of the function

$$A \mapsto \frac{d}{dA}\Phi(A) = \sqrt{\frac{\pi}{A}}\varphi\left(\sqrt{\frac{A}{\pi}}\right) + \varphi'\left(\sqrt{\frac{A}{\pi}}\right)$$

In other words,  $\hat{\varphi} : [0, \infty[ \mapsto \mathbb{R}$  is the unique (up to a set of zero measure) non-decreasing function such that, for every  $k \leq 0$ ,

$$\begin{aligned} \text{meas}\left(\{A \geq 0; \hat{\varphi}(A) \leq k\}\right) &= \\ \text{meas}\left(\left\{A \geq 0; \sqrt{\frac{\pi}{A}}\varphi\left(\sqrt{\frac{A}{\pi}}\right) + \varphi'\left(\sqrt{\frac{A}{\pi}}\right) \leq k\right\}\right). \end{aligned} \quad (4.3.1)$$

**Theorem 2.** Assume that, for some constant  $A_0$ , the non-increasing rearrangement  $\hat{\varphi}$  satisfies

$$g(A) \doteq 2c\sqrt{\pi A} + \int_0^A \hat{\varphi}(s) ds > 0 \quad \text{for every } A > A_0. \quad (4.3.2)$$

Then, if the initial set  $S_0$  has measure  $m_2(S_0) > A_0$ , uniform confinement is not possible. Indeed, for any choice of the control  $\xi(\cdot)$  one has

$$m_2(S(t)) \rightarrow \infty \quad \text{as } t \rightarrow \infty. \quad (4.3.3)$$

**Proof.** The area of the set  $S(t)$  evolves in time according to

$$\frac{d}{dt}m_2(S(t)) = c \cdot m_1(\partial S(t)) + \int_{S(t)} \text{div } \mathbf{v}. \quad (4.3.4)$$

Here  $\partial S$  denotes the boundary of the set  $S$ , while  $m_1$  is the one-dimensional Hausdorff measure, normalized so that  $m_1(\gamma)$  gives the usual length of a smooth curve  $\gamma$ .

If  $m_2(S(t)) = \pi r^2(t)$  for some  $r(t)$ , then the isoperimetric inequality yields

$$m_1(\partial S(t)) \geq 2\pi r(t) = 2\sqrt{\pi m_2(S(t))}. \quad (4.3.5)$$

This provides a lower bound on the first term on the right hand side of (4.3.4).

To achieve a bound on the second term we observe that, by the definition of  $\hat{\varphi}$ ,

$$\int_S \text{div } \mathbf{v} \geq \inf \left\{ \int_{S'} \text{div } \mathbf{v}; S' \subset \mathbb{R}^2, m_2(S') = m_2(S) \right\} = \int_0^{m_2(S)} \hat{\varphi}(\zeta) d\zeta. \quad (4.3.6)$$

Using (4.3.5) and (4.3.6) in (4.3.4), we obtain

$$\frac{d}{dt}m_2(S(t)) \geq g(m_2(S(t))),$$

where  $g : ]A_0, \infty[ \mapsto \mathbb{R}_+$  is the continuous, strictly positive function introduced at (4.3.2).

A standard comparison argument for ODEs now yields (4.3.3).  $\square$



**Example 1.** Consider the case where  $\varphi(r) = ae^{-br}$ , as in (4.1.5). Calling  $r = |x|$ , we have

$$\operatorname{div} \mathbf{v}(x) = \left( \frac{\varphi(r)}{r} + \varphi'(r) \right) = \left( \frac{1}{r} - b \right) ae^{-br} = \left( \sqrt{\frac{\pi}{A}} - b \right) ae^{-b\sqrt{A/\pi}}$$

Hence  $\operatorname{div} \mathbf{v}(x) \leq 0$  if and only if  $|x| \geq b^{-1}$ . For every set  $S \subset \mathbb{R}^2$  we thus have

$$\int_S \operatorname{div} \mathbf{v} \geq \int_{|x| \geq 1/b} \operatorname{div} \mathbf{v} = -2\pi\varphi(1/b) = -\frac{2\pi a}{e}.$$

In particular, if the initial set  $S_0$  has area  $m_2(S_0) > \pi a^2/c^2 e^2$ , then its perimeter satisfies  $c \cdot m_1(\partial S_0) \geq 2c\sqrt{\pi m_2(S_0)} > 2\pi a/e$ , and the corresponding sets  $S(t)$  become arbitrarily large:  $m_2(S(t)) \rightarrow \infty$  as  $t \rightarrow \infty$ .

**Example 2.** For the function  $\varphi(r)$  defined at (4.1.6) we have

$$\int_S \operatorname{div} \mathbf{v} \geq -2\pi\alpha\sigma.$$

A similar computation shows that, if the initial set  $S_0$  has area  $m_2(S_0) > \pi\alpha^2\sigma^2/c^2$ , then its perimeter satisfies  $c \cdot m_1(\partial S_0) \geq 2c\sqrt{\pi m_2(S_0)} > 2\pi\alpha\sigma$ , and  $m_2(S(t)) \rightarrow \infty$  as  $t \rightarrow \infty$ .

**Example 3.** In the case  $\varphi(r) = \min\{\beta, \alpha r^{-\gamma}\}$ , setting  $r^* \doteq (\alpha/\beta)^{1/\gamma}$  we compute

$$\operatorname{div} \mathbf{v}(x) = \begin{cases} \beta/r & \text{if } |x| < r^*, \\ \alpha(1-\gamma)|x|^{-\gamma-1} & \text{if } |x| > r^*. \end{cases}$$

Notice that, if  $\gamma \leq 1$ , then  $\operatorname{div} \mathbf{v}(x) > 0$  for all  $x \in \mathbb{R}^2$ . In this case the measure  $m_2(S(t))$  will be always increasing in time, and uniform confinement is impossible. On the other hand, if  $\gamma > 1$ , then

$$\int_S \operatorname{div} \mathbf{v} \geq \int_{|x| \geq r^*} \operatorname{div} \mathbf{v} = -2\pi r^* \varphi(r^*) = -2\pi\alpha^{1/\gamma}\beta^{1-1/\gamma}.$$

If the initial set  $S_0$  has area  $m_2(S_0) > \pi\alpha^2\beta^{2-2/\gamma}/c^2$ , then its perimeter satisfies  $c \cdot m_1(\partial S_0) \geq 2c\sqrt{\pi m_2(S_0)} > 2\pi\alpha^{1/\gamma}\beta^{1-1/\gamma}$ , and  $m_2(S(t)) \rightarrow \infty$  as  $t \rightarrow \infty$ .

### 4.3.2 A steering problem

Next, we consider the problem of steering the set  $S(t)$ , initially inside a disc  $\overline{B}(P_1, r_1)$ , to another disc  $\overline{B}(P_2, r_2)$ . To state a positive result in this direction, an auxiliary function needs to be introduced.

Fix a radius  $r_0 \geq 0$ , and consider a probability distribution  $\mu$  uniformly distributed along the circumference centered at the origin with radius  $r_0$ . Consider the “averaged” vector field

$$\mathbf{w}(x) \doteq \int_{|\xi|=r_0} \varphi(|x-\xi|) \frac{x-\xi}{|x-\xi|} d\mu(\xi). \quad (4.3.7)$$

Clearly this vector field is radially symmetric, having the form

$$\mathbf{w}(x) = \phi(|x|, r_0) \frac{x}{|x|}. \quad (4.3.8)$$

The function  $\phi$  can be computed using the divergence theorem. Indeed, for every  $0 < r < r_0$  we have

$$2\pi r \phi(r, r_0) = \int_{|\xi|=r_0} \left( \int_{B(0,r)} \operatorname{div} \mathbf{v}(x, \xi) \right) d\mu(\xi) = \int_{B(0,r)} \operatorname{div} \mathbf{v}(x, P), \quad (4.3.9)$$

where  $P$  is any point having distance  $r_0$  from the origin. Taking  $P = (r_0, 0) \in \mathbb{R}^2$ , the right hand side of (4.3.7) is computed by

$$\phi(r, r_0) = \frac{1}{2\pi r} \int_{r_0-r}^{r_0+r} 2s \left( \frac{\varphi(s)}{s} + \varphi'(s) \right) \arccos \left( \frac{s^2 + r_0^2 - r^2}{2r_0 s} \right) ds. \quad (4.3.10)$$

**Theorem 3.** Assume that  $\varphi : \mathbb{R}_+ \mapsto \mathbb{R}_+$  satisfies (A1) and let  $\phi$  be the function defined at (4.3.7)-(4.3.8). Let  $0 < r_2 \leq r_1$  and assume that

$$\inf_{\rho > r} \phi(r, \rho) < -c \quad \text{for all } r \in [r_2, r_1]. \quad (4.3.11)$$

Let the initial condition satisfy  $S_0 \subseteq \overline{B}(P_1, r_1)$  for some point  $P_1$ . Then, for any point  $P_2 \in \mathbb{R}^2$  there exists a smooth control function  $t \mapsto \xi(t)$  and  $T > 0$  such that the corresponding set satisfies  $S(T) \subseteq \overline{B}(P_2, r_2)$ .

**Proof. 1.** Let the assumption (4.3.11) hold. Then for every  $r \in [r_2, r_1]$  there exists  $\varepsilon > 0$  and a probability measure  $\mu_{\rho(r)}$ , uniformly distributed along the circumference  $\partial B(P_1, \rho(r))$  centered at  $P_1$  with radius  $\rho(r) > r + \varepsilon$ , such that the following holds. At some time  $\tau > 0$ , every solution to the differential inclusion

$$\dot{x} \in G(x, \mu_{\rho(r)}), \quad x(0) \in \overline{B}(P_1, r + \varepsilon)$$

satisfies

$$x(\tau) \in \overline{B}(P_1, r - \varepsilon).$$

**2.** Since the interval  $[r_2, r_1]$  is compact, by a covering argument we can find  $\tau, \varepsilon > 0$  and radii  $R_k$  with

$$r_1 = R_0 > R_1 > \dots > R_N = r_2$$

such that the following holds. For every  $k = 1, \dots, N$ , every solution to the differential inclusion

$$\dot{x} \in G(x, \mu_{\rho(R_k)}), \quad x(0) \in \overline{B}(P_1, R_k)$$

satisfies

$$x(\tau) \in \overline{B}(P_1, R_{k+1} - \varepsilon).$$

By Theorem 1, for every  $k$  there exists a control function  $\xi_k : [0, \tau] \mapsto \mathbb{R}^2$  such that every solution to the differential inclusion

$$\dot{x} \in G(x, \xi_k(t)), \quad x(0) \in \overline{B}(P_1, R_k)$$

satisfies

$$x(\tau) \in \overline{B}(P_1, R_{k+1}).$$

Consider the control function  $\xi : [0, N\tau] \mapsto \mathbb{R}^2$  defined as the concatenation

$$\xi(t) \doteq \xi_k(t - (k-1)\tau) \quad t \in [(k-1)\tau, k\tau].$$

Then every solution of the differential inclusion

$$\dot{x} \in G(x, \xi(t)), \quad x(0) \in \overline{B}(P_1, r_1)$$

satisfies

$$x(N\tau) \in \overline{B}(P_1, r_2).$$

This already proves the theorem in the case  $P_2 = P_1$ .

**3.** Next, consider the unit vector  $\mathbf{e} = (P_2 - P_1)/|P_2 - P_1|$  and choose an integer  $m$  large enough so that

$$\delta = \frac{|P_2 - P_1|}{m} < r_1 - r_2.$$

By the previous step, for every  $j \geq 1$  there exists a control function  $\xi_j : [0, N\tau] \mapsto \mathbb{R}^2$  such that every solution of

$$\dot{x} \in G(x, \xi_j(t)), \quad x(0) \in \overline{B}(P_1 + (j-1)\delta\mathbf{e}, r_1)$$

satisfies

$$x(N\tau) \in \overline{B}(P_1 + (j-1)\delta\mathbf{e}, r_2) \subset \overline{B}(P_1 + j\delta\mathbf{e}, r_1).$$

After  $m+1$  steps, the concatenation of these controls  $\xi_j(\cdot)$  yields a control  $\xi(\cdot)$  satisfying the requirements of the theorem, with  $T = (m+1)N\tau$ .  $\square$

Next, we provide a sufficient condition for the solvability of the steering problem. Given a probability measure  $\mu$  on  $\mathbb{R}^2$ , we recall that  $G(x, \mu)$  denotes the averaged velocity set defined at (4.2.2).

**Theorem 4.** Assume that  $\varphi : \mathbb{R}_+ \mapsto \mathbb{R}_+$  satisfies (A1). Consider any bounded open set  $\Omega \subset \mathbb{R}^2$  with smooth boundary, and any velocity vector  $\mathbf{e}$ . Assume that there exists a probability distribution  $\mu$  such that, calling  $\mathbf{n}(x)$  the unit outer normal to  $\Omega$  at the boundary point  $x$ , one has

$$\langle \mathbf{n}(x), \mathbf{v} - \mathbf{e} \rangle < -c \quad \text{for all } x \in \partial\Omega, \quad \mathbf{v} \in G(x, \mu). \quad (4.3.12)$$

If  $S_0$  is any compact set contained in  $\Omega$ , then there exists a continuous control function  $t \mapsto \xi(t)$  such that the corresponding reachable set in (4.1.15) satisfies

$$S(t) \subset \Omega + t\mathbf{e} \quad \text{for all } t \geq 0. \quad (4.3.13)$$

**Proof. 1.** Define the multifunction  $G^-(x, \xi) \doteq G(x, \xi) - \mathbf{e}$ . Assume that there exists a control function  $\xi^-(\cdot)$  such that every solution of

$$\dot{x} \in G^-(x, \xi^-(t)), \quad x(0) \in S_0 \quad (4.3.14)$$

satisfies

$$x(t) \in \Omega \quad \text{for all } t \geq 0. \quad (4.3.15)$$

Since  $G$  is translation invariant, i.e.  $G(x, \xi) = G(x + t\mathbf{e}, \xi + t\mathbf{e})$ , the control  $\xi(t) = \xi^-(t) + t\mathbf{e}$  then satisfies the conclusion of the theorem. To prove Theorem 4, it thus suffices to construct a control function  $\xi^-$  such that (4.3.15) holds, for every solution of (4.3.14). **2.** Call  $d(x, \partial\Omega)$  the signed distance of a point  $x$  to the boundary of  $\Omega$ . By assumption,  $d(\cdot, \partial\Omega)$  is smooth in a neighborhood of  $\partial\Omega$  and satisfies

$$\begin{cases} d(x, \partial\Omega) < 0 & \text{if } x \in \Omega, \\ d(x, \partial\Omega) > 0 & \text{if } x \notin \overline{\Omega}, \end{cases}$$

Consider the sublevel sets

$$\Lambda_{-c} \doteq \{x; \psi(x) \leq -c\}.$$

Thanks to the assumption (4.3.12), we can find  $c > 0$  such that the set  $\Lambda_{-c}$  is strongly invariant for the differential inclusion

$$\dot{x} \in G^-(x, \mu). \quad (4.3.16)$$

In fact, choosing a sufficiently small constant  $c$ , satisfying

$$\max_{x \in S_0} \psi(x) < -c < 0,$$

the following stronger statement is true. Every solution  $t \mapsto x(t)$  of (4.3.16) with  $x(0) \in \Lambda_{-c/2}$  satisfies

$$x(t) \in \Lambda_{-c/2} \quad \text{for all } t \geq 0, \quad x(1) \in \Lambda_{-c}.$$

By Theorem 1, there exists a control function  $\xi^- : [0, 1] \mapsto \mathbb{R}^2$  such that every solution of

$$\dot{x} \in G^-(x, \xi^-(t)), \quad x(0) \in \Lambda_{-c/2}$$

satisfies

$$x(t) \in \Lambda_{-c/4} \quad \text{for all } t \in [0, 1], \quad x(1) \in \Lambda_{-c/2}.$$

Extending  $\xi^-(\cdot)$  by periodicity, so that  $\xi^-(t+1) = \xi^-(t)$ , we obtain a  $\xi^- : \mathbb{R}_+ \mapsto \mathbb{R}^2$  with the desired property. Namely, every solution of (4.3.14) satisfies (4.3.15). This achieves the proof.  $\square$

**Example 4.** Assume that, for some  $0 < r < r_0$  and  $\delta > 0$ , the function  $\phi$  in (4.3.10) satisfies

$$\phi(r, r_0) = -c - \delta. \quad (4.3.17)$$

Let  $\mu_0$  be the probability measure uniformly distributed along the circumference  $\{x = (x_1, x_2); |x| = r_0\}$ , and let  $\mu^-$  be the probability measure uniformly distributed along the half circumference  $\{x = (x_1, x_2); |x| = r_0, x_1 \leq 0\}$ . Let  $\Omega \doteq \overline{B}(0, r)$ . By (4.3.17) one has

$$\frac{c}{c + \delta} \left\langle \mathbf{n}(x), \nabla \Phi^{\mu_0}(x) \right\rangle = -c \quad \text{for all } x \in \partial\Omega. \quad (4.3.18)$$

Choose  $\eta > 0$  such that

$$\left\langle \mathbf{n}(x), \nabla \Phi^{\mu_-}(x) - \eta \mathbf{e}_1 \right\rangle < 0 \quad \text{for all } x \in \partial\Omega. \quad (4.3.19)$$

Then the assumptions of Theorem 4 are satisfied with

$$\mu \doteq \frac{c}{c+\delta} \mu_0 + \frac{\delta}{c+\delta} \mu_-, \quad \mathbf{e} = \frac{\eta\delta}{c+\delta} \mathbf{e}_1.$$

## 4.4 Asymptotic shape of a rotating solution

In this section we study in more detail the evolution of the set  $S(t)$ , in case where the point  $\xi(t)$  moves along a circumference, with constant angular speed  $\omega$ .

To fix the ideas, assume that

$$\xi(t) = R(\cos \omega t, -\sin \omega t),$$

with  $\omega = \varepsilon^{-1}$  very large. Consider a set of rotating coordinates, determined by the orthonormal frame  $\{\mathbf{e}_1(t), \mathbf{e}_2(t)\}$ , with  $\mathbf{e}_1(t) = (\cos \omega t, -\sin \omega t)$ .

Consider the vector fields

$$\mathbf{w}(x) \doteq \begin{pmatrix} -x_2 \\ x_1 \end{pmatrix}, \quad (4.4.1)$$

$$\mathbf{v}(x) \doteq \varphi(|x - \xi|) \cdot \frac{x - \xi}{|x - \xi|}, \quad \xi = (\xi_1, \xi_2) = (R, 0). \quad (4.4.2)$$

In the above system of rotating coordinates, the sets  $S(t)$  are determined as the reachable sets for the differential inclusion

$$\dot{x} \in B\left(\frac{1}{\varepsilon} \mathbf{w}(x) + \mathbf{v}(x), c\right). \quad (4.4.3)$$

For a suitable class of initial data  $S_0$ , as  $t \rightarrow \infty$  we expect that  $S(t) \rightarrow \bar{S}$ , for some invariant set  $\bar{S}$ . In polar coordinates, this set has the representation

$$\bar{S} = \left\{ (r \cos \alpha, r \sin \alpha); \quad r \leq \rho_\varepsilon(\alpha) \right\},$$

where  $\alpha \mapsto \rho_\varepsilon(\alpha)$  provides a periodic solution to the ODE

$$\frac{d\rho}{d\alpha} = g_\varepsilon(\alpha, \rho). \quad (4.4.4)$$

With reference to Fig. 4.1, left, if the point  $x = (\rho \cos \alpha, \rho \sin \alpha)$  moves according to  $\dot{x} = \mathbf{v}^+(x)$ , then its polar coordinates satisfy (4.4.4). The function  $g_\varepsilon$  is determined by

$$\begin{aligned} g_\varepsilon(\alpha, \rho) &= \frac{\cos \theta}{|x|} = \sup_{|\mathbf{y}| \leq c} \frac{\left\langle x, \varepsilon^{-1} \mathbf{w}(x) + \mathbf{v}(x) + \mathbf{y} \right\rangle}{|x|^2 \cdot |\varepsilon^{-1} \mathbf{w}(x) + \mathbf{v}(x) + \mathbf{y}|} \\ &= \varepsilon \cdot \sup_{|\mathbf{y}| \leq c} \frac{\left\langle x, \mathbf{v}(x) + \mathbf{y} \right\rangle}{|x|^2 \cdot |\mathbf{w}(x) + \varepsilon \mathbf{v}(x) + \varepsilon \mathbf{y}|}. \end{aligned} \quad (4.4.5)$$

For  $\varepsilon = 0$  we have  $g_0(\alpha, \rho) \equiv 0$  and every constant function is a periodic solution. To find periodic solutions for  $\varepsilon > 0$  we use a bifurcation technique. Call  $r \mapsto F_\varepsilon(r)$  the return map for (4.4.4). Calling  $\alpha \mapsto \rho_\varepsilon(\alpha, r)$  the solution of (4.4.4) with initial data  $\rho(0) = r$ , consider the function

$$F(r, \varepsilon) \doteq \rho_\varepsilon(2\pi, r) - r. \quad (4.4.6)$$

Zeroes of  $F$  correspond to periodic solutions. Since  $F(r, 0) \equiv 0$  for all  $r$ , by standard bifurcation theory we have

- (i) If  $\frac{\partial F}{\partial \varepsilon}(\bar{r}, 0) \neq 0$ , then in a neighborhood of the point  $(\bar{r}, 0)$  the only solutions of (4.4.6) are those with  $\varepsilon = 0$ .
- (ii) If  $\frac{\partial F}{\partial \varepsilon}(\bar{r}, 0) = 0$  and  $\frac{\partial^2 F}{\partial r \partial \varepsilon}(\bar{r}, 0) \neq 0$ , then there exists a nontrivial branch of solutions of the form  $r = r^*(\varepsilon)$ , with

$$r^*(0) = \bar{r}, \quad \frac{\partial r^*}{\partial \varepsilon}(0) = -\frac{\partial^2 F}{\partial \varepsilon^2}(\bar{r}, 0) \cdot \left( \frac{\partial^2 F}{\partial r \partial \varepsilon}(\bar{r}, 0) \right)^{-1}.$$

Consider the formal asymptotic expansions

$$g_\varepsilon(\alpha, \rho) = \varepsilon g_1(\alpha, \rho) + \varepsilon^2 g_2(\alpha, \rho) + o(\varepsilon^2), \quad (4.4.7)$$

$$\rho_\varepsilon(\alpha, r) = r + \varepsilon \rho_1(\alpha, r) + \varepsilon^2 \rho_2(\alpha, r) + o(\varepsilon^2), \quad (4.4.8)$$

$$r^*(\varepsilon) = \bar{r} + \varepsilon r_1 + \varepsilon^2 r_2 + o(\varepsilon^2). \quad (4.4.9)$$

The conditions in (ii) for the existence of a nontrivial branch of solutions, bifurcating from the trivial branch at  $(\bar{r}, 0)$ , can be written as

$$\frac{\partial F}{\partial \varepsilon}(\bar{r}, 0) = \rho_1(2\pi, \bar{r}) = 0, \quad (4.4.10)$$

$$\frac{\partial^2 F}{\partial \varepsilon \partial r}(\bar{r}, 0) = \frac{\partial \rho_1}{\partial r}(2\pi, \bar{r}) \neq 0. \quad (4.4.11)$$

Inserting (4.4.7)-(4.4.8) in (4.4.4) and equating coefficients, to first order we obtain

$$\rho_1(2\pi, r) = \int_0^{2\pi} g_1(\beta, r) d\beta. \quad (4.4.12)$$

Hence (4.4.10) yields

$$\int_0^{2\pi} g_1(\beta, \bar{r}) d\beta = \int_0^{2\pi} \frac{\partial g_\varepsilon}{\partial \varepsilon}(\beta, \bar{r}) d\beta = 0. \quad (4.4.13)$$

Moreover, (4.4.11) yields

$$\int_0^{2\pi} \frac{\partial}{\partial r} g_1(\beta, \bar{r}) d\beta = \int_0^{2\pi} \frac{\partial^2 g_\varepsilon}{\partial \varepsilon \partial r}(\beta, \bar{r}) d\beta \neq 0. \quad (4.4.14)$$

Introducing the vector  $x(\alpha, r) \doteq (r \cos \alpha, r \sin \alpha)$ , from (4.4.5) and the definitions of the vector fields  $\mathbf{w}, \mathbf{v}$  at (4.4.1)-(4.4.2), it follows

$$g_1(\alpha, \rho) = c + \frac{1}{\rho} \left\langle \mathbf{v}(x(\alpha, \rho)), x(\alpha, \rho) \right\rangle.$$

Defining the function

$$\psi(r, R) \doteq \int_0^{2\pi} \left\langle \mathbf{v}(x(\alpha, r)), \frac{x(\alpha, r)}{r} \right\rangle d\alpha, \quad (4.4.15)$$

the conditions (4.4.13) and (4.4.14) can be written as

$$\psi(\bar{r}, R) = -2\pi c. \quad (4.4.16)$$

$$\left. \frac{d}{dr} \psi(r, R) \right|_{r=\bar{r}} \neq 0. \quad (4.4.17)$$

**Theorem 5.** *Assume that there exists a unique radius  $\bar{r}$  for which (4.4.16) hold, and for such value  $\bar{r}$  assume that the inequality (4.4.17) holds as well. Then, for every  $\varepsilon > 0$  small enough, the following holds.*

- (i) *The ODE (4.4.4) has a unique periodic solution  $r = r^*(\alpha)$ .*
- (ii) *The region  $S^* \doteq \{(r \cos \alpha, r \sin \alpha); 0 \leq r \leq r^*(\alpha), \alpha \in [0, 2\pi]\}$  is positively invariant for the differential inclusion (4.4.3).*
- (iii) *If, in addition,  $\psi(r) > -2\pi c$  for all  $0 < r < \bar{r}$ , then for any initial set  $S_0 \subseteq S^*$ , the corresponding reachable set  $S(t)$  satisfies*

$$\lim_{t \rightarrow \infty} d_H(S(t), S^*) = 0. \quad (4.4.18)$$

*Moreover, for all  $t$  sufficiently large the set  $S(t)$  admits a polar coordinate representation*

$$S(t) = \{r(\cos \theta, \sin \theta); 0 \leq r \leq r(t, \theta)\} \quad (4.4.19)$$

*with  $\lim_{t \rightarrow \infty} r(t, \theta) = r^*(\theta)$  uniformly for  $\theta \in [0, 2\pi]$ .*

**Proof. 1.** By standard results of bifurcation theory [29], the existence and uniqueness of the periodic solution are an immediate consequence of the assumptions.

**2.** The positive invariance of the set  $S^*$  follows from the definition (4.4.5). Indeed, calling  $T_{S^*}(x)$  the tangent cone to the set  $S^*$  at any boundary point  $x$ , (4.4.5) implies

$$B(\mathbf{w}(x) + \varepsilon \mathbf{v}(x), c\varepsilon) \subseteq T_{S^*}(x). \quad (4.4.20)$$

Moreover, for every  $x \in S^*$ ,

$$B(-\mathbf{w}(x) - \varepsilon \mathbf{v}(x), c\varepsilon) \cap T_{S^*}(x) \neq \emptyset. \quad (4.4.21)$$

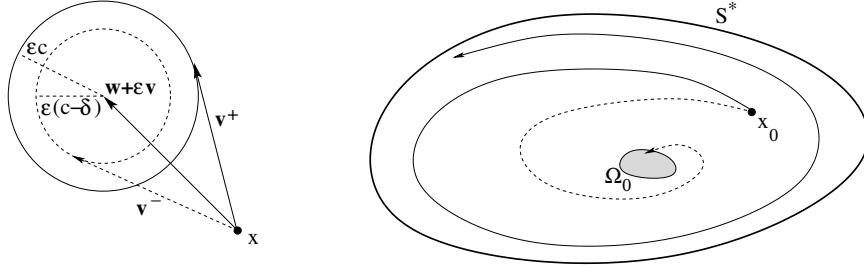


Figure 4.1: Left: construction of the vector fields  $\mathbf{v}^+$ ,  $\mathbf{v}^-$ . Right: any trajectory of  $\dot{x} = \mathbf{v}^+(x)$  (solid curve) approaches the periodic orbit providing the boundary of  $S^*$ . Any trajectory of  $\dot{x} = \mathbf{v}^-(x)$  (dashed curve) enters the set  $\Omega_0$ .

Since the right hand side of (4.4.3) is a Lipschitz continuous multifunction, by (4.4.20) every trajectory of (4.4.3) starting at a point  $x_0 \in S^*$  remains inside  $S^*$  for all times  $t \in [0, \infty[$ . On the other hand, by (4.4.21), for every point  $x_0 \in S^*$  there exists a trajectory  $t \mapsto x(t) \in S^*$  defined for  $t \in ]-\infty, 0]$  with  $x(0) = x_0$ . Together, these two properties yield the positive invariance of  $S^*$ .

**3.** In the remainder of the proof we assume that  $\psi(r) < 2\pi c$  for all  $0 < r < \bar{r}$ . Since  $\psi(r) \rightarrow 0$  as  $r \rightarrow 0+$  and  $\psi(\bar{r}) = -2\pi c$ , by continuity we can find  $\delta > 0$  such that  $\psi(r) < 2\pi(c - \delta)$  for all  $r \in [0, \bar{r}]$ .

It is convenient to introduce the vector fields  $\mathbf{v}^+$ ,  $\mathbf{v}^-$ , as in Fig. 4.1. At a given point  $x$ , these are defined as the tangents to the circumferences centered at  $\mathbf{w}(x) + \varepsilon \mathbf{v}(x)$  and with radii  $\varepsilon c$ ,  $\varepsilon(c - \delta)$ , respectively. By Pythagoras' theorem,

$$\begin{aligned} |\mathbf{v}^+(x)| &= \sqrt{|\mathbf{w}(x) + \varepsilon \mathbf{v}(x)|^2 - \varepsilon^2 c^2}, \\ |\mathbf{v}^-(x)| &= \sqrt{|\mathbf{w}(x) + \varepsilon \mathbf{v}(x)|^2 - \varepsilon^2 (c - \delta)^2}, \end{aligned} \quad (4.4.22)$$

and the vectors  $\mathbf{v}^+(x)$ ,  $\mathbf{v}^-(x)$  are well defined as soon as the right hand sides of (4.4.22) are  $\geq 0$ .

Observe that the above assumptions on the function  $\psi$  in (4.4.15) imply that, for every  $\varepsilon > 0$  sufficiently small, the following holds.

- The vector field  $\mathbf{v}^+$  has a unique periodic solution. This is precisely the boundary of the domain  $S^*$ . In polar coordinates, it corresponds to a periodic solution of (4.4.4).
- The vector field  $\mathbf{v}^-$  has no periodic solution inside  $S^*$ .

Consider any point  $x_0 \in S^*$ , and denote by  $t \mapsto x(t, x_0)$  the solution of

$$\dot{x} = \mathbf{v}^-(x), \quad x(0) = x_0.$$

Notice that this trajectory is well defined, as long as it does not touch the set

$$\Omega_0^- \doteq \left\{ x; \quad |\mathbf{w}(x) + \varepsilon \mathbf{v}(x)| \leq \varepsilon(c - \delta) \right\} \subset \Omega_0 \doteq \left\{ x; \quad |\mathbf{w}(x) + \varepsilon \mathbf{v}(x)| \leq \varepsilon c \right\}.$$

Since  $S^*$  is positively invariant, we have  $x(t) \in S^*$ . By the Poincaré-Bendixson theorem,  $x(\cdot)$  must either approach a periodic orbit, or a point where  $\mathbf{v}^- = 0$ . By assumption, there



are no periodic orbits inside  $S^*$ . We conclude that there exists a time  $\tau \geq 0$  such that  $|\mathbf{w}(x(\tau)) + \varepsilon \mathbf{v}(x(\tau))| \leq \varepsilon(c - \frac{\delta}{2})$ . Hence,  $x(\tau)$  lies in the interior of  $\Omega_0$ .

By the above arguments, for every initial set  $S_0 \subseteq S^*$  there exists  $\tau \geq 0$  such that  $S(\tau, S_0) \cap \text{int}\Omega_0 \neq \emptyset$ .

**4.** For  $\varepsilon \ll 1$ ,  $\Omega_0 = \left\{x; |\mathbf{w}(x) + \varepsilon \mathbf{v}(x)| \leq \varepsilon c\right\}$  is convex and diffeomorphic to disk  $B(o, \varepsilon c)$ . Consider the one-to-one map  $x \mapsto H(x) \doteq \mathbf{w}(x) + \varepsilon \mathbf{v}(x)$ . Notice that  $\mathbf{v}(x)$  is smooth and  $\lim_{|x| \rightarrow \infty} |\mathbf{v}(x)| = 0$ ,

$$\mathcal{J}_H(x) = \begin{pmatrix} 0 & -1 \\ 1 & 0 \end{pmatrix} + \varepsilon \mathcal{J}_{\mathbf{v}}(x), \quad (4.4.23)$$

hence,  $\mathcal{J}_H(x)$  is invertible and continuous when  $\varepsilon$  is very small.  $H(x)$  is the diffeomorphism we need, provided  $\varepsilon \ll 1$ . There exist a point  $x_0 \in \Omega_0$  which is the preimage of the origin.

$$H(x) = \mathbf{w}(x) + \varepsilon \mathbf{v}(x) \approx \mathcal{J}_H(x_0)(x - x_0) + o(\varepsilon) \approx \begin{pmatrix} 0 & -1 \\ 1 & 0 \end{pmatrix} (x - x_0) + o(\varepsilon).$$

**5.** By a straightforward comparison argument, if  $S(\tau, S_0) \supseteq S_1$ , then  $S(\tau+t, S_0) \supseteq S(t, S_1)$ . To prove the convergence (4.4.18), by the previous step it is thus not restrictive to assume that  $S_0 \subseteq \Omega_0$ . By definition,  $\Omega_0$  is the set of stationary points for the differential inclusion (4.4.3). In other words, if  $\bar{x} \in \Omega_0$ , then  $x(t) \equiv \bar{x}$  is a solution to (4.4.3). The assumption  $S_0 \subseteq \Omega_0$  thus implies

$$S(t, S_0) \supseteq S(s, S_0) \supset S_0 \quad \text{for all } t \geq s \geq 0. \quad (4.4.24)$$

Therefore, the closure of the union

$$S_\infty \doteq \overline{\bigcup_{t \geq 0} S(t, S_0)} \subseteq S^*$$

must be a positively invariant set, consisting of all the trajectories of  $\mathbf{v}^+$  starting inside  $\Omega_0$ . Hence the boundary  $\partial S_\infty$  should be a periodic orbit of  $\mathbf{v}^+$ . By uniqueness, we conclude that  $S_\infty = S^*$ .

**6.** Finally, we show that the stronger convergence (4.4.19) holds.

Denote by  $\Gamma^* \doteq \partial S^*$ ,  $\Gamma(t) \doteq \partial S(t)$  the boundaries of  $S^*$  and  $S(t)$ , respectively. By the previous analysis we know that  $\Gamma^*$  is a smooth curve and that

$$\lim_{t \rightarrow +\infty} d_H(\Gamma(t), \Gamma^*) = 0. \quad (4.4.25)$$

To prove the Lipschitz regularity of the curve  $\Gamma(t)$  we use the fact that each  $S(t)$  satisfies an interior ball condition [26]:

*There exists a constant  $\rho > 0$  such that, for all  $t \geq 1$ , every point  $P \in S(t)$  is contained in some closed disc  $D \subseteq S(t)$  of radius  $\rho$ .*

For convenience, we consider the transformation mapping the point  $P = r(\cos \theta, \sin \theta)$  to the point  $P' = \frac{r}{r^*(\theta)}(\cos \theta, \sin \theta)$ , where  $r^*(\cdot)$  yields the polar representation of the curve  $\Gamma^*$ . Relying on this change of coordinates, it is not restrictive to assume that the set  $S^*$

is the closed unit disc, so that  $\Gamma^* = \{x \in \mathbb{R}^2; |x| = 1\}$ . The images of the sets  $S(t)$  in these new coordinates will satisfy an interior ball condition, possibly with a different radius  $\rho > 0$ .

By (4.4.25), for any  $\varepsilon > 0$  we can find  $t_\varepsilon$  sufficiently large such that

$$\Gamma(t) \subseteq \left\{x \in \mathbb{R}^2; 1 - \varepsilon \leq |x| \leq 1\right\} \quad \text{for all } t \geq t_\varepsilon.$$

Choosing  $\varepsilon = \rho/2$ , we claim that, for  $t \geq t_\varepsilon$ , the curve  $\Gamma(t)$  can be written in polar coordinates as

$$\Gamma(t) = \left\{r^{(t)}(\theta)(\cos \theta, \sin \theta); \theta \in [0, 2\pi]\right\} \quad (4.4.26)$$

for some Lipschitz continuous function  $r^{(t)}$ . Indeed, fix an angle  $\alpha$ , and define

$$r^{(t)}(\alpha) \doteq \max \left\{r \geq 0; \lambda(\cos \alpha, \sin \alpha) \in S(t) \text{ for all } \lambda \in [0, r]\right\}.$$

Referring to Fig. 4.2, consider the point

$$P = r^{(t)}(\alpha)(\cos \alpha, \sin \alpha) \in \Gamma(t).$$

Let  $B_1, B_2$  be the two closed discs with radius  $\rho$ , tangent to  $\Gamma^*$  and containing  $P$  as a boundary point. Consider the open region  $\Sigma$ , bounded between  $\Gamma^*$  and the two discs. By construction, if  $Q \in \Sigma$ , then  $Q \notin \Gamma(t)$ , because there exists no disc of radius  $\rho$  containing  $Q$  and contained in  $S(t)$ . The above argument shows that, for every  $t \geq t_\varepsilon$ , the set  $\Gamma(t)$  admits the polar coordinate representation (4.4.26), where the function  $r^{(t)}$  satisfies an estimate of the form

$$1 - \varepsilon \leq r^{(t)}(\beta) \leq r^{(t)}(\alpha) + C|\beta - \alpha|.$$

for some uniform constant  $C$ , valid for all times  $t \geq t_\varepsilon$  and all angles  $\alpha, \beta$ . Hence  $r^{(t)}$  is Lipschitz continuous with Lipschitz constant  $C$ .

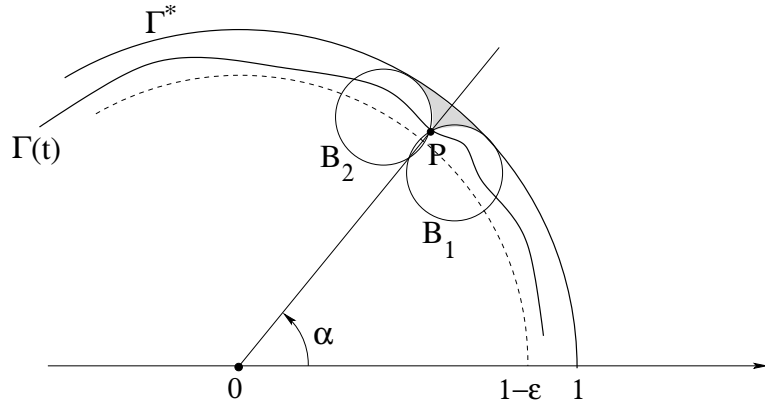


Figure 4.2: No point of  $\Gamma(t)$  can lie in the shaded area, because the interior ball condition would otherwise be violated.

**Example 6.** Consider the “scare function”  $\varphi(r) = ae^{-br}$  as in (4.1.5), assuming  $a > c, b > 1$ . We wish to understand for which radii  $\bar{r}$ ,  $0 < \bar{r} < R$ , the conditions (4.4.16)-(4.4.17) hold. First, a direct computation yields

$$\begin{aligned}
\frac{d}{dr}\psi(r) &= \frac{d}{dr} \left( \int_0^{2\pi} \left\langle \mathbf{v}(x(\alpha, r)), \frac{x(\alpha, r)}{r} \right\rangle d\alpha \right) \\
&= \int_0^{2\pi} \frac{d}{dr} \left( \frac{\varphi(|x - \xi|)}{|x - \xi|} (r - R \cos \alpha) \right) d\alpha \\
&= \int_0^{2\pi} \frac{\varphi(|x - \xi|)}{|x - \xi|} \left( 1 - (b + \frac{1}{|x - \xi|}) \frac{(r - R \cos \alpha)^2}{|x - \xi|^2} \right) d\alpha \quad (4.4.27) \\
&\leq \int_0^{2\pi} \frac{\varphi(|x - \xi|)}{|x - \xi|} \left( 1 - (b + \frac{1}{R + r}) \frac{(R - r)^2}{(R + r)^2} \right) d\alpha \\
&\leq \int_0^{2\pi} \frac{\varphi(|x - \xi|)}{|x - \xi|} \left( 1 - b \frac{(R - r)^2}{(R + r)^2} \right) d\alpha < 0,
\end{aligned}$$

provided  $r < \frac{\sqrt{b}-1}{\sqrt{b}+1}R$ .

Hence,  $\psi(r)$  is strictly monotone decreasing in  $(0, \frac{\sqrt{b}-1}{\sqrt{b}+1}R)$ , which make condition (4.4.17) holds.

Now we check condition (4.4.16). Recall the equivalent formula of  $\psi(r)$  in (4.3.10).

$$\psi(r) = 2\pi\phi(r, R) = \frac{2}{r} \int_{R-r}^{R+r} \varphi(s)(1 - bs) \arccos \left( \frac{s^2 + R^2 - r^2}{2Rs} \right) ds. \quad (4.4.28)$$

For any fixed  $R$ , we first need to make sure  $\psi(r) < 0$ , which require  $1 - bs < 0$ , for all  $s \in (R - r, R + r)$ . So, together with the monotone condition (4.4.27), we have

$$R - r > R - \frac{\sqrt{b}-1}{\sqrt{b}+1}R = \frac{2R}{\sqrt{b}+1} > \frac{1}{b}, \quad (4.4.29)$$

provided  $b > \max \left\{ 1, \left( \frac{1 + \sqrt{1 + 8R}}{4R} \right)^2 \right\}$ .

Then we can always choose parameter  $a$  large enough to make sure  $\min \psi(r) < -2\pi c$ .

$$\frac{2\pi a}{r} \left( se^{-bs} \right) \Big|_{R-r}^{R+r} = \frac{2\pi}{r} \int_{R-r}^{R+r} \varphi(s)(1 - bs) ds < \psi(r) < -2\pi c, \quad (4.4.30)$$

provided  $a > cr \max \{ (be)^{-1}, \psi(R + r)/a, \psi(R - r)/a \}$ .

Notice that  $\psi(r) \rightarrow 0$  when  $r \rightarrow 0$ , we claim there is a  $\bar{r} \in (0, \frac{\sqrt{b}-1}{\sqrt{b}+1}R)$  satisfy condition (4.4.27) such that  $\psi(\bar{r}) = -2\pi c$ .

# References

- [1] D. ACEVEDO-GARCIA, K. A. LOCHNER, T. L. OSYPUK, AND S. V. SUBRAMANIAN, *Future directions in residential segregation and health research: a multilevel approach*, American journal of public health, 93 (2003), pp. 215–221.
- [2] M. ALI, Y. WAGATSUMA, M. EMCH, AND R. F. BREIMAN, *Use of a geographic information system for defining spatial risk for dengue transmission in bangladesh: role for aedes albopictus in an urban outbreak*, The American journal of tropical medicine and hygiene, 69 (2003), pp. 634–640.
- [3] R. ANDERSON, J. MANN, AND D. TARANTOLA, *The spread of hiv and sexual mixing patterns*, AIDS in the World II, 2 (1996), pp. 71–86.
- [4] R. ANDERSON AND R. MAY, *Infectious diseases of humans: dynamics and control*, vol. 26, Wiley Online Library, 1992.
- [5] F. ANDREU, V. CASELLES, AND J. M. MAZÓN, *A strongly degenerate quasilinear equation: the parabolic case*, Archive for rational mechanics and analysis, 176 (2005), pp. 415–453.
- [6] F. ANDREU, V. CASELLES, J. M. MAZÓN, AND S. MOLL, *Finite propagation speed for limited flux diffusion equations*, Archive for rational mechanics and analysis, 182 (2006), pp. 269–297.
- [7] S. ANITA, V. ARNAUTU, AND V. CAPASSO, *An Introduction to Optimal Control Problems in Life Sciences and Economics: From Mathematical Models to Numerical Simulation with MATLAB®*, Springer, 2011.
- [8] J.-P. AUBIN, *Mutational equations in metric spaces*, Set-Valued Analysis, 1 (1993), pp. 3–46.
- [9] —, *Mutational and morphological analysis: tools for shape evolution and morphogenesis*, Springer, 1999.
- [10] J. P. AUBIN AND A. CELLINA, *Differential inclusions: set-valued maps and viability theory*, Springer-Verlag New York, Inc., 1984.
- [11] A. BANDURA ET AL., *Health promotion by social cognitive means*, Health education and behavior, 31 (2004), pp. 143–164.

- [12] C. BAUCH AND D. EARN, *Vaccination and the theory of games*, Proceedings of the National Academy of Sciences of the United States of America, 101 (2004), p. 13391.
- [13] C. T. BAUCH, A. P. GALVANI, AND D. J. EARN, *Group interest versus self-interest in smallpox vaccination policy*, Proceedings of the National Academy of Sciences, 100 (2003), pp. 10564–10567.
- [14] N. BECKER AND L. EGERTON, *A transmission model for hiv with application to the australian epidemic*, Mathematical biosciences, 119 (1994), pp. 205–224.
- [15] H. BEHNCKE, *Optimal control of deterministic epidemics*, Optimal control applications and methods, 21 (2000), pp. 269–285.
- [16] N. BELLOMO AND C. DOGBE, *On the modeling of traffic and crowds: A survey of models, speculations, and perspectives*, SIAM review, 53 (2011), pp. 409–463.
- [17] L. BIAN, *Spatial approaches to modeling dispersion of communicable diseases—a review*, Transactions in GIS, 17 (2013), pp. 1–17.
- [18] L. BOLZONI, V. TESSONI, M. GROPPi, AND G. A. DE LEO, *React or wait: which optimal culling strategy to control infectious diseases in wildlife*, Journal of mathematical biology, (2013), pp. 1–25.
- [19] D. BREDa, O. DIEKMANN, W. DE GRAAF, A. PUGLIESE, AND R. VERMIGLIO, *On the formulation of epidemic models (an appraisal of kermack and mckendrick)*, (2012).
- [20] D. BREDa AND D. VISETTI, *Existence, multiplicity and stability of endemic states for an age-structured s-i epidemic model*, Mathematical biosciences, (2011).
- [21] S. BRENNER AND R. SCOTT, *The mathematical theory of finite element methods*, vol. 15, Springer, 2007.
- [22] A. BRESSAN, *Differential inclusions and the control of forest fires*, Journal of Differential Equations, 243 (2007), pp. 179–207.
- [23] A. BRESSAN AND B. PICCOLI, *Introduction to the mathematical theory of control*, vol. 2, American institute of mathematical sciences Springfield, 2007.
- [24] A. BRESSAN AND T. WANG, *Equivalent formulation and numerical analysis of a fire confinement problem*, ESAIM: Control, Optimisation and Calculus of Variations, 16 (2010), pp. 974–1001.
- [25] D. L. BRITO, E. SHESHINSKI, AND M. D. INTRILIGATOR, *Externalities and compulsory vaccinations*, Journal of Public Economics, 45 (1991), pp. 69–90.
- [26] P. CANNARSA AND C. SINISTRARI, *Semiconcave functions, Hamilton-Jacobi equations, and optimal control*, vol. 58, Springer, 2004.

- [27] T. CARACO, S. GLAVANAKOV, G. CHEN, J. E. FLAHERTY, T. K. OHSUMI, AND B. K. SZYMANSKI, *Stage-structured infection transmission and a spatial epidemic: a model for lyme disease*, The American Naturalist, 160 (2002), pp. 348–359.
- [28] F. H. CHEN, *Rational behavioral response and the transmission of stds*, Theoretical Population Biology, 66 (2004), pp. 307–316.
- [29] S.-N. CHOW AND J. K. HALE, *Methods of bifurcation theory*, Springer, 1982.
- [30] A. CLIFF AND P. HAGGETT, *Spatial aspects of epidemic control*, Progress in Human Geography, 13 (1989), pp. 315–347.
- [31] R. M. COLOMBO AND M. LÉCUREUX-MERCIER, *An analytical framework to describe the interactions between individuals and a continuum*, Journal of nonlinear science, 22 (2012), pp. 39–61.
- [32] M. CONNER AND P. NORMAN, *Predicting health behaviour: a social cognition approach*, Predicting health behaviour, (2005), pp. 1–27.
- [33] C. DE COSTER AND P. HABETS, *An overview of the method of lower and upper solutions for odes*, Progress in Nonlinear Differential Equations and their Applications, 43 (2001), pp. 3–22.
- [34] M. DELGADO, M. MOLINA-BECERRA, AND A. SUÁREZ, *A nonlinear age-dependent model with spatial diffusion*, Journal of mathematical analysis and applications, 313 (2006), pp. 366–380.
- [35] R. J. DORAN AND S. W. LAFFAN, *Simulating the spatial dynamics of foot and mouth disease outbreaks in feral pigs and livestock in queensland, australia, using a susceptible-infected-recovered cellular automata model*, Preventive Veterinary Medicine, 70 (2005), pp. 133–152.
- [36] S. EUBANK, H. GUCLU, V. A. KUMAR, M. V. MARATHE, A. SRINIVASAN, Z. TOROCZKAI, AND N. WANG, *Modelling disease outbreaks in realistic urban social networks*, Nature, 429 (2004), pp. 180–184.
- [37] L. C. EVANS, *Partial differential equations: Graduate studies in mathematics*, American Mathematical Society, 2 (1998).
- [38] J. M. EYLER, *The changing assessments of john snow’s and william farr’s cholera studies*, Sozial-und Präventivmedizin, 46 (2001), pp. 225–232.
- [39] S. FUNK, M. SALATHÉ, AND V. JANSEN, *Modelling the influence of human behaviour on the spread of infectious diseases: a review*, Journal of The Royal Society Interface, 7 (2010), pp. 1247–1256.
- [40] A. P. GALVANI, T. C. RELUGA, AND G. B. CHAPMAN, *Long-standing influenza vaccination policy is in accord with individual self-interest but not with the utilitarian optimum*, Proceedings of the National Academy of Sciences, 104 (2007), pp. 5692–5697.

- [41] G. GARNETT, R. ANDERSON, G. GARNETT, AND R. ANDERSON, *Factors controlling the spread of hiv in heterosexual communities in developing countries: patterns of mixing between different age and sexual activity classes*, Philosophical Transactions of the Royal Society of London. Series B: Biological Sciences, 342 (1993), pp. 137–159.
- [42] J. GARNIER, L. ROQUES, AND F. HAMEL, *Success rate of a biological invasion in terms of the spatial distribution of the founding population*, Bulletin of mathematical biology, 74 (2012), pp. 453–473.
- [43] E. C. GREEN, D. T. HALPERIN, V. NANTULYA, AND J. A. HOGLE, *Uganda's hiv prevention success: the role of sexual behavior change and the national response*, AIDS and Behavior, 10 (2006), pp. 335–346.
- [44] B. GRENFELL, A. KLECZKOWSKI, C. GILLIGAN, AND B. BOLKER, *Spatial heterogeneity, nonlinear dynamics and chaos in infectious diseases*, Statistical Methods in Medical Research, 4 (1995), pp. 160–183.
- [45] T. GROSS, C. D'LIMA, AND B. BLASIUS, *Epidemic dynamics on an adaptive network*, Physical review letters, 96 (2006), p. 208701.
- [46] G. HESS, S. RANDOLPH, P. ARNEBERG, C. CHEMINI, C. FURLANELLO, J. HARWOOD, M. ROBERTS, AND J. SWINTON, *Spatial aspects of disease dynamics*, The ecology of wildlife diseases, (2002), pp. 102–118.
- [47] E. HOLMES, M. LEWIS, J. BANKS, AND R. VEIT, *Partial differential equations in ecology: spatial interactions and population dynamics*, Ecology, (1994), pp. 17–29.
- [48] E. C. HOLMES AND S. S. BURCH, *The causes and consequences of genetic variation in dengue virus*, Trends in microbiology, 8 (2000), pp. 74–77.
- [49] E. E. HOLMES, *Basic epidemiological concepts in a spatial context*, Spatial ecology: the role of space in population dynamics and interspecific interactions. Princeton University Press, Princeton, NJ, (1997), pp. 111–136.
- [50] S. HU AND N. PAPAGEORGIOU, *Handbook of multivalued analysis, vol. i theory 1997*, Mathematics and its Applications, (1997).
- [51] J. P. HUGHES, J. M. BAETEN, J. R. LINGAPPA, A. S. MAGARET, A. WALD, G. DE BRUYN, J. KIARIE, M. INAMBAO, W. KILEMBE, C. FARQUHAR, ET AL., *Determinants of per-coital-act hiv-1 infectivity among african hiv-1-serodiscordant couples*, Journal of Infectious Diseases, (2012), p. jir747.
- [52] J. HYMAN, J. LI, AND E. STANLEY, *Threshold conditions for the spread of the hiv infection in age-structured populations of homosexual men*, Journal of Theoretical Biology, 166 (1994), pp. 9–31.
- [53] H. INABA, *Endemic threshold results in an age-duration-structured population model for hiv infection*, Mathematical biosciences, 201 (2006), pp. 15–47.

- [54] H. R. JOSHI, S. LENHART, H. LOU, AND H. GAFF, *Harvesting control in an integrodifference population model with concave growth term*, Nonlinear Analysis: Hybrid Systems, 1 (2007), pp. 417–429.
- [55] J. P. KELLER, L. GERARDO-GIORDA, AND A. VENEZIANI, *Numerical simulation of a susceptible–exposed–infectious space-continuous model for the spread of rabies in raccoons across a realistic landscape*, Journal of biological dynamics, 7 (2013), pp. 31–46.
- [56] W. O. KERMACK AND A. G. MCKENDRICK, *Contributions to the mathematical-theory of epidemics. II. the problem of endemicity*, Proceedings of the Royal Society of London, 138 (1932), pp. 55–83.
- [57] ———, *Contributions to the mathematical-theory of epidemics. III. further studies of the problem of endemicity*, Proceedings of the Royal Society of London, 141 (1933), pp. 94–122.
- [58] B. L. KEYFITZ AND N. KEYFITZ, *The mckendrick partial differential equation and its uses in epidemiology and population study*, Mathematical and Computer Modelling, 26 (1997), pp. 1–9.
- [59] C. KIRCHNER, M. HERTY, S. GOTTLICH, AND A. KLAR, *Optimal control for continuous supply network models*, Networks and Heterogeneous Media, 1 (2006), pp. 675–688.
- [60] J. KLAMKA, *Controllability of dynamical systems*, Kluwer Academic Publishers Dordrecht,, The Netherlands, 1991.
- [61] E. F. LAMBIN, A. TRAN, S. O. VANWAMBEKE, C. LINARD, AND V. SOTI, *Pathogenic landscapes: interactions between land, people, disease vectors, and their animal hosts*, International journal of health geographics, 9 (2010), pp. 1–13.
- [62] S. LENHART, E. BODINE, P. ZHONG, AND H. R. JOSHI, *Illustrating optimal control applications with discrete and continuous features*, in Advances in Applied Mathematics, Modeling, and Computational Science, Springer, 2013, pp. 209–238.
- [63] S. LENHART AND J. T. WORKMAN, *Optimal control applied to biological models*, CRC Press, 2007.
- [64] D. LI AND P. E. KLOEDEN, *On the dynamics of nonautonomous periodic general dynamical systems and differential inclusions*, Journal of Differential Equations, 224 (2006), pp. 1–38.
- [65] A. L. LLOYD AND V. A. JANSEN, *Spatiotemporal dynamics of epidemics: synchrony in metapopulation models*, Mathematical biosciences, 188 (2004), pp. 1–16.
- [66] T. LORENZ, *Mutational analysis: a joint framework for Cauchy problems in and beyond vector spaces*, vol. 1996, Springer, 2010.



- [67] D. LOUZ, H. E. BERGMANS, B. P. LOOS, AND R. C. HOEBEN, *Emergence of viral diseases: mathematical modeling as a tool for infection control, policy and decision making*, Critical reviews in microbiology, 36 (2010), pp. 195–211.
- [68] M. L. N. MBAH AND C. A. GILLIGAN, *Optimal control of disease infestations on a lattice*, Mathematical Medicine and Biology, (2013), p. dqt012.
- [69] J. MEDLOCK AND M. KOT, *Spreading disease: integro-differential equations old and new*, Mathematical Biosciences, 184 (2003), pp. 201–222.
- [70] V. S. MELNIK AND J. VALERO, *On attractors of multivalued semi-flows and differential inclusions*, Set-Valued Analysis, 6 (1998), pp. 83–111.
- [71] V. MÉNDEZ, *Epidemic models with an infected-infectious period*, Physical Review E, 57 (1998), pp. 3622–3624.
- [72] V. MÉNDEZ, T. PUJOL, AND J. FORT, *Dispersal probability distributions and the wave-front speed problem*, Physical review-series E-, 65 (2002), pp. 041109–041109.
- [73] L. A. MEYERS, B. POURBOHLOUL, M. E. NEWMAN, D. M. SKOWRONSKI, AND R. C. BRUNHAM, *Network theory and sars: predicting outbreak diversity*, Journal of theoretical biology, 232 (2005), pp. 71–81.
- [74] R. MILLER NEILAN AND S. LENHART, *Optimal vaccine distribution in a spatiotemporal epidemic model with an application to rabies and raccoons*, Journal of Mathematical Analysis and Applications, 378 (2011), pp. 603–619.
- [75] D. MOLLISON, *Spatial contact models for ecological and epidemic spread*, Journal of the Royal Statistical Society. Series B (Methodological), (1977), pp. 283–326.
- [76] R. PARR AND W. YANG, *Density-functional theory of atoms and molecules*, vol. 16, Oxford University Press, USA, 1994.
- [77] C. PETERS AND J. PETERS, *An introduction to ebola: the virus and the disease*, Journal of Infectious Diseases, 179 (1999), pp. ix–xvi.
- [78] N. PUNYACHAROENSIN, W. EDMUNDS, D. DE ANGELIS, AND R. WHITE, *Mathematical models for the study of hiv spread and control amongst men who have sex with men*, European journal of epidemiology, (2011), pp. 1–15.
- [79] B. RAPATSKI, F. SUPPE, AND J. YORKE, *Hiv epidemics driven by late disease stage transmission*, JAIDS Journal of Acquired Immune Deficiency Syndromes, 38 (2005), pp. 241–253.
- [80] T. RELUGA, C. BAUCH, AND A. GALVANI, *Evolving public perceptions and stability in vaccine uptake*, Mathematical biosciences, 204 (2006), pp. 185–198.
- [81] T. C. RELUGA AND A. P. GALVANI, *A general approach for population games with application to vaccination*, Mathematical Biosciences, 230 (2011), pp. 67–78.

- [82] T. C. RELUGA AND J. LI, *Games of age-dependent prevention of chronic infections by social distancing*, Journal of Mathematical Biology, (2012).
- [83] T. C. RELUGA, J. MEDLOCK, AND A. P. GALVANI, *A model of spatial epidemic spread when individuals move within overlapping home ranges august 2, 2011*, (2011).
- [84] T. C. RELUGA, J. MEDLOCK, E. POOLMAN, AND A. P. GALVANI, *Optimal timing of disease transmission in an age-structured population*, Bulletin of Mathematical Biology, 69 (2007), pp. 2711–2722.
- [85] K. R. RIOS-SOTO, C. CASTILLO-CHAVEZ, M. G. NEUBERT, E. S. TITI, AND A. YAKUBU, *Epidemic spread in populations at demographic equilibrium*, Contemporary Mathematics, 410 (2006), pp. 297–310.
- [86] R. E. ROWTHORN, R. LAXMINARAYAN, AND C. A. GILLIGAN, *Optimal control of epidemics in metapopulations*, Journal of the Royal Society Interface, 6 (2009), pp. 1135–1144.
- [87] J. F. RUSHBY AND K. HANSON, *Calculating and presenting disability adjusted life years (dalys) in cost-effectiveness analysis*, Health policy and planning, 16 (2001), pp. 326–331.
- [88] M. SALATHÉ AND S. BONHOEFFER, *The effect of opinion clustering on disease outbreaks*, Journal of The Royal Society Interface, 5 (2008), pp. 1505–1508.
- [89] L. SALICRUP AND L. FEDORKOVA, *Challenges and opportunities for enhancing biotechnology and technology transfer in developing countries*, Biotechnology advances, 24 (2006), pp. 69–79.
- [90] M. SMALLMAN-RAYNOR AND A. D. CLIFF, *Epidemic diffusion processes in a system of us military camps: Transfer diffusion and the spread of typhoid fever in the spanish-american war, 1898*, Annals of the Association of American Geographers, 91 (2001), pp. 71–91.
- [91] J. SNOW, *On the mode of communication of cholera*, John Churchill, 1855.
- [92] M. J. TILDESLEY, T. A. HOUSE, M. C. BRUHN, R. J. CURRY, M. O’NEIL, J. L. ALLPRESS, G. SMITH, AND M. J. KEELING, *Impact of spatial clustering on disease transmission and optimal control*, Proceedings of the National Academy of Sciences, 107 (2010), pp. 1041–1046.
- [93] A. R. TUIITE, J. TIEN, M. EISENBERG, D. J. EARN, J. MA, AND D. N. FISMAN, *Cholera epidemic in haiti, 2010: using a transmission model to explain spatial spread of disease and identify optimal control interventions*, Annals of internal medicine, 154 (2011), pp. 593–601.
- [94] N. D. WOLFE, C. P. DUNAVAN, AND J. DIAMOND, *Origins of major human infectious diseases*, Nature, 447 (2007), pp. 279–283.

- [95] M. WOOLHOUSE AND E. GAUNT, *Ecological origins of novel human pathogens*, Critical reviews in microbiology, 33 (2007), pp. 231–242.
- [96] D. ZANETTE AND S. RISAU-GUSMÁN, *Infection spreading in a population with evolving contacts*, Journal of biological physics, 34 (2008), pp. 135–148.

# Appendix

## Details of Chapter 2

### Analysis of the disease dynamics with continuous-age-structure

Recall the population-scale dynamics (2.2.2), we assume  $\beta(a, a_I, z)$  has a simple form:

$$\beta(a, a_I, z) \doteq \xi(a) q(a_I, z). \quad (0.1)$$

This will induce the general separable inter-cohort form of the infection pressure

$$\lambda(a, t) = \xi(a) \int_0^{a_{\max}} \int_0^{a_I} q(a_I, z) I(a_I, t, z) dz da_I, \quad (0.2)$$

where  $\xi \in L^\infty(0, a_{\max})$ ,  $q \in L_2(0, a_{\max}) \times (0, a_{\max})$ ,  $q(a_I, z), \xi(a) \geq 0$ . For convenience, we denote

$$K(a) \doteq e^{-\int_0^a \mu(\tau) d\tau}. \quad (0.3)$$

which is the survival probability, meaning the probability at birth of surviving to age  $a$ , and for given  $\bar{c}_S(a)$ ,

$$\sigma(a) \doteq \sigma(a, \bar{c}_S(a)). \quad (0.4)$$

Integrating  $S$  along the characteristics, we obtain

$$S(a, t) = rK(a) e^{-\int_0^a \lambda(\tau, t-a+\tau) \sigma(\tau) d\tau}, \quad \text{for } t \geq a. \quad (0.5)$$

Further more, using Eq. (0.5) and integrating  $I$  along the characteristics, we have

$$I(a, t, z) = rK(a-z) \sigma(a-z) \lambda(a-z, t-z) e^{-\int_0^{a-z} \sigma(\tau) \lambda(\tau, t-a+\tau) d\tau} e^{-\alpha z - \int_{a-z}^a \mu(\tau) d\tau}, \quad \text{for } t \geq a. \quad (0.6)$$

If we define

$$W(t) \doteq \int_0^{a_{\max}} \int_0^{a_I} q(a_I, z) I(a_I, t, z) dz da_I, \quad (0.7)$$

then Eq. (0.6) can be represented by

$$I(a, t, z) = rK(a)\sigma(a-z)\xi(a-z)W(t-z) e^{-\int_0^{a-z} \sigma(\tau)\xi(\tau)W(t-a+\tau)d\tau} e^{-\alpha z}, \quad \text{for } t \geq a. \quad (0.8)$$

### Existence and uniqueness of steady state solution

For steady state analysis, we only consider  $t \rightarrow \infty$  and  $\alpha = 0$ , plug Eq. (0.8) into Eq. (0.2), we obtain

$$W(t) = \int_0^{a_{\max}} \int_0^{a_I} rK(a_I)q(a_I, z)\sigma(a_I - z)\xi(a_I - z)W(t - z) e^{-\alpha z - \int_0^{a_I - z} \sigma(\tau)\xi(\tau)W(t - a_I + \tau)d\tau} dz da_I. \quad (0.9)$$

1. The disease-free equilibrium corresponding to the trivial solution  $W(t) = W^* = 0$  is:

$$\begin{cases} S(a) = rK(a), \\ I(a, z) = 0. \end{cases} \quad (0.10)$$

2. The endemic equilibrium provided by  $W(t) = A > 0$ . Constant  $A$  is given by rearrange the integration of Eq. (0.9) along the characteristic first, then cancel the repeated non-zero constant  $A$  on both side of the equation, we obtain:

$$F(A) \doteq \int_0^{a_{\max}} e^{-A \int_0^{a_0} \sigma(\tau)\xi(\tau)d\tau} \left\{ \int_0^{a_{\max} - a_0} q(a_0 + z, z)rK(a_0 + z)\sigma(a_0)\xi(a_0)e^{-\alpha z} dz \right\} da_0, \quad (0.11)$$

the desirable  $A$  has to be the solution for  $F(A) = 1$  if the solution exist. Notice that  $\frac{dF(A)}{dA} < 0$ ,  $F(A)$  is monotone decreasing. So, it is sufficient to impose  $F(A = 0) > 1$  as the condition for the existence and uniqueness of the endemic steady state solution.

To summarize, define the basic epidemic reproduction number  $R_0$  as

$$R_0 \doteq \int_0^{a_{\max}} \int_0^{a_I} q(a_I, z)rK(a_I)\sigma(a_I - z)\xi(a_I - z)e^{-\alpha z} dz da_I = F(0). \quad (0.12)$$

**Theorem 0.1.** If  $R_0 < 1$ , there exist an unique disease-free equilibrium. If  $R_0 > 1$ , there exist an unique endemic equilibrium.

### Stability of the disease-free equilibrium and basic reproduction number $R_0$

For the stability of steady-state solution, we consider functional derivative in calculus of variation, see reference [76] for example.

$$W(t) = W^* + \epsilon\omega(t), \quad (0.13)$$

we linearize  $W(t) = L(W(t))$  around the steady state  $W^*$ , such that

$$\omega(t) = \frac{d}{d\epsilon} L(W^* + \epsilon\omega(t))|_{\epsilon=0}, \quad (0.14)$$

where the linear operator  $L$  is the integration of  $W(t)$  in Eq. (0.9). To simplify the notation, we denote

$$\Psi(a_I, z) \doteq rK(a_I)q(a_I, z)\sigma(a_I - z)\xi(a_I - z)e^{-\alpha z}. \quad (0.15)$$

$$\begin{aligned} \omega(t) = & \int_0^{a_{\max}} \int_0^{a_I} \omega(t - z) \Psi(a_I, z) e^{-W^* \int_0^{a_I - z} \sigma(\tau) \xi(\tau) d\tau} dz da_I \\ & - W^* \int_0^{a_{\max}} \int_0^{a_I} \Psi(a_I, z) e^{-W^* \int_0^{a_I - z} \sigma(\tau) \xi(\tau) d\tau} \\ & \left\{ \int_0^{a_I - z} \sigma(\tau) \xi(\tau) \omega(t - a_I + \tau) d\tau \right\} dz da_I. \end{aligned} \quad (0.16)$$

In the case of the disease-free equilibrium Eq. (0.10), Eq. (0.16) will take a much simple form, by changing the integration order, we obtain

$$\begin{aligned} \omega(t) = & \int_0^{a_{\max}} \left\{ \int_{a_{\max} - z}^{a_{\max}} \Psi(a_I, z) e^{-W^* \int_0^{a_I - z} \sigma(\tau) \xi(\tau) d\tau} da_I \right\} \omega(t - z) dz \\ = & \int_0^{a_{\max}} \Phi(z) \omega(t - z) dz, \end{aligned} \quad (0.17)$$

where  $\Phi(z)$  is defined as the corresponding the convolution kernel.

To study the local asymptotic stability of this disease-free equilibrium, we consider the characteristic equation by substituting  $\omega(t) = e^{st}$ ,  $s \in \mathbb{C}$  in Eq. (0.17).

$$e^{st} = \int_0^{a_{\max}} \Phi(z) e^{s(t-z)} dz = e^{st} \int_0^{a_{\max}} \Phi(z) e^{-sz} dz. \quad (0.18)$$

Hence, we have the characteristic equation

$$1 - \hat{\Phi}(s) = 0, \quad \text{where} \quad \hat{\Phi}(s) = \int_0^{+\infty} e^{-sz} \Phi(z) dz. \quad (0.19)$$

**Theorem 0.2.** If  $R_0 < 1$ , the disease-free equilibrium is stable. If  $R_0 > 1$ , the disease-free equilibrium is unstable.

*Proof.* First, recall the definition of  $R_0$  in Eq. (0.12), notice that

$$\hat{\Phi}(0) = \int_0^{a_{\max}} \Phi(z) dz = F(0) = R_0. \quad (0.20)$$

If  $R_0 < 1$ ,  $\hat{\Phi}(0) < 1$ . Then, suppose  $s \in \mathbb{C}$  has a positive real part,

$$|\hat{\Phi}(s)| = \left| \int_0^{a_{\max}} e^{-sz} \Phi(z) dz \right| \leq \int_0^{a_{\max}} e^{-\operatorname{Re}(s)z} \Phi(z) dz \leq \hat{\Phi}(0) < 1. \quad (0.21)$$

Hence, the characteristic equation (0.19) has no non-zero root with positive real part.

If  $R_0 > 1$ ,  $\hat{\Phi}(0) > 1$ . Notice that  $\hat{\Phi}(s)$  is a monotone decreasing function and  $\hat{\Phi}(s) \rightarrow 0$  as  $s \rightarrow \infty$ , which means characteristic equation  $1 - \hat{\Phi}(s) = 0$  has exactly one root located on the positive real line. Hence, the disease-free equilibrium is unstable in this case.  $\square$

## Derivation of optimality conditions using adjoint-calculus

To use the standard adjoint-variable approach for problem (2.2.6) as in [59], we first need to reformulate the constraint on  $p_S$  and  $p_I$  in a weak form. The idea is to do integration-by-parts on the adjoint function to get the initial and boundary condition involved. We reformulate the constraint  $C(p_S, p_I, c_S) = 0$  as

$$\langle V, C(p_S, p_I, c_S) \rangle = 0 \quad (0.22)$$

for all continuous  $V \in C_0(\mathbb{R}) \times C_0(\mathbb{R}^2) \times C_0(\mathbb{R})$ , where the inner product

$$\begin{aligned} \langle V, C \rangle &= \int_0^{a_{\max}} e^{-ha} V_S(a) \left[ \frac{dp_S}{da} + \mu(a)p_S + \sigma(c_S(a))\tilde{\lambda}(a)p_S \right] da \\ &\quad + \int_0^{a_{\max}} e^{-ha} \int_0^a V_I(a, z) \left[ \frac{dp_I}{da} + \frac{dp_I}{dz} + \gamma(a, z)p_I(a, z) \right] dz da \\ &\quad + \int_0^{a_{\max}} e^{-ha} V_{c_S}(a) c_S(a) da. \end{aligned} \quad (0.23)$$

The  $e^{-ha}$  is weighting of the inner product that so that the adjoint variable can be interpreted as present-values of each state at the corresponding age. Integrating by parts,

$$\begin{aligned} \langle V, C \rangle &= - \int_0^{a_{\max}} e^{-ha} \left\{ \frac{dV_S}{da} - [h + \mu(a) + \sigma(c_S(a))\tilde{\lambda}(a)] V_S \right\} p_S(a) da \\ &\quad + \left|_0^{a_{\max}} e^{-ha} V_S(a) p_S(a) + \int_0^{a_{\max}} \left|_{a=0}^{a_{\max}} e^{-ha} V_I(a, z) p_I(a, z) \chi_{[0, a](z)} dz \right. \right. \\ &\quad + \int_0^{a_{\max}} \left|_{z=0}^a e^{-ha} V_I(a, z) p_I(a, z) da + \int_0^{a_{\max}} e^{-ha} V_{c_S}(a) c_S(a) da \right. \\ &\quad \left. - \int_0^{a_{\max}} \int_0^a e^{-ha} \left\{ \frac{\partial V_I}{\partial a} + \frac{\partial V_I}{\partial z} - [h + \gamma(a, z)] V_I \right\} p_I(a, z) dz da. \right. \end{aligned} \quad (0.24)$$

So our Lagrangian finally has the form

$$\begin{aligned} \mathcal{L} &= \int_0^{a_{\max}} e^{-ha} \left\{ [u_S(a) - c_S(a)] p_S(a) + \int_0^a u_I(a, z) p_I(a, z) dz \right\} da \\ &\quad + \int_0^{a_{\max}} e^{-ha} \left\{ \frac{\partial V_S}{\partial a} - [h + \mu(a) + \sigma(c_S(a))\tilde{\lambda}(a)] V_S \right\} p_S(a) da \\ &\quad + V_S(0) p_S(0) - e^{-hT} V_S(T) p_S(T) \\ &\quad + \int_0^{a_{\max}} \int_0^a e^{-ha} \left\{ \frac{dV_I}{da} + \frac{\partial V_I}{\partial z} - [h + \gamma(a, z)] V_I \right\} p_I(a, z) dz da \\ &\quad + \int_0^{a_{\max}} e^{-ha} V_I(a, 0) \sigma(c_S(a)) \tilde{\lambda}(a) p_S(a) da \\ &\quad + \int_0^{a_{\max}} e^{-ha} V_{c_S}(a) c_S(a) da. \end{aligned} \quad (0.25)$$

Thus, optimizing the Lagrangian now corresponds to setting all the functional derivatives with respect to  $p_S$ ,  $p_I$  and  $c_S$  equal to zero:

$$0 = \frac{\delta \mathcal{L}[p_S]}{\delta p_S}, \quad 0 = \frac{\delta \mathcal{L}[p_I]}{\delta p_I}, \quad 0 = \frac{\delta \mathcal{L}[c_S]}{\delta c_S}. \quad (0.26)$$

The inequality constraint for  $c_S(a) \geq 0$  provide additional requirement:

$$\text{either } c_S = 0, V_{c_S} \geq 0, \text{ or } c_S(a) > 0, V_{c_S} = 0. \quad (0.27)$$

Now we compute the strong form to the above system. Starting with the equation for  $-e^{-ha}V_I(a, z)$ , we differentiate the Lagrangian with respect to  $p_I$  to obtain

$$\int_0^{a_{\max}} \int_0^a e^{-ha} \left\{ u_I + \frac{\partial V_I}{\partial a} + \frac{\partial V_I}{\partial z} - [h + \gamma] V_I \right\} \delta p_I dz da = 0, \quad \text{for all } \delta p_I(a, z). \quad (0.28)$$

This is clearly the weak formulation of

$$-\frac{dV_I}{da} - \frac{dV_I}{dz} = u_I(a, z) - [h + \gamma(a, z)] V_I(a, z), \quad V_I(a_{\max}, z) = 0. \quad (0.29)$$

Similarly, for the equation for  $-e^{-ha}V_S(a)$ , we differentiate the Lagrangian with respect to  $p_S$ , and get

$$\int_0^{a_{\max}} e^{-ha} \left\{ [u_S - c_S] + \frac{\partial V_S}{\partial a} - [h + \mu + \sigma \tilde{\lambda}] V_S + V_I(a, 0) \sigma \tilde{\lambda} \right\} \delta p_S da = 0, \quad (0.30)$$

for all  $\delta p_S(a)$ .

This is exactly the weak formulation of the terminal value problem

$$-\frac{dV_S}{da} = u_S(a) - c_S(a) + \sigma(c_S(a)) \tilde{\lambda}(a) [V_I(a, 0) - V_S(a)] - [h + \mu(a)] V_S(a), \quad V_S(a_{\max}) = 0. \quad (0.31)$$

Finally, we have the equation for  $c_S$  as

$$\left\{ \frac{\partial \sigma}{\partial c_S} - \frac{1}{\tilde{\lambda}(a) [V_I(a, 0) - V_S(a)]} \right\} c_S = 0, \quad c_S \geq 0. \quad (0.32)$$

Therefore, the evolution for the adjoint variables is described by equations as follows

$$-\frac{dV_S}{da} = u_S(a) - c_S(a) + \sigma(c_S(a)) \tilde{\lambda}(a) [V_I(a, 0) - V_S(a)] - [h + \mu(a)] V_S(a) \quad (0.33a)$$

$$-\frac{dV_I}{da} - \frac{dV_I}{dz} = u_I(a, z) - [h + \gamma(a, z)] V_I(a, z) \quad (0.33b)$$

If  $c_S^*(a)$  is a Nash equilibrium, then  $c_S^* = 0$  or it must be a positive solution of the equation

$$\frac{\partial \sigma}{\partial c_S} - \frac{1}{\tilde{\lambda}(a) [V_I(a, 0) - V_S(a)]} = 0. \quad (0.34)$$



## Details of the numerical scheme used in simulation

Our main interest deals with a numerical approximation to the continuous problem given in section 4, that describes the dynamics of the disease transmission in the framework of the utility maximization for each individual when engaged in epidemic games.

We assume the spatial domain for  $(a, z)$  to be given by triangle  $\Omega = [0, a_{\max}] \times [0, a]$ . Notice that our dynamic Eqs. (2.3.7) have characteristic lines  $a(z) = z + a_0$  which never intersect over time, we discretized our triangular domain by means of uniform triangular mesh. For the numerical integration involved in our algorithm, we pick the first order Gauss quadrature for triangular domain which evaluate the function at the barycenter of each triangle with weight 0.5 as shown in [21].

First,  $V_I(a, z)$  can be integrated on its own which is independent of any strategy an individual might choose. Given the terminal condition  $V(a_{\max}, z) = 0$ , we can use the exponential Euler method to solve this differential equation along each characteristic line backwards in time to get  $V_I(a, z)$ . Only  $V_I(a, 0)$  at the barycenter of each triangular element need to be stored for further computation.

Second, we can compute the best response  $c_S^B$  and  $V_S(a)$  for any given infection pressure  $\tilde{\lambda}$  in general using optimality condition (2.3.4) that we derived previously. With  $V_I(a, 0)$  precomputed already, these can be implemented by computing  $c_S(a)$  first at each time step, then use the exponential Euler method backwards in time to calculate  $V_S(a - dt)$ . Additionally, with  $c_S^B$  and  $\tilde{\lambda}$  known, we can compute  $S(a)$  using the exponential Euler method. Density of infected people  $I(a, z)$  can also be computed with the exponential Euler method along characteristics.

Finally, we need to clarify how to compute the steady-state infection pressure  $\tilde{\lambda}$ , given the aggregated investment strategy of the population  $\bar{c}_S(a)$ . Recall the steady-state condition (2.3.10), which takes different form depends on the transmission type. So, we listed different numerical method accordingly for efficiency concern. In general, all the methods we picked here have taken in to account the advantage that our dynamic equations has characteristic lines.

### Scalar transmission case

For the case  $\beta(a, a_I, z) = \beta$ , which is a scalar constant, we recall the condition (2.4.4) for desired  $\tilde{\lambda}$ . It shows that  $\tilde{\lambda}$  should also be a scalar. We rearrange the double integral in Eq. (2.4.4) to first integrate along each characteristic lines which do share the same coefficient of  $\tilde{\lambda}$ , then integrate along different initial value  $a_0$  for each characteristic line. This provide us a new form of function  $F$  as

$$F(\tilde{\lambda}) = \int_0^{a_{\max}} e^{-\tilde{\lambda} \int_0^{a_0} \sigma(\bar{c}_S(\tau)) d\tau} \times \int_0^{a_{\max}-a_0} \beta \sigma(\bar{c}_S(a_0)) r e^{-\int_0^{a_0} \mu(\tau) d\tau} e^{-\int_0^z \gamma(a_0+\tau, \tau) d\tau} dz da_0.$$

We could furthermore use vector inner product to replace the out layer integral if we store  $e^{-\tilde{\lambda} \int_0^{a_0} \sigma(t, c_S(t)) dt}$  and the left part as two vectors for each  $a_0$ . Notice that  $F(\tilde{\lambda})$  is monotone

decreasing function of  $\tilde{\lambda}$ . The rest can be done by root finding of  $F(\tilde{\lambda}) - 1 = 0$ , using bisection or optimization techniques.

### Separable transmission case

For such case as  $\beta(a, a_I, z) := \Theta(a, a_I)\phi(z)$ . As we analyzed previously, the steady-state infection pressure  $\tilde{\lambda}(a) = A \cdot \phi(a)$  where  $A$  has to satisfy the condition (2.4.9). Similar as the previous case, notice the existence of characteristic lines  $a(z) = a_0 + z$  for  $I(a_I, z)$ . We rearrange the double integral in Eq. (2.4.9) as

$$F(A) = \int_0^{a_{\max}} e^{-A \int_0^{a_0} \xi(\tau)\sigma(c_S(\tau))d\tau} \int_0^{a_{\max}-a_0} \xi(a_0+z)\phi(z)\xi(a_0)\sigma c_S(a_0)) \times \\ r e^{-\int_0^{a_0} \mu(\tau)d\tau} e^{-\int_0^z \gamma(a_0+\tau,\tau)d\tau} dz da_0.$$

We compute the inner integral of  $z$  for each  $a_0$  along characteristic first and store it in a vector. The rest will be the same following the scalar case. The results are shown in the figures accordingly.

### General transmission case

Here the transmission rate  $\beta(a, a_I, z)$  can be given as a matrix or a multivariable function which might not provide our  $\tilde{\lambda}(a)$  any special structure. We have to evaluate it according to general condition (2.3.10). But we do want to point out here that we can still rearrange the double integral to integrate variable  $z$  along characteristic line first if possible, provided that  $\beta(a, a_I, z)$  is independent of  $z$  as our example in section 4.3

$$\tilde{\lambda}(a) = \int_0^{a_{\max}} \Theta(a, a_0) \tilde{\lambda}(a_0) \sigma(c_S(a_0)) r e^{-\int_0^{a_0} \tilde{\lambda}(\tau)\sigma(c_S(\tau)) + \mu(\tau)d\tau} \times \\ \int_0^{a_{\max}-a_0} \phi(z) e^{-\int_0^z \gamma(a_0+\tau,\tau)d\tau} dz da_0.$$

Here we can only speed up the algorithm by replacing the integral with vector produce accordingly.

At the end we do want to summarize our iterative method step by step. We always start by initially imposing  $\bar{c}_S(a) = 0$ , then we compute the steady-state  $\tilde{\lambda}$  to get an idea that how bad the disease will play in the population without any social distancing investment. Then, we compute the best response  $c_S^B(\bar{c}_S, \tilde{\lambda})$ . Update  $\bar{c}_S = c_S^B$ , repeat the iteration until they converge to  $c_S^*$ . Alternatively, we can also set the stopping criteria by checking the convergence of  $\tilde{\lambda}$  to  $\lambda^*$  if there exists a unique steady state infection pressure. Both ways, we should identify the game equilibria  $c_S^*(c_S^*; \lambda^*)$ .

## **Vita**

### **Dongmei Zhang**

Dongmei Zhang is a Ph.D. candidate in the Department of Mathematics at the Pennsylvania State University - University Park. Along her training in Mathematics, she has also completed her Ph.D. Minor in Computational Science administered by the Department of Aerospace Engineering in the College of Engineering. Prior to her education in the United State of America, she received her Bachelor's degree of Computational Mathematics at University of Science and Technology of China in 2008.